Title
A Tale of Two Methyltransferases: A Role for Methylation in the Control of Phosphorylation-Mediated Cell Signaling

Author
MacKay, Kennen Burke

Publication Date
2012

Peer reviewed|Thesis/dissertation

UNIVERSITY OF CALIFORNIA

Los Angeles

A Tale of Two Methyltransferases:

A Role for Methylation in the Control of Phosphorylation-Mediated Cell Signaling

A dissertation submitted in partial satisfaction of the requirements for the degree of

Doctor of Philosophy in Biochemistry and Molecular Biology

by

Kennen Burke MacKay

2012

ABSTRACT OF THE DISSERTATION

A Tale of Two Methyltransferases:

A Role for Methylation in the Control of Phosphorylation Pathways

by

Kennen Burke MacKay

Doctor of Philosophy in Biochemistry and Molecular Biology

University of California, Los Angeles, 2012

Professor Steven G. Clarke, Chair

The leucine carboxyl methyltransferase and the protein L-isoaspartyl methyltransferase are two carboxyl methyltransferases responsible for mediating two protein modification chemistries. The leucine carboxyl methyltransferase, coded for by the *Lcmt1* gene in mice, has only one known substrate, the C-terminal residue of protein phosphatase 2A (PP2A), a modification countered by protein phosphatase methylesterase 1. The protein L-isoaspartyl methyltransferase, coded for by the *Pcmt1* gene in mice, is responsible for methylating a multitude of

substrates, targeting isomerized aspartic acid residues for conversion, through methylation, to normal aspartic acid residues. Isoaspartyl residues are formed spontaneously in proteins from aspartyl and asparaginyl residues. Both of these enzymes have been implicated in the etiology of various disease states: PCMT1 in the onset of seizure disorders and spina bifida and LCMT1 as a tumor suppressor. Interestingly both enzymes have been implicated in the onset of Alzheimer's disease suggesting an important link to brain homeostasis.

Mice lacking the isoaspartyl methyltransferase demonstrate increased brain growth despite a decreased overall body size, hyperproliferation of T-cells and early death due to tonic clonic seizures. Although insulin signaling is constitutively activated in the brains of these animals, it is unclear whether this is involved in seizure onset. Additionally the convergence point between the isoaspartyl methyltransferase and the increased insulin signaling observed in *Pcmt1*$^{-/-}$ mice remains unknown. Recent work has implicated the isomerization/repair cycle mediated by the isoaspartyl methyltransferase in the regulation of a variety of proteins from cell surface receptors to p53, the "guardian of the genome". From my work, I hypothesize that an isoaspartyl-forming residue within a protein involved in the insulin signaling pathway may be responsible for the constitutive activation of this pathway seen in *Pcmt1*$^{-/-}$ mice. Through wortmannin-induced amelioration of the phosphatidylinositol 3-kinase-dependent insulin signaling pathway, I suggest the culpable residue or site of PCMT1 interaction may be the central effector of insulin signaling, the Akt kinase.

Expanding on the role of carboxyl methylation in the control of cell signaling, I characterized a mouse model hypomorphic for the leucine carboxyl methyltransferase, examining the tissue-specific decreases in PP2A methylation as well as a weak, but significant increase in insulin resistance in these animals. In an effort to discover as of yet unknown relationships between these two methyltransferases and the governance of cell signaling, I then attempted to define the LCMT1 and PCMT1 dependent "phosphome". Utilizing brain tissue from *Pcmt1*$^{-/-}$ animals as well as brain and muscle tissue from *Lcmt1*$^{-/-}$ animals, I employed a mass-spectrometry-based phosphoproteomic approach to identify tissues specific sites of phosphorylation sensitive to the levels of these two methyltransferases. These data will provide the foundation for future work examining the relationship between these two protein modification chemistries and their physiological role in mammalian cells.

The dissertation of Kennen Burke MacKay is approved.

_____

Catherine F. Clarke

_____

Stephen G. Young

_____

James W. Gober

_____

Kym F. Faull

_____

Steven G. Clarke, Committee Chair

University of California, Los Angeles 2012

This work is dedicated to my parents Drs. Deborah Burke and Don MacKay.

Without them I would never have pursued a career in academia

or a life of the mind.

TABLE OF CONTENTS

LIST OF FIGURES

LIST OF TABLES

ACKNOWLEDGEMENTS

I am deeply indebted to Dr. Steven Clarke for the hours he has spent discussing science and analyzing data with me. Dr. Clarke is responsible for teaching me not only the correct way to structure a scientific hypothesis but also how to organize ideas into coherent scientific arguments. My time with Dr. Clarke has instilled in me a cautious scientific objectivism, a trait I believe is vital to analyzing any form of obscure data. Working with one of the world's premier scientific thought leaders has been one of the highlights of my life and I will look back on my early halcyon years of scientific study in Dr. Clarke's lab with fondness for the rest of my life. Napoleon Bonaparte said, "a leader is a dealer in hope", and when it became apparent that 5 years into my dissertation work at UCLA I was still struggling with each of my projects, Dr. Clarke proved he is not only a thought leader, but also a consummate leader of people. Assuming a role not far from therapist, Dr. Clarke consistently provided hope through supportive advice and was able to talk me down from the metaphoric edge, for which I will be perpetually grateful to him.

The following acknowledgements are chronicled in the order through which they are reflected in this dissertation. CHAPTER 2 of this dissertation is a reprint of the article entitled "Wortmannin Reduces Insulin Signaling and Death in Seizure-Prone *Pcmt1*$^{-/-}$ Mice" from the journal PLOS ONE (Vol. 7(10): e46719). I would like to thank my co-author Dr. Jon Lowenson for performing the mouse breeding

necessary for this study as well as helping with the administration of wortmannin so I could take an occasional weekend day off while the 6 months of daily wortmannin dosing was being performed. I would additionally like to thank Dr. Lowenson for his terrific experimental ideas, critical proofreading, as well as his expert mouse care advice.

CHAPTER 3 of this dissertation would not be possible without the generous gift of *Lcmt1*$^{+/-}$ mice from Dr. Stephen Young. I would like to take this chance to thank him as well as members of his laboratory, Drs. Loren Fong and Yiping Tu, who were incredibly generous with their time and provided invaluable advice and collaboration concerning mammalian tissue culture, inverse PCR and the design of primers appropriate for genotyping knockout animals.

CHAPTER 4 of this dissertation was made possible through collaboration with a former undergraduate student of Dr. Clarke, Nick Hertz, as well as collaboration with the Al Burlingame and Kevan Shokat laboratories at the University of California, San Francisco. I am deeply grateful to each of these two professors for accommodating me in their labs on multiple occasions as well as nearly unlimited access to their laboratory supplies and instrumentation. Additionally this experience at UCSF expanded my horizons and opened my eyes to my career prospects in science and academia.

Additionally I would like to thank Austin Gable, an undergraduate student collaborator in Dr. Clarke's lab who tirelessly performed repetitious, mundane, yet scientifically crucial experiments such as mouse genotyping and bulk Western blotting.

I would like to personally thank my advisory committee Drs. Catherine Clarke, Stephen Young, Jim Gober, and Kym Faull. Dr. Faull's unabashedly honest evaluation of my projects consistently provided valuable insight and helped shaped my current abjectly objective scientific viewpoint. Lastly, but very importantly, I would like to thank Dr. Jon Wanagat for invaluable career advice as well as the countless hours he has invested in me, mentoring me on clinical medicine as well as rodent biology.

VITA

2001-2005	B.A. Biochemistry The Colorado College Colorado Springs, CO
2001-2005	NCAA D-III Team Academic All-American, Swimming
2004	Crecelius Family Research Award, $500
2004	Alfred W. Alberts Summer Research Prize, $3000
2006-2007	Teaching Assistant University of California, Los Angeles Department of Chemistry Advisor: Stacie Nakamoto
2006-2009	UCLA Cellular & Molecular Biology Training Grant

PUBLICATIONS AND PRESENTATIONS

MacKay KB, Lowenson JD, Clarke SG (2012) Wortmannin reduces insulin signaling and death in seizure-prone *Pcmt1*$^{-/-}$ mice. PloS ONE 7: e46719.

MacKay KB, Clarke SG (2012) Identification of Methylation-Dependent Protein Phosphatase 2A Activity Correlated with Changes in Insulin Secretion and Glucose Tolerance in Mice with Hypomorphic Expression of the LCMT1 Protein Carboxyl Methyltransferase, American Society for Biochemistry and Molecular Biology Annual Meeting, poster presentation, San Diego, CA**.**

MacKay KB, Hertz N, Clarke SG (2011) A Phosphoproteomic Look at PP2A's Methylation Dependent Targeting, CMB Retreat, poster presentation, Lake Arrowhead, CA.

MacKay KB, Young S, Clarke SG (2010) Deconvoluting Methylation Dependent Phosphatase Signaling. CMB Retreat, oral presentation, Lake Arrowhead, CA.

MacKay KB , Grover N (2005) Thermodynamic Analysis of the HIV-1 tat/TAR Interaction. American Society for Biochemistry and Molecular Biology Annual Meeting, poster presentation, San Diego, CA

MacKay KB , Grover N (2004) Thermodynamics of the HIV-1 TAR Base Triple. , PEW Undergraduate Research Conference, poster presentation, Chicago, Il.

CHAPTER 1

Introduction to the Dissertation

Post-translational phosphorylation is one of the most common mechanisms through which eukaryotic organisms regulate protein function[1]. Protein phosphorylation entered the scientific limelight relatively early due to its involvement in controlling cell cycle, growth, apoptosis, and signal transduction. Understanding mammalian cell's capacity for control of protein phosphorylation is vital for understanding disease biology[2,3,4]. This thesis sheds light on the recent discovery that two methyltransferases play an integral role in control of phosphorylation-perpetuated signal transduction as well as the reversal of protein phosphorylation mediated by a protein phosphatase.

The protein isoaspartyl methyltransferase gene in mice (*Pcmt1*) encodes a protein (PCMT1) initially discovered to methylate L-isoaspartyl and D-aspartyl residues formed from the spontaneous isomerization, racemization, and deamidation of aspartyl and asparaginyl residues[5]. This enzymatic reaction can initiate the conversion of these abnormal residues to normal L-aspartyl residues[6,7]. Due to the time-dependent formation of altered aspartyl residues and their buildup in proteins over time, it was initially believed that PCMT1 was an enzyme involved solely in repairing the protein damage associated with aging[8].

Formation of an isoaspartyl residue causes an increase in the length of the peptide backbone, and alters the spatial position of the side chain's negative charge [7]. Early experiments hinted at the initial damage/repair hypothesis by showing that accumulation of this "damage" modification could alter protein structure and decrease the activity of an enzyme, potentially contributing to age-related decreases in cellular function[7]. *In vivo* experiments that generated isoaspartyl

methyltransferase deficient *E. coli* and *C. elegans* contributed to the paradigm of the isoaspartyl methyltransferase protecting against aging as knockouts were sensitive to aging related stressors [9,10]. Conversely overexpression of this enzyme in *E. coli* and *D. melanogaster* protected against age-related stressors, buttressing the anti-aging repair enzyme paradigm [11,12]. This involvement of this enzyme in aging and repair is perhaps best exemplified in plants, where it has been shown to increase seed longevity and germination vigor[13] and its activity is correlated with heat stress[14].

Studying this enzyme in mammals, however, revealed a much more complex picture. *Pcmt1*$^{-/-}$ mice display decreased body size, yet an increased brain size compared to wild-type animals and die of massive tonic clonic seizures after an average of approximately 45 days of age[15,16,17]. Exploration of the main growth pathways within these animals revealed an increase in insulin signaling, a potential cause of the increased brain size[16,18]. The pleiotropic seizure sensitive *Pcmt1*$^{-/-}$ mice proved to be more complicated than what might be expected from the "early aging" model that the repair paradigm suggested. This mouse model suggested isoaspartyl residues and PCMT1 might provide an alternative, much more complex, cellular function. The aberrant signaling in this model provided the first evidence that isoaspartyl accumulation or the isoaspartyl methyltransferase may be a confluence point between cell signaling pathways and cytosolic functioning[16,18].

The question, however, remains whether this effect is mediated through an interaction with the methyltransferase itself or through the accumulation of general or specific isoaspartyl residues. Multiple biological examples for the latter exist in

the literature. For instance, it has been reported that isoaspartyl residues represent a crucial age/condition dependent switch activating specific integrin isoforms [19]. Additionally isoaspartyl residues have been proposed to function as cellular sensors guarding induction of apoptosis via mammalian p53 and Bcl-XL[20,21]. These experiments provide further evidence that isoaspartyl formation may act as a molecular switch, similar to phosphorylation, to regulate protein function. Exploring this new paradigm within the *Pcmt1* mouse model it becomes apparent that an isoaspartyl molecular switch could provide the answer to the aberrant insulin signaling observed in these animals.

Work in CHAPTER 2 of this thesis attempts to answer whether phosphoinositide 3-kinase mediated insulin signaling is responsible for the increases in brain size seen in *Pcmt1*$^{-/-}$ animals and to localize the site of interplay between the methyltransferase and the insulin signaling pathway. Additionally, as increases in brain size increase pressure within the cranial cavity which can itself lead to seizures [22,23], I attempted to determine whether seizure onset in these animals is due to their increased brain size, or an alternative etiologic, potentially isoaspartyl induced, cause. This work suggested small molecule-induced amelioration of insulin signaling could decrease brain size of *Pcmt1*$^{-/-}$ animals to near wild-type levels and extend lifespan, but not to that seen in wild-type animals, suggesting that insulin signaling and brain size is only partially responsible for seizure onset and early death in these animals. Additionally drug administration did not ameliorate all aspects of PI3K-mediated signaling in *Pcmt1*$^{-/-}$ animals,

particularly relating to mTOR activation, localizing a potential interaction point for isoaspartyl residues or the methyltransferase in this pathway[24].

During the course of my dissertation, additional work emerged suggesting the isoaspartyl methyltransferase influenced not only the insulin-signaling pathway but additional cell-signaling pathways such as the mitogen-activated signaling cascade [25,26], suggesting that the absence of the PCMT1 protein itself or isoaspartyl accumulation in the methyltransferase's absence, contributes to other specific alterations in protein phosphorylation. Work in CHAPTER 4 attempts to outline the global phosphorylation changes in *Pcmt1*$^{-/-}$ mice as compared to their wild-type littermates utilizing a quantitative phosphoproteomic approach. By labeling phosphopeptides with iTRAQ tags followed by mass spectrometric analysis using an LTQ-Orbitrap Velos instrument, I was able to compile libraries of significantly altered phosphopeptides in *Pcmt1*$^{-/-}$ animals. These libraries suggest PCMT1 may play a role in controlling phosphorylation of structural proteins such as tau and tubulin, previously known endogenous substrates of the enzyme[27,28]. This study emphasizes the pervasive nature of the isoaspartyl methyltransferase and provides a significant resource through which to further investigate novel interactions of this enzyme.

Due to the cyclical nature of isoaspartyl formation and repair through methylation, and the requirement of successive rounds of methylation for the repair of isoaspartyl residues[29], PCMT1 has been thought to be one of the major regulators of its methyl-donor *S*-adenosylmethionine (AdoMet) in the cell[30]. *Pcmt1*-deficient animals display increased cytosolic AdoMet and decreased *S*-

adenosylhomocysteine (AdoHcy) [30]. This increase in the AdoMet/AdoHcy ratio in *Pcmt1*$^{-/-}$ animals could result in potential interplay with, or activation of, other methyltransferases sharing the same co-substrate and contribute to the alterations in protein phosphorylation observed in *Pcmt1*$^{-/-}$ animals. One obvious AdoMet-dependent methyltransferase candidate known to affect phosphorylation is the leucine carboxyl methyltransferase, responsible for methylating and potentially activating the protein phosphatase 2A (PP2A)[31]. Indeed, I was able to show the activity of this methyltransferase was increased in *Pcmt1*$^{-/-}$ animals as evidenced by increased methylation of its only known substrate, PP2A.

Delving further into the role of carboxyl methylation in regulating protein phosphorylation I began investigating the role of methylation of protein phosphatase 2A (PP2A) by the leucine carboxyl methyltransferase (LCMT1) in CHAPTER 3. The relationship between these two enzymes presents an interesting dichotomy: LCMT1 is one of the most chaste of methyltransferases, refusing to methylate even peptide homologs of PP2A, yet it is responsible for controlling PP2A, one of the most promiscuous of enzymes with thousands of cellular substrates. This minor modification to PP2A propagates drastic alterations in phosphatase targeting as well as cellular function. The importance of this methylation is highlighted by work in *S. cerevisiae* demonstrating that loss of the methyltransferase ortholog results in severe growth defects and temperature sensitivity [32]. PP2A methylation is thought to alter the subunit composition of the heterotrimeric phosphatase, specifically regulating the binding of subunits responsible for targeting the enzyme to various cellular substrates[33].

Fortuitously BayGenomics, a global gene trapping consortium, had recently reported the successful insertion of a gene trap cassette within *Lcmt1* in mouse embryonic stem cells[34]. Obtaining chimeric *Lcmt1* gene trapped mice from this group, I was able to backcross them into a C57BL/6 background, and eventually generate what appeared to be *Lcmt1*$^{-/-}$ animals, a mutation previously reported to be lethal in mice[35]. Localizing the gene trap through long range sequencing experiments revealed a large section of the 5' end of the gene trap had been lost during insertion into the first intron of *Lcmt1*. This loss could potentially decrease the strength of the gene trap's splice acceptor site during RNA processing. Additionally a weak splice donor site on the 3' end of *Lcmt1* exon 1 could contribute to alternative splicing around the gene trap. Utilizing quantitative RT-PCR I was able to detect intact *Lcmt1* transcript, as well as intact LCMT1 protein through immunoblotting, albeit both at reduced levels in *Lcmt1*$^{-/-}$ animals. This reduction in LCMT1 appeared to function in a tissue specific manner, perhaps alluding to a difference in *Lcmt1* splicing and RNA processing in different tissues. Decreases in LCMT1 methyltransferase activity were also quantitated in these animals through *in vitro* radiolabelling experiments as well as through methylation sensitive antibodies and immunoblotting.

Through the characterization of these animals it rapidly became apparent that the gene trap was not functioning correctly; instead of creating a "knockout" animal our *Lcmt1*$^{-/-}$ animals represented a "knockdown" model hypomorphic for *Lcmt1*, perhaps the only reason these *Lcmt1*$^{-/-}$ animals were able to survive. It thus appears that we have been able to create a much more valuable model for probing

the role of this methyltransferase than could be had with the embryonic lethal full knockout. In addition to finding decreased *Lcmt1* transcript product and activity as well as decreased methylation of PP2A, I also quantitated the relative levels of steady state PP2A in tissue of *Lcmt1*$^{-/-}$ animals demonstrating a significant decrease in the cytosolic methylated pool of PP2A.

In order to study the effect of reduced methylation of PP2A on targeting of PP2A and global phosphorylation I again turned to an iTRAQ mediated quantitative phosphoproteomic approach as chronicled in CHAPTER 4. Applying the same method utilized to quantitate alterations in protein phosphorylation in *Pcmt1*$^{-/-}$ mice I was again able to generate libraries of phosphosites both increased and decreased in *Lcmt1*$^{-/-}$ hypomorphic mice. These data support the idea that this methylation reaction alters the targeting of this phosphatase with phosphosites discovered to be decreased in *Lcmt1*$^{-/-}$ animals reflecting sites of increased targeting in the absence of methylation, and sites discovered to display increased phosphorylation reflecting phosphosubstrates of PP2A requiring methylation for effective targeting.

REFERENCES

1. Cohen P (2000) The regulation of protein function by multisite phosphorylation--a 25 year update. Trends in biochemical sciences 25: 596-601.
2. Caenepeel S, Charydczak G, Sudarsanam S, Hunter T, Manning G (2004) The mouse kinome: discovery and comparative genomics of all mouse protein kinases. Proceedings of the National Academy of Sciences of the United States of America 101: 11707-11712.
3. Manning G, Whyte DB, Martinez R, Hunter T, Sudarsanam S (2002) The protein kinase complement of the human genome. Science 298: 1912-1934.
4. Walsh G, Jefferis R (2006) Post-translational modifications in the context of therapeutic proteins. Nature biotechnology 24: 1241-1252.
5. Clarke S (1985) Protein carboxyl methyltransferases: two distinct classes of enzymes. Annual review of biochemistry 54: 479-506.
6. Lowenson J, Clarke S (1988) Does the chemical instability of aspartyl and asparaginyl residues in proteins contribute to erythrocyte aging? The role of protein carboxyl methylation reactions. Blood cells 14: 103-118.
7. Clarke S (2003) Aging as war between chemical and biochemical processes: protein methylation and the recognition of age-damaged proteins for repair. Ageing research reviews 2: 263-285.
8. Desrosiers RR, Fanelus I (2011) Damaged proteins bearing L-isoaspartyl residues and aging: a dynamic equilibrium between generation of isomerized forms and repair by PIMT. Current aging science 4: 8-18.

9. Li C, Clarke S (1992) A protein methyltransferase specific for altered aspartyl residues is important in Escherichia coli stationary-phase survival and heat-shock resistance. Proceedings of the National Academy of Sciences of the United States of America 89: 9885-9889.

10. Ota IM, Ding L, Clarke S (1987) Methylation at specific altered aspartyl and asparaginyl residues in glucagon by the erythrocyte protein carboxyl methyltransferase. The Journal of biological chemistry 262: 8522-8531.

11. Kindrachuk J, Parent J, Davies GF, Dinsmore M, Attah-Poku S, Napper S (2003) Overexpression of L-isoaspartate O-methyltransferase in Escherichia coli increases heat shock survival by a mechanism independent of methyltransferase activity. The Journal of biological chemistry 278: 50880-50886.

12. Chavous DA, Jackson FR, O'Connor CM (2001) Extension of the Drosophila lifespan by overexpression of a protein repair methyltransferase. Proceedings of the National Academy of Sciences of the United States of America 98: 14814-14818.

13. Oge L, Bourdais G, Bove J, Collet B, Godin B, Granier F, Boutin JP, Job D, Jullien M, Grappin P (2008) Protein repair L-isoaspartyl methyltransferase 1 is involved in both seed longevity and germination vigor in Arabidopsis. The Plant cell 20: 3022-3037.

14. Villa ST, Xu Q, Downie AB, Clarke SG (2006) Arabidopsis Protein Repair L-Isoaspartyl Methyltransferases: Predominant Activities at Lethal Temperatures. Physiologia plantarum 128: 581-592.

15. Kim E, Lowenson JD, Clarke S, Young SG (1999) Phenotypic analysis of seizure-prone mice lacking L-isoaspartate (D-aspartate) O-methyltransferase. The Journal of biological chemistry 274: 20671-20678.

16. Farrar C, Houser CR, Clarke S (2005) Activation of the PI3K/Akt signal transduction pathway and increased levels of insulin receptor in protein repair-deficient mice. Aging cell 4: 1-12.

17. Farrar CE, Huang CS, Clarke SG, Houser CR (2005) Increased cell proliferation and granule cell number in the dentate gyrus of protein repair-deficient mice. The Journal of comparative neurology 493: 524-537.

18. Ikegaya Y, Yamada M, Fukuda T, Kuroyanagi H, Shirasawa T, Nishiyama N (2001) Aberrant synaptic transmission in the hippocampal CA3 region and cognitive deterioration in protein-repair enzyme-deficient mice. Hippocampus 11: 287-298.

19. Corti A, Curnis F (2011) Isoaspartate-dependent molecular switches for integrin-ligand recognition. Journal of cell science 124: 515-522.

20. Lee JC, Kang SU, Jeon Y, Park JW, You JS, Ha SW, Bae N, Lubec G, Kwon SH, Lee JS, Cho EJ, Han JW (2012) Protein L-isoaspartyl methyltransferase regulates p53 activity. Nature communications 3: 927.

21. Cimmino A, Capasso R, Muller F, Sambri I, Masella L, Raimo M, De Bonis ML, D'Angelo S, Zappia V, Galletti P, Ingrosso D (2008) Protein isoaspartate methyltransferase prevents apoptosis induced by oxidative stress in endothelial cells: role of Bcl-Xl deamidation and methylation. PloS one 3: e3258.

22. Mokri B (2001) The Monro-Kellie hypothesis: applications in CSF volume depletion. Neurology 56: 1746-1748.

23. McNamara B, Ray J, Menon D, Boniface S (2003) Raised intracranial pressure and seizures in the neurological intensive care unit. British journal of anaesthesia 90: 39-42.

24. Mackay KB, Lowenson JD, Clarke SG (2012) Wortmannin reduces insulin signaling and death in seizure-prone pcmt1(-/-) mice. PloS one 7: e46719.

25. Kosugi S, Furuchi T, Katane M, Sekine M, Shirasawa T, Homma H (2008) Suppression of protein l-isoaspartyl (d-aspartyl) methyltransferase results in hyperactivation of EGF-stimulated MEK-ERK signaling in cultured mammalian cells. Biochemical and biophysical research communications 371: 22-27.

26. Ryu J, Song J, Heo J, Jung Y, Lee SJ, Hong S, Cho JY (2011) Cross-regulation between protein L-isoaspartyl O-methyltransferase and ERK in epithelial mesenchymal transition of MDA-MB-231 cells. Acta pharmacologica Sinica 32: 1165-1172.

27. Zhu JX, Doyle HA, Mamula MJ, Aswad DW (2006) Protein repair in the brain, proteomic analysis of endogenous substrates for protein L-isoaspartyl methyltransferase in mouse brain. The Journal of biological chemistry 281: 33802-33813.

28. Watanabe A, Takio K, Ihara Y (1999) Deamidation and isoaspartate formation in smeared tau in paired helical filaments. Unusual properties of the

microtubule-binding domain of tau. The Journal of biological chemistry 274: 7368-7378.

29. McFadden PN, Clarke S (1987) Conversion of isoaspartyl peptides to normal peptides: implications for the cellular repair of damaged proteins. Proceedings of the National Academy of Sciences of the United States of America 84: 2595-2599.

30. Farrar C, Clarke S (2002) Altered levels of S-adenosylmethionine and S-adenosylhomocysteine in the brains of L-isoaspartyl (D-Aspartyl) O-methyltransferase-deficient mice. The Journal of biological chemistry 277: 27856-27863.

31. Shi Y (2009) Assembly and structure of protein phosphatase 2A. Science in China Series C, Life sciences / Chinese Academy of Sciences 52: 135-146.

32. Wei H, Ashby DG, Moreno CS, Ogris E, Yeong FM, Corbett AH, Pallas DC (2001) Carboxymethylation of the PP2A catalytic subunit in Saccharomyces cerevisiae is required for efficient interaction with the B-type subunits Cdc55p and Rts1p. The Journal of biological chemistry 276: 1570-1577.

33. Shi Y (2009) Serine/threonine phosphatases: mechanism through structure. Cell 139: 468-484.

34. Nord AS, Chang PJ, Conklin BR, Cox AV, Harper CA, Hicks GG, Huang CC, Johns SJ, Kawamoto M, Liu S, Meng EC, Morris JH, Rossant J, Ruiz P, Skarnes WC, Soriano P, Stanford WL, Stryke D, von Melchner H, Wurst W, Yamamura K, Young SG, Babbitt PC, Ferrin TE (2006) The International Gene Trap

Consortium Website: a portal to all publicly available gene trap cell lines in mouse. Nucleic acids research 34: D642-648.

35. Lee JA, Pallas DC (2007) Leucine carboxyl methyltransferase-1 is necessary for normal progression through mitosis in mammalian cells. The Journal of biological chemistry 282: 30974-30984.

CHAPTER 2

Wortmannin Reduces Insulin Signaling and Death in Seizure-Prone *Pcmt1*$^{-/-}$ Mice

OPEN ACCESS Freely available online

PLOS ONE

Wortmannin Reduces Insulin Signaling and Death in Seizure-Prone *Pcmt1*$^{-/-}$ Mice

Kennen B. MacKay, Jonathan D. Lowenson, Steven G. Clarke*

Department of Chemistry and Biochemistry and the Molecular Biology Institute, University of California Los Angeles, Los Angeles, California, United States of America

Abstract

L-isoaspartyl (D-aspartyl) *O*-methyltransferase deficient mice (*Pcmt1*$^{-/-}$) accumulate isomerized aspartyl residues in intracellular proteins until their death due to seizures at approximately 45 days. Previous studies have shown that these mice have constitutively activated insulin signaling in their brains, and that these brains are 20–30% larger than those from age-matched wild-type animals. To determine whether insulin pathway activation and brain enlargement is responsible for the fatal seizures, we administered wortmannin, an inhibitor of the phosphoinositide 3-kinase that catalyzes an early step in the insulin pathway. Oral wortmannin reduced the average brain size in the Pcmt1$^{-/-}$ animals to within 6% of the wild-type DMSO administered controls, and nearly doubled the lifespan of Pcmt1$^{-/-}$ at 60% survival of the original population. Immunoblotting revealed significant decreases in phosphorylation of Akt, PDK1, and mTOR in Pcmt1$^{-/-}$ mice and Akt and PDK1 in wild-type animals upon treatment with wortmannin. These data suggest activation of the insulin pathway and its resulting brain enlargement contributes to the early death of Pcmt1−/− mice, but is not solely responsible for the early death observed in these animals.

Citation: MacKay KB, Lowenson JD, Clarke SG (2012) Wortmannin Reduces Insulin Signaling and Death in Seizure-Prone *Pcmt1*$^{-/-}$ Mice. PLoS ONE 7(10): e46719. doi:10.1371/journal.pone.0046719

Editor: Shree Ram Singh, National Cancer Institute, United States of America

Received July 20, 2012; **Accepted** September 1, 2012; **Published** October 5, 2012

Funding: This work was funded by National Institutes of Health grants GM026020 and GM007185 (www.nih.gov) and by the Ellision Medical Foundation (www.elllisonfoundation.org). The funders had no role in study design, data collection and analysis, decision to publish, or preparation of the manuscript.

Competing Interests: The authors have declared that no competing interests exist.

* E-mail: clarke@mbi.ucla.edu

Introduction

Successful aging is dependent upon an organism's ability to protect its macromolecular machinery over time, and if this is not sufficient, to repair or replace that machinery [1,2,3]. Protein damage due to the spontaneous deamidation and isomerization of asparagine and aspartic acid residues, respectively, can build up over time and lead to alterations in tertiary protein structure and enzyme activity [4]. Additionally, isoaspartyl formation can act as an age-timed molecular switch altering enzyme function [5]. Organisms respond to such damage with the L-isoaspartyl (D-aspartyl) *O*-methyltransferase (PCMT1), a protein repair methyltransferase that initiates the conversion of L-isoaspartyl residues to normal L-aspartyl residues [4]. Pcmt1 is conserved from bacteria to humans and overexpression of this protein has been linked to extended lifespan in *Escherichia coli*, *Caenorhabditis elegans*, and *Drosophilia melanogaster* [6,7,8].

Although there are no reports of Pcmt1 overexpression in mammals, genetic deletion of this enzyme in mice leads to a significant increase in isoaspartyl residues in intracellular proteins [9,10]. Additionally these mice display reduced overall body size, enlarged brains, and have been reported to die at approximately 45 days of age from tonic-clonic seizures [11,12,13]. Although the cause of the seizure and reduced body size phenotypes remains to be resolved, the enlarged brain size is thought to be attributed, at least in part, to aberrantly increased insulin signaling in neuronal tissues [12,13,14]. This theory is reinforced by data showing similar effects in mice genetically modified to have increased insulin signaling [15]. Down-regulation of PCMT1 in human epileptic hippocampus suggests there may be a conserved role of PCMT1 in seizure disorders [16].

A conserved link between the insulin signaling pathway and the isoaspartyl repair methyltransferase also appears in the nematode *C. elegans*, where lifespan extension due to overexpression of the methyltransferase requires the activity of the DAF-16 transcription factor that is inactivated by insulin signaling [7,17]. On the other hand, repair methyltransferase-deficient mutants of *C. elegans* demonstrate diminished expression of at least some DAF-16 target genes [7]. Consistent with these observations, the loss of the repair methyltransferase in *C. elegans* results in a reduced starvation response and decreased lifespan under stress [18]. It has been hypothesized that either the accumulation of damaged proteins in methyltransferase knockouts acts as a direct switch activating insulin signaling or that the methyltransferase may directly interfere with the insulin-signaling pathway independent of isoaspartyl accumulation [7].

The sudden death phenotype of *Pcmt1*$^{-/-}$ mice clearly precludes their use as an aging model and prevents the discovery of the role of isoaspartyl accumulation in aging. Some progress has been made in developing *Pcmt1*$^{-/-}$ mice expressing transgenic L-isoaspartyl methyltransferase on a neuron-specific promoter [19]. These mice express low levels of this enzyme in the brain and display increased survival. In these mice, there appears to be a proteolytic system that engages at approximately 100 days of age to compensate for the rising level of L-isoaspartyl-containing proteins [19]. In *C. elegans* this link is further reinforced by evidence suggesting that the absence of the repair methyltransferase reduces

autophagy, indicating a direct link between PCMT1 and protein turnover [20].

We hypothesized that the aberrant growth signaling pathways and/or the enlarged brains in repair methyltransferase-deficient mice could be contributing to the seizure phenotype. Although the underlying cause of the increased brain size in *Pcmt1*$^{-/-}$ animals is currently unknown, the aberrant insulin signaling in the brains of these animals is theorized to be the leading cause of the enlarged brain size observed [12]. In this study we sought to knock down the insulin-signaling cascade through the use of the phosphoinositide 3-kinase (PI3K) inhibitor wortmannin [21–22]. PI3K is an essential element of the insulin cascade responsible for recruiting the AGC family of kinases, including Akt, PDK1 and mTORC2, to the membrane where Akt is phosphorylated and activated [23] [17]. If the increased activity of the insulin-signaling pathway is indeed involved in the seizure phenotype, inhibition of PI3K may reduce the brain size of *Pcmt1*$^{-/-}$ animals, limit seizure activity, and prolong their lifespan. We directly tested this hypothesis by maintaining mice on wortmannin and tracking their growth, lifespan, and insulin-signaling activation. Our results suggest the isoaspartyl methyltransferase may affect insulin signaling at or after the PI3K-dependent activation of Akt. We show that reduction of PI3K activity in *Pcmt1*$^{-/-}$ mice prevents the insulin-signaling cascade from exerting its downstream pleiotropic effects and establishes the aberrantly increased insulin signaling in the brains of these animals as the causative factor for their increased brain size. Additionally, wortmannin partially ameliorated seizure onset and extended lifespan in Pcmt1$^{-/-}$ animals.

Methods

Ethics Statement

This study was performed in accordance with animal use protocols approved by the UCLA Animal Research Committee (Protocol 1993-109-62). Mice were scheduled to be euthanized if they met any early removal criteria (kyphosis, lack of grooming behavior). However, this did not occur with any of the animals in our study.

Animal Husbandry

Mice were kept on a 12-hour light/dark cycle and allowed *ad libitum* access to water and NIH-31 7013 pellet chow (18% protein, 6% fat, 5% fiber, Harlan Teklad, Madison, WI). *Pcmt1*$^{-/-}$ animals were generated through breeding of *Pcmt1*$^{+/-}$ animals as reported previously [9,12]. These animals have been interbred for fifteen years to obtain a genetically homogeneous population. *Pcmt1*$^{-/-}$ and *Pcmt1*$^{+/+}$ offspring were used in this study. Experimental animals were weaned at 21 or 22 days of age; and we then began the administration of wortmannin or control solutions once per day until the mice reached 44 days of age. At this time, they were fasted for 15 hours and sacrificed by carbon dioxide asphyxiation for tissue extraction. Wortmannin (Alexis Biochemicals, San Diego, CA; lot 24089) was stored at −20°C in a 25 mg/ml solution in DMSO. Immediately prior to administration, mice were weighed. A fresh aliquot of wortmannin was diluted 1:10 in a grape-flavored sugar-based drink (Inter-American Products, Cincinnati, OH) and animals were administered oral doses using a calibrated Gilson P20 Pipetman containing 1.5 mg drug/kg body weight in the evening hours. Control animals were given a corresponding 1:10 dilution of DMSO in grape drink at the same time. A fresh pipet tip was used for each animal, and the mouse was held until the solution was observed to be swallowed. Animals were administered either drug or DMSO in a blinded fashion based on cage numbers and animal markings without knowledge of the genotype. Animals were housed in same-sex cages with two or three other mice.

Brain Extraction and Western Blotting

Following their final dose of wortmannin or control solution, 44 day-old mice were fasted overnight for 15 h and subsequently euthanized on their 45th day of age in a CO_2 chamber prior to surgical brain removal. Brain tissue (excluding the olfactory bulbs) was dissected, weighed, and added to 3 ml/g of RIPA buffer (50 mM Tris-HCl pH 8, 150 mM NaCl, 0.5% sodium deoxycholate, 1% Triton X-100, 1 mM PMSF) with phosphatase (HALT, Thermo-Pierce, Rockford, IL) and protease inhibitors (Complete, Roche, Mannheim, Germany) and homogenized using a Polytron homogenizer with a PTA-7 generator. The protein concentration of the crude extracts was determined after trichloroacetic acid precipitation by the Lowry method [24]. Aliquots containing 20 µg of protein were added to 10 µl of a 2X SDS-sample loading buffer (100 mM Tris-HCl, pH 6.8, 200 mM β-mercaptoethanol, 4% SDS, 0.1% bromophenol blue, 20% glycerol) and then brought to a final volume of 20 µl with water and heated for 5 min at 100°C. The samples were then loaded into lanes of twelve-well, 10 cm by 10 cm, 4–12% RunBlue SDS gels (Expedeon, San Diego, CA) in an Invitrogen XCell SureLock Mini-Cell apparatus along with parallel lanes of rainbow molecular weight markers (RPN-800V, GE Healthcare, Buckinghamshire, England). Electrophoresis was performed at 180 V for 1 h. Proteins were transferred from gels to PVDF membranes (Amersham Hybond-P, GE Healthcare) by electrophoretic transfer at 25 V for 3 h using the Invitrogen Blot Module and NuPAGE transfer buffer (Invitrogen, Grand Island, NY). Membranes were blocked overnight using 5% bovine serum albumin and then probed with the primary antibodies diluted in TBS-T buffer as described in Table 1. After the blot was washed in TBS-T buffer, it was incubated with horseradish peroxidase-labeled secondary antibodies as described in Table 1. Peroxidase activity was visualized after treating the blot with ECL Prime Chemiluminescent Agent (GE Healthcare) and detected on Hyblot CL film (Denville, Metuchen, NJ). Exposure times were optimized to allow linear responses. Film densitometry was performed using ImageJ densitometry software.

Quantitation of L-isoaspartyl Residues in Soluble Mouse Brain Extracts

The content of L-isoaspartyl residues in soluble mouse brain proteins was determined with an assay similar to that used previously [19]. Briefly, recombinant human L-isoaspartyl methyltransferase was used as a reagent to catalyze the transfer of ^{14}C-methyl groups from *S*-adenosyl-[*methyl*-^{14}C] methionine to L-isoaspartyl residues. After hydrolysis of the methyl esters formed, ^{14}C-methanol was quantified using a vapor diffusion assay. Samples were prepared by diluting the mouse brain crude homogenates described above two-fold with RIPA buffer, centrifugation at 20,800×g for 20 min at 4°C, and collection of the supernatant. The isoaspartyl methyltransferase assay mixture consisted of 5 µL of RIPA buffer containing 2 to 4 µg of protein from the supernatant fraction of *Pcmt1*$^{-/-}$ brain extract or 20 µg of protein from *Pcmt1*$^{+/+}$ brain extract, 10 µM *S*-adenosyl [*methyl*-^{14}C]methionine (48.8 mCi/mmol; Amersham Biosciences), 2.24 µg of recombinant human L-isoaspartyl methyltransferase (8944 pmol/min/mg protein), 160 mM bis-Tris-HCl buffer at pH 6.4 in a final volume of 40 µl. After a 3 h incubation at 37°C, ^{14}C-methyl ester content was quantitated as described [19]. All samples were assayed in triplicate. As a negative control, the brain sample was substituted with an equal volume of RIPA buffer.

Table 1. Source of Antibodies and Immunoblotting Protocols.

Target	Name	Source	Dilution	Incubation time	Temperature	Polypeptide size
p-S241-PDK1	Phospho-PDK1 (Ser241) (C49H2) Rabbit mAb #3438	Cell Signaling	1:10,000	1 h	25°C	58 kDa
Akt (pan)	Akt (pan) (C67E7) Rabbit mAb #4691	Cell Signaling	1:10,000	1 h	25°C	60 kDa
p-S473-Akt	Phospho-Akt (Ser473) (D9E) XP Rabbit mAb #4060	Cell Signaling	1:15,000	1 h	25°C	60 kDa
p-T308-Akt	Phospho-Akt (Thr308) (C31E5E) Rabbit mAb #2965	Cell Signaling	1:10,000	1 h	25°C	60 kDa
p-S2481-mTOR	Phospho-mTOR (Ser2481) Antibody #2974	Cell Signaling	1:10,000	18 h	25°C	289 kDa
p-S2448-mTOR	Phospho-mTOR (Ser2448) (D9C2) XP Rabbit mAb #5536	Cell Signaling	1:10,000	18 h	25°C	289 kDa
mTOR	mTOR (7C10) Rabbit mAb #2983	Cell Signaling	1:10,000	24 h	25°C	289 kDa
GAPDH	GAPDH (14C10) Rabbit mAb	Cell Signaling	1:40,000	1 h	25°C	37 kDa
PCMT1	Anti-PCMT1 cultured in rabbit (non-commercial)	Gift from Dr. Mark Mamula	1:1000	1 h	4°C	25 kDa
Anti-Rabbit	Anti-Rb Goat HRP conjugated secondary (ab6721)	Abcam	1:100,000	1 h	25°C	NA

doi:10.1371/journal.pone.0046719.t001

Radioactivity measured here was subtracted from the protein-containing samples. As a positive control, the brain sample was replaced with RIPA buffer and L-isoaspartyl-containing ovalbumin (80 mg/mL; Sigma-Aldrich A5503) dissolved in the bis-Tris buffer [19]. The positive control demonstrated that the RIPA buffer in the assay did not inhibit the recombinant isoaspartyl methyltransferase, and that there was enough methyltransferase activity and *S*-adenosyl[*methyl*-^{14}C]methionine in each incubation to methylate more than 25-fold more L-isoaspartyl residues than were detected in the mouse brain samples.

Results

Decreased Body Weights in Wortmannin-treated Mice

In an effort to test whether inhibition of the increased insulin signaling in *Pcmt1*$^{-/-}$ mice may alleviate the early death and growth phenotypes displayed by these animals, we treated groups of mice with daily 1.5 mg/kg oral doses of the PI3K inhibitor wortmannin beginning 21 or 22 days after birth at the time of weaning [22,25]. This dose was chosen based on two published reports that oral wortmannin administration at similar dosage levels significantly reduced β-amyloid deposition in an Alzheimer's disease model mouse [26] and tumor growth in a mouse cancer model [27], and had no adverse effects on these animals. Just prior to drug treatment, we confirmed the smaller size of *Pcmt1*$^{-/-}$ mice compared to their *Pcmt1*$^{+/+}$ littermates (Figure 1) as has been previously reported [9]. Although wortmannin has been used orally as an inhibitor of the kinase in mice [26,27] and in rats [28,29], it has not been established if such treatment would inhibit insulin-signaling activity. We thus treated *Pcmt1*$^{-/-}$ and wild-type mice as described above with wortmannin dissolved in DMSO, or DMSO alone, both diluted ten-fold in a grape flavored sugar drink. This drug administration was not done by gavage; instead, these mice were observed to swallow the 5–12 μL solution that was placed in their mouth via a Gilson P20 Pipetman. We found that the increase in body weight following weaning was identical for *Pcmt1*$^{-/-}$ and *Pcmt1*$^{+/+}$ mice when grouped by treatment and sex (Figure 2, panels A-D; Figure S1, panels A-D). Additionally, the body weight of the animals in the control group was similar to those of previously studied mice on the same NIH-31 7013 diet in the absence of DMSO and the sugar drink [9], suggesting that the DMSO and the additional sugar in the drink does not significantly alter growth.

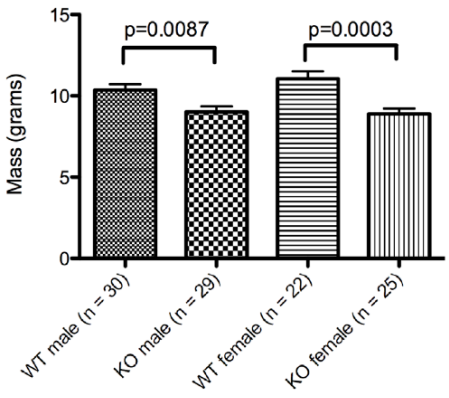

Figure 1. Body weight of wild-type and *Pcmt1*$^{-/-}$ mice at time of weaning. *Pcmt1*$^{-/-}$ mice are significantly smaller than their wild-type littermates when they are weaned at 21 or 22 days of age. The average weight +/− the standard deviation is shown as well as p-values calculated by Student's t-test.
doi:10.1371/journal.pone.0046719.g001

The average body weight of all groups of animals treated with wortmannin decreased significantly regardless of *Pcmt1* genotype (Figure 2, panels E-H; Figure S1, panels E-H). At 44 days of age, male wild-type animals weighed on average 22.1 g in the DMSO control group while animals administered wortmannin weighed on average 17.1 g. This decrease in mass was also seen in the male *Pcmt1*$^{-/-}$ animals, which had average weights at this time of 20.5 g (DMSO) and 15.2 g (wortmannin). Female wild-type control and wortmannin groups weighed 18.6 g and 15.8 g respectively. Because no female control *Pcmt1*$^{-/-}$ animals on DMSO survived the experimental time period, no data on their final body weight was available; however, female *Pcmt1*$^{-/-}$ animals on wortmannin had an average mass of 13.8 g at day 44.

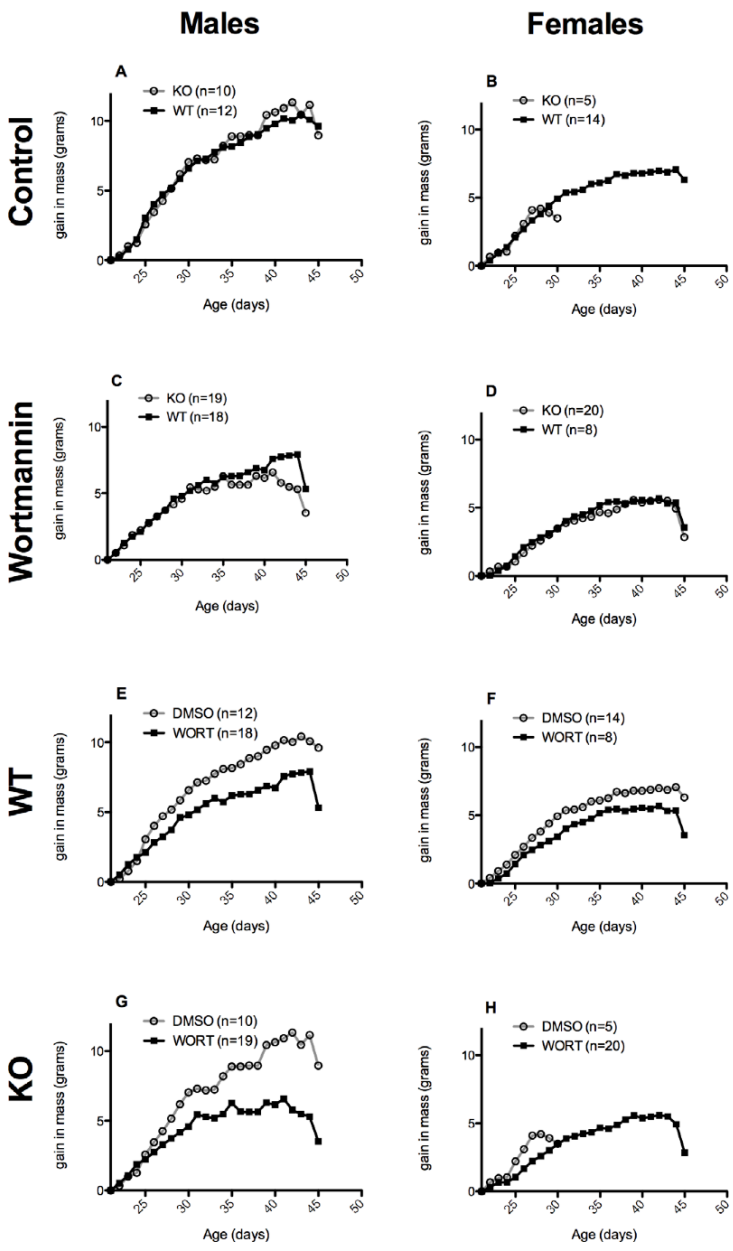
Males
Females
Control
Wortmannin
WT
KO
A
KO (n=10)
WT (n=12)
B
KO (n=5)
WT (n=14)
C
KO (n=19)
WT (n=18)
D
KO (n=20)
WT (n=8)
E
DMSO (n=12)
WORT (n=18)
F
DMSO (n=14)
WORT (n=8)
G
DMSO (n=10)
WORT (n=19)
H
DMSO (n=5)
WORT (n=20)
gain in mass (grams)
Age (days)

Figure 2. Effect of wortmannin (WORT) on the post-weaning weight gain of wild-type (WT) and protein L-isoaspartyl methyltransferase-deficient (*Pcmt1*$^{-/-}$) (KO) mice. In panels A-D, wild-type weight gains are shown in closed squares and *Pcmt1*$^{-/-}$ weight gains are shown in open circles. In panels E-H, weight gains of wortmannin-treated animals are shown in closed squares while those of DMSO-treated control mice are shown in open circles. In all cases animals treated with wortmannin showed significant growth retardation compared to their sex or genotype matched control counterparts.
doi:10.1371/journal.pone.0046719.g002

At 44 days, all animals were fasted in preparation for tissue analyses. Animals were fasted in order to ensure there were no differences in food consumption and blood sugar levels prior to analysis, as well as to ensure we were assaying baseline insulin signaling levels. Although statistically insignificant, all sex and genotype paired animal groups administered wortmannin lost a larger percentage of their body mass during overnight fasting than their DMSO control counterparts. In male wild-type animals the body mass loss amounted to 13.0% in the DMSO-treated group but 15.1% in the wortmannin-treated group. Similarly, male *Pcmt1*$^{-/-}$ mice lost 10.7% and 13.6% loss for control and wortmannin animals respectively. Finally, in female wild-type animals the losses amounted to 11.2% and 12.0% in DMSO and wortmannin animals respectively.

The large reduction in body weight over the course of drug administration suggests that the oral administration of wortmannin does in fact decrease insulin signaling-related growth, presumably by the inhibition of the PI3K. Attenuation of insulin signaling, through genetic knockouts as well as by RNA interference of pathway components (including PI3K variants), has been shown to generally result in decreased body size and stature [30].

Decreased Brain Weights in Wortmannin-treated Mice

Although *Pcmt1*$^{-/-}$ animals have a decreased body size they exhibit enlarged brains [10,12,14]. Such an increase in brain size was confirmed here in the control group of male mice (lanes 1 and 2 of Figure 3A). In male mice treated with wortmannin, brain size decreased for both *Pcmt1*$^{-/-}$ and wild-type animals (Figure 3A, lanes 1 and 3; lanes 2 and 4, respectively). These results confirm the role of insulin signaling in the increased brain size in *Pcmt1*$^{-/-}$ animals [12,13,14].

Male *Pcmt1*$^{-/-}$ animals treated with wortmannin on average had a brain mass 0.06 g less than those in the DMSO control group, while wild-type animals treated with wortmannin had brains on average 0.02 g smaller than control animals. Male *Pcmt1*$^{-/-}$ animals thus lost about three times as much brain weight with wortmannin treatment as compared to wild-type animals. Interestingly, male mice of both genotypes treated with wortmannin showed similar losses in body mass: 5 grams for male wild-type animals and 5.3 grams for male *Pcmt1*$^{-/-}$ animals. These results suggest that there is an interaction of the insulin-signaling pathway and the protein repair methyltransferase in the brain that may not occur generally in the rest of the body. Female wild-type animals on wortmannin lost on average 0.03 g of brain mass as compared to control treated animals. The lack of female *Pcmt1*$^{-/-}$ control animal survivors precludes our ability to make this calculation for female *Pcmt1*$^{-/-}$ animals. The tripling in brain weight lost in male *Pcmt1*$^{-/-}$ animals upon wortmannin treatment suggests wortmannin is reducing the brain specific insulin signaling in *Pcmt1*$^{-/-}$ animals.

Comparing the increase in brain size due to the absence of PCMT1 expression in the DMSO-control *Pcmt1*$^{-/-}$ group (0.08 g; lanes 2 and 1 in Figure 3A) with that of the wortmannin-treated group (0.04 g; lanes 4 and 3 in Figure 3A) enables us to map the location of *Pcmt1*'s influence within the insulin-signaling pathway. The fact that wortmannin-treated *Pcmt1*$^{-/-}$ animals still display enlarged brains compared to wild-type DMSO-treated animals suggests three possibilities. First, there may be incomplete PI3K inhibition through wortmannin-treatment. Second, the effect of the protein repair

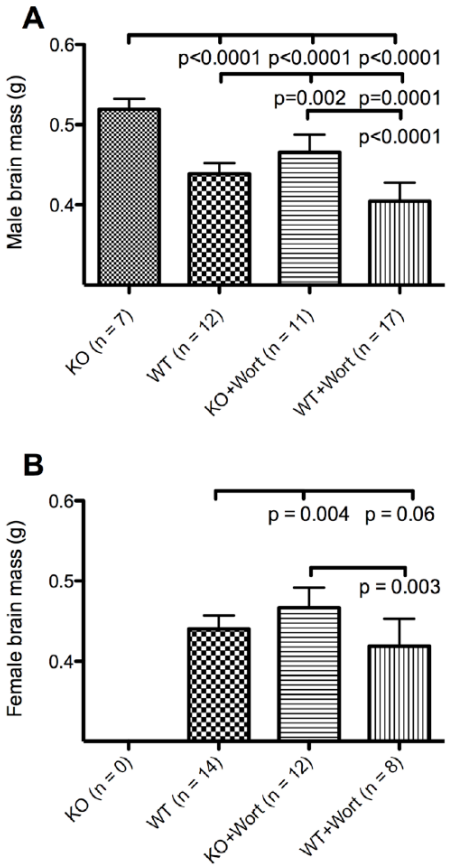

Figure 3. Comparison of brain weights at 45 days of wortmannin (WORT) and control DMSO treated wild-type (WT) and *Pcmt1*$^{-/-}$ (KO) mice. Panel A: Male mice. Panel B: Female mice. No female KO mice without WORT survived to 45 days of age. In each case the patterned bars indicate the average of 'n' treated animals +/− the standard deviation. The horizontal bars indicate the p values obtained by the Student's t-test (two-tailed, unpaired) in the indicated comparisons.
doi:10.1371/journal.pone.0046719.g003

methyltransferase may converge on the insulin-signaling pathway downstream of this kinase. Finally, there may be an alternate growth pathway influenced by the repair methyltransferase.

Lifespan Extension by Wortmannin in *Pcmt1*$^{-/-}$ Mice

To discover whether wortmannin treatment could alleviate the fatal tonic clonic seizures in *Pcmt1*$^{-/-}$ animals, we plotted lifespan data collected over the course of this experiment (Figure 4A). In order to increase sample size and statistical significance, we combined data from male and female animals as data collected during the maintenance of our mouse colony over the last 3 years shows that there is no difference in the survival of male and female *Pcmt1*$^{-/-}$ animals (Figure S2). We have now observed that wortmannin-treated *Pcmt1*$^{-/-}$ animals live significantly longer than their DMSO-treated control counterparts. As only one wild-type animal died over the experimental period, the effect of wortmannin on wild-type survival remains unknown. The decreased fatalities with wortmannin treatment, presumably due to prolonged time before seizure onset [9,11,19], correlates well with the decreased brain size seen in Figure 3.

Direct Analysis of the Insulin-signaling Pathway in Wortmannin-treated *Pcmt1*$^{-/-}$ and *Pcmt1*$^{+/+}$ Mice

By immunoblotting brain extracts for the activated phosphorylated components of the insulin-signaling system, we first confirmed that insulin signaling was potentiated in DMSO-treated *Pcmt1*$^{-/-}$ mice as previously described [12]. Phosphorylation of Ser-241 of PDK1, as well as Ser-473 and Thr-308 of Akt were each seen to be significantly increased in the *Pcmt1*$^{-/-}$ mice (Figure 5), suggesting that the DMSO treatment in our current experiments does not significantly alter brain phosphorylation patterns from the untreated animals described previously [12]. No change in total Akt protein levels was observed. Additionally we quantitated phosphorylation sites of Ser-2448 and Ser-2481 of mTOR. The former is associated with the active mTORC1 complex, the latter with the active mTORC2 complex [31]. Both mTOR phosphorylation sites appear to increase significantly in the *Pcmt1*$^{-/-}$ extracts, suggesting there is an overall increase in activated mTOR kinase in both mTORC1 and mTORC2 complexes. PCMT1 was also assayed in order to confirm the genotype of the *Pcmt1*$^{-/-}$ animals.

We then established the baseline effect of wortmannin treatment on 15 hour-fasted wild-type animals (Figure 6). Western blots showed that wortmannin significantly reduced PDK1 phosphor-

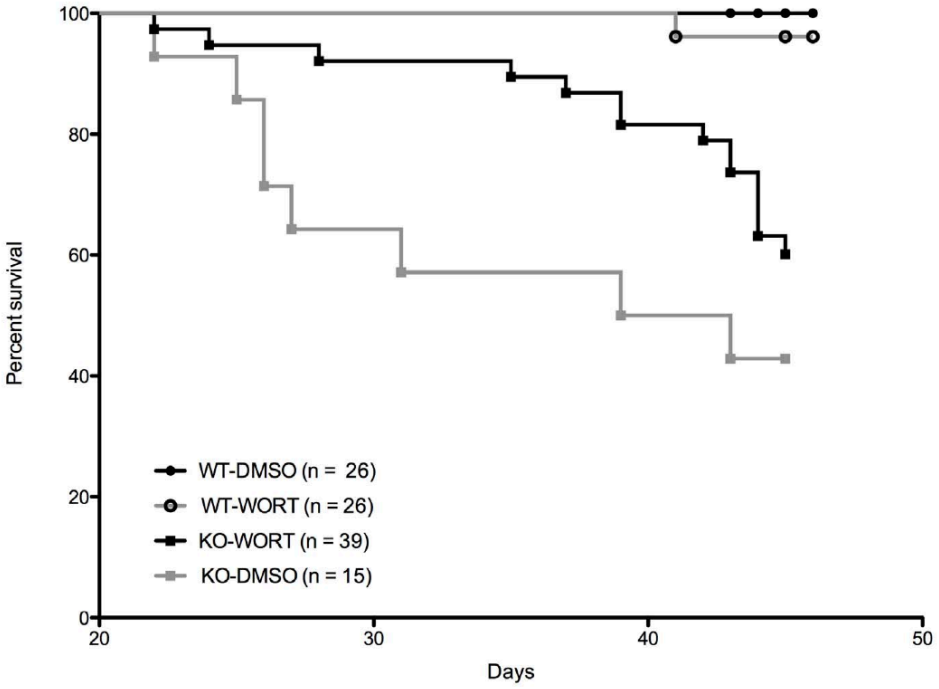

Figure 4. Survival curves of wortmannin (WORT)- and control (DMSO)–treated wild-type (WT) and *Pcmt1*$^{-/-}$ (KO) mice. The number of mice (both male and female) in each group is indicated in the legend. The survival of the KO group on wortmannin is significantly longer than the control KO group treated with DMSO according to the Gehan-Breslow-Wilcoxon Test ($p = 0.049$).
doi:10.1371/journal.pone.0046719.g004

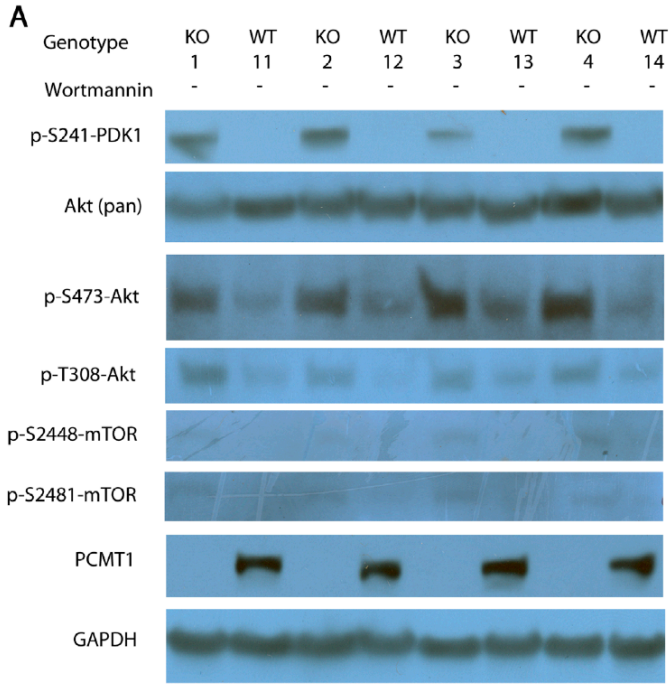
A
Genotype
KO 1
WT 11
KO 2
WT 12
KO 3
WT 13
KO 4
WT 14
Wortmannin
p-S241-PDK1
Akt (pan)
p-S473-Akt
p-T308-Akt
p-S2448-mTOR
p-S2481-mTOR
PCMT1
GAPDH

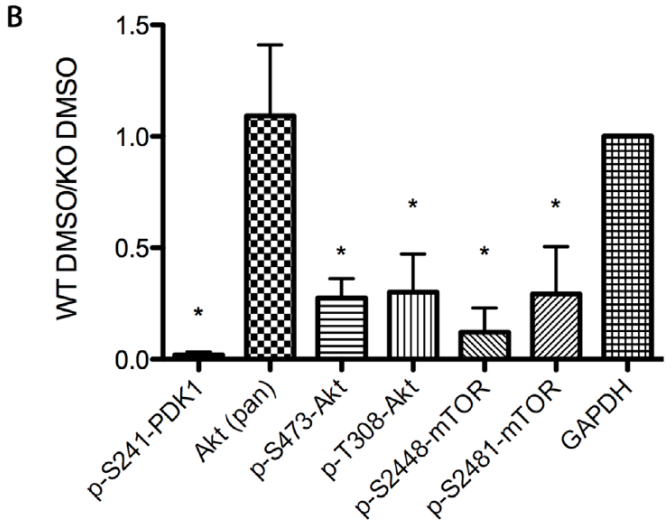
B
WT DMSO/KO DMSO
1.5
1.0
0.5
0.0
p-S241-PDK1
Akt (pan)
p-S473-Akt
p-T308-Akt
p-S2448-mTOR
p-S2481-mTOR
GAPDH

Figure 5. Western blot analysis of the phosphoproteins of the insulin-signaling cascade in homogenized whole-brains from male wild-type (WT) and *Pcmt1*$^{-/-}$ (KO) animals in the absence of wortmannin. Panel A: representative Western blots from four KO and four WT animals. Each row represents an independent exposure. Panel B: averaged densitometry results from all animals analyzed (n = 7 for KO; n = 12 for WT), standardized to GAPDH band densities to ensure equal protein loading. The molecular weight of each of the bands as determined in comparison with rainbow markers was consistent with the known weight of the target protein (Table 1). The error bars denote standard deviations; asterisks indicate statistical significance ($p<0.05$) by Student t-test between the WT and KO samples.
doi:10.1371/journal.pone.0046719.g005

ylation at Ser-241, an auto-phosphorylation site necessary for PDK1 activation and downstream signaling [32]. Although wortmannin reduced phosphorylation of Akt Thr-308 in these wild-type animals, it did not appear to statistically alter phosphorylation of the Ser-473 site. Additionally no effect was seen on mTOR phosphorylation (data not shown). These results show that orally administered wortmannin is an effective inhibitor of the insulin-signaling pathway in the brain as shown by the reduction in PDK1 and Akt phosphorylation [32,33].

Finally, we examined the effect wortmannin treatment had on *Pcmt1*$^{-/-}$ animals using Western blots with these brain extracts run side by side with *Pcmt1*$^{-/-}$ control extracts (Figure 7). In *Pcmt1*$^{-/-}$ mice, wortmannin decreased all of the phosphorylation sites related to canonical insulin signaling that were examined. Ser-241 of PDK1 had a nearly 10-fold decrease in phosphorylation. Downstream, phosphorylation of Thr-308 on Akt (the target of PDK1) was significantly reduced under wortmannin treatment. The Ser-473 site of Akt, phosphorylated by mTORC2, was also observed to be significantly decreased in wortmannin-treated *Pcmt1*$^{-/-}$ animals, suggesting insulin signaling mediated by Akt in the brains of *Pcmt1*$^{-/-}$ animals has been significantly ameliorated, a result also reflected in the reduced brain size of these animals compared to their *Pcmt1*$^{-/-}$ control counterparts. Auto-phosphorylation of mTOR as a result of PI3K/Akt signaling on the Ser-2481 site [34–35] as well as phosphorylation of Ser-2448 by the ribosomal protein S6 kinase [36,37] is significantly decreased in *Pcmt1*$^{-/-}$ animals in the presence of wortmannin. As the mTOR phosphorylation sites were not seen to have decreased in wild-type animals subject to wortmannin treatment yet presented significant decreases in *Pcmt1*$^{-/-}$ animals this could potentially represent the point of convergence between the insulin signaling pathway and the isoaspartyl repair methyltransferase.

These data suggest *Pcmt1*$^{-/-}$ animals react to a reduction in insulin signaling in a distinctly different manner than wild-type mice. Wortmannin treated *Pcmt1*$^{-/-}$ mice show similar inhibition of PDK1 to wild-type animals, and yet show a much greater inhibition of mTOR and Akt1. This suggests that these sites are aberrantly activated in *Pcmt1*$^{-/-}$ mice, yet subject to the effects of wortmannin. Interestingly, despite larger reduction in insulin signaling upon wortmannin treatment in *Pcmt1*$^{-/-}$ mice, these animals still have larger brains than control treated wild-type animals. This observation suggests that the isoaspartyl methyltransferase could affect the insulin-signaling pathway downstream of Akt, or the existence of an alternative growth pathway that is activated in *Pcmt1*$^{-/-}$ animals.

Effect of Wortmannin on the Accumulation of L-isoaspartyl Residues in Wild-type and Knockout *Pcmt1*$^{-/-}$ Mice

Another phenotype that has been observed in Pcmt1−/− mice is the 8- to 14-fold accumulation of isoaspartyl residues in intracellular brain proteins [9,10,19]. Partial extension of the short lifespan of these mice was achieved by inserting a *Pcmt1* transgene on a weak neuron-specific promoter, and this was correlated with a partial decrease in isoaspartate accumulation in the brain [19]. To determine whether wortmannin's protective effect is linked to isoaspartyl accumulation either through repair or by an increase in proteolytic degradation, we quantified the number of isoaspartyl residues in both *Pcmt1*$^{-/-}$ and wild-type animals. As expected, control *Pcmt1*$^{-/-}$ animals accumulated about 2500 pmol of methylatable isoaspartyl residues per milligram of protein while control wild-type animals had only approximately 200 pmol/mg (Figure 8). Interestingly, wortmannin had no effect on isoaspartyl accumulation in either wild-type or *Pcmt1*$^{-/-}$ animals, suggesting that the overall number of isoaspartyl residues in the brain proteins is not contributing to the prolonged survival of *Pcmt1*−/− mice afforded by wortmannin.

Discussion

In this study we found evidence that the PI3K inhibitor wortmannin can decrease insulin signaling in both *Pcmt1*$^{-/-}$ as well as wild-type mice, decrease the enlarged brain phenotype typical of *Pcmt1*$^{-/-}$ animals, and prolong the survival of *Pcmt1*$^{-/-}$ mice. Our observations suggest that the *Pcmt1*$^{-/-}$ activated growth pathways are confined to brain tissue as we find an approximate 20% increase in brain mass over wild-type animals at 45 days of age, yet a reduced overall body weight. This growth paradox highlights the importance of PCMT1 in the brain and suggests a role for this enzyme in brain growth and development. It is currently unknown, however, whether unrepaired isoaspartyl residues are acting as molecular switches triggering brain growth or whether the methyltransferase itself has a moonlighting role in mammalian development and growth. Our observation that a near complete reduction of phosphorylation of PDK1, mTOR and Akt1 does not completely abolish the enlarged brains of *Pcmt1*$^{-/-}$ animals suggests that the convergence of this methyltransferase with the insulin signaling pathway either occurs at, or downstream of, the kinase Akt. Alternatively, PCMT1 could be influencing brain growth through a different, Akt independent, growth pathway. For example, Kosugi et al. have shown that PCMT1 activity is also required for normal signaling through the MAPK pathway in cultured human embryonic kidney cells upon addition of EGF [38]. Additionally, although wortmannin was able to partially decrease the size of the enlarged brains of *Pcmt1*$^{-/-}$ animals, it succeeded only in prolonging the time until death (seizure onset), not preventing the early death phenotype. This suggests that the enlarged brain phenotype of *Pcmt1*$^{-/-}$ mice may be a contributing factor toward, but not the entire underlying cause of, the seizure phenotype and early death these mice experience.

The Akt kinase is at the center of the insulin-signaling pathway [30]. Interestingly mice have three genes expressing highly similar forms of the enzyme designated Akt1, Akt2, and Akt3 [30]. Akt1 is expressed ubiquitously outside of the brain and is responsible for global growth [39]. Akt2 is primarily responsible for maintaining insulin sensitivity to changing blood glucose levels and is confined to brown fat, skeletal muscle and the β-islet cells of the pancreas [40]. Akt3, of most interest to the present study, is expressed only in neurons and testis, and when genetically deleted has been shown to decrease brain size, indicating that it is largely responsible for brain growth and development [41–42]. Conversely, mutations leading to consti-

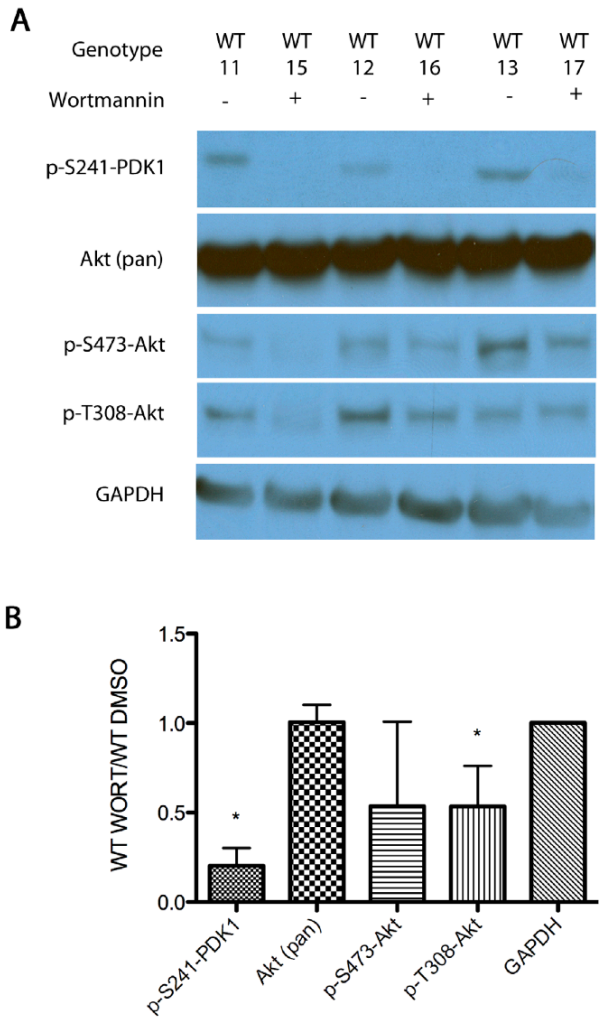

Figure 6. Western blot analysis of the phosphoproteins of the insulin-signaling cascade in homogenized whole-brains from male wild-type (WT) animals treated with wortmannin (+) or the DMSO control (-). Panel A: Representative Western blots from three DMSO control- and three wortmannin-treated animals. The molecular weight of each of the bands as determined in comparison with rainbow markers was consistent with the known weight of the target protein (Table 1). Each row represents an independent exposure. Panel B gives the results of densitometry from the entire group of 12 control and 17 wortmannin-treated animals. All bands were standardized to GAPDH controls to ensure equal protein loading. The error bars denote standard deviations; asterisks indicate statistical significance ($p<0.05$) by Student t-test between the wortmannin and DMSO control samples.
doi:10.1371/journal.pone.0046719.g006

tutive activation of this gene result in an enlarged brain and seizure phenotype [43], not dissimilar from the phenotypes observed in our *Pcmt1*$^{-/-}$ mice [9,10,11,12,14,19]. Our findings suggest that the Akt3 enzyme presents a brain-specific convergence point between PCMT1 and growth pathways and could provide a unique age-sensitive point of regulation of Akt3, either

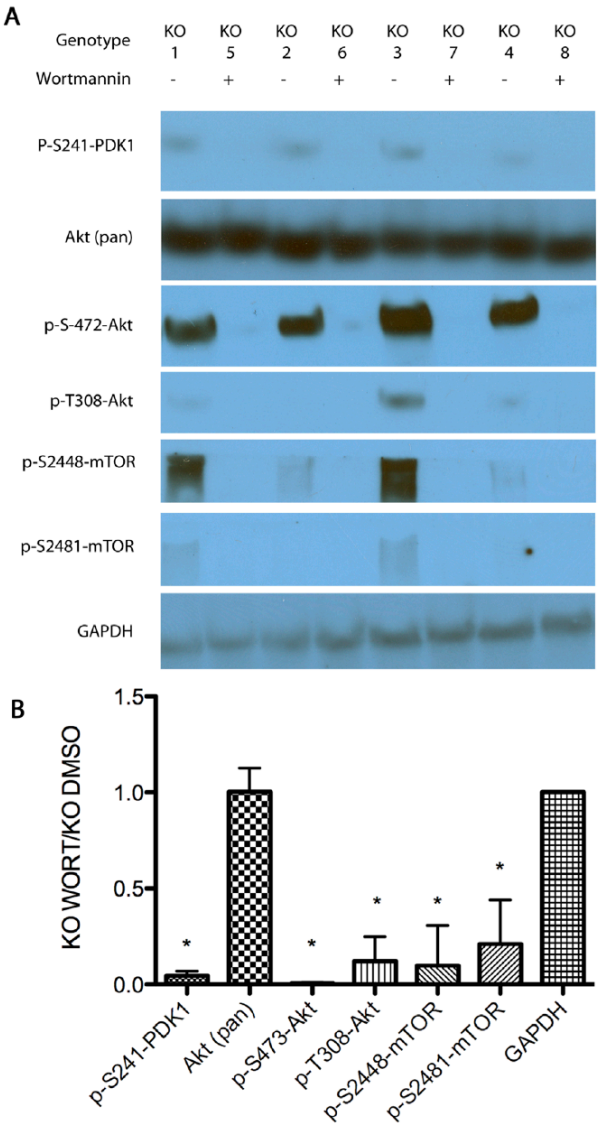

Figure 7. Western blot analysis of the insulin-signaling cascade in homogenized whole-brains from male animals. Panel A shows representative Western blots from four DMSO-control and four wortmannin-treated male *Pcmt1*$^{-/-}$ animals. The polypeptide molecular weight of each of the bands as determined in comparison with rainbow markers was consistent with the known weight of the target protein (Table 1). Each row represents an independent exposure. Panel B gives the results of densitometry from the entire group of 7 control and 11 wortmannin-treated animals. All bands were standardized to GAPDH controls to ensure equal protein loading. The error bars denote standard deviations; asterisks indicate a statistical significance ($p<0.05$) by Student t-test between the wortmannin and DMSO control samples.
doi:10.1371/journal.pone.0046719.g007

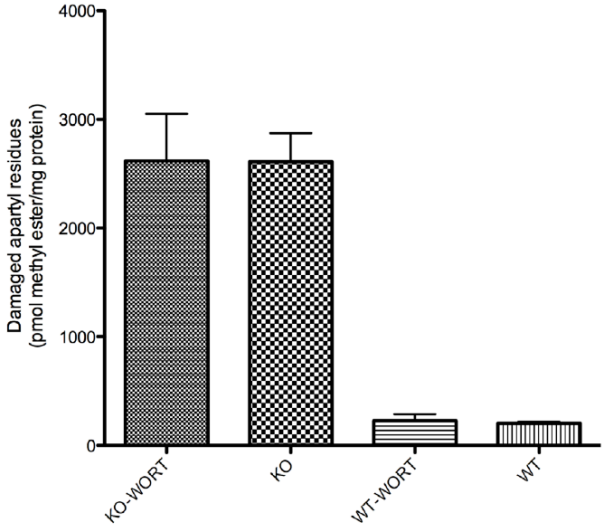

Figure 8. Quantitation of damaged aspartyl and asparaginyl residues in brain extracts. L-isoaspartyl residues arising *in vivo* in soluble brain polypeptides and proteins were labeled *in vitro* using recombinant human Pcmt1 and S-adenosyl- [^{14}C] methionine. The resulting [^{14}C] methyl esters were converted to [^{14}C] methanol with sodium hydroxide and allowed to diffuse from filter paper into scintillation fluid, which was counted in a scintillation counter. There are significantly more damaged residues in KO brains than in WT brains, but no significant change due to wortmannin treatment (n = 7 for each experimental group).
doi:10.1371/journal.pone.0046719.g008

by an isoaspartyl "switch" or through interaction with PCMT1 itself.

The possibility that Akt3 contains an isoaspartyl-regulated switch like that proposed for BCL-xL [44,45] and p53 [46] is supported by the fact that Akt3 has 9 additional potential isoaspartyl-forming asparagine and aspartic acid residues compared to Akt1, and 7 potential isoaspartyl-forming residues more than Akt2. Interestingly, some of these residues in Akt3 flank the crucial hydrophobic motif that is necessary for mTOR binding and activation [47,48,49]. The Akt3 isoform has also been linked to aberrant brain growth and seizure onset in humans [50]. We can propose the possibility that the isoaspartyl forms of Akt3 are more active than the methylated or non-isomerized forms (Figure 9); this model would account for the activation of the insulin-signaling pathway in *Pcmt1*$^{-/-}$ animals. Although other growth pathways have been shown to be sensitive to, or regulated by, PCMT1 activity such as the MAPK/ERK pathway [51] [38] [52–54], they do not rely on brain specific constituents and provide unlikely explanations for the aberrant brain growth phenotype observed in *Pcmt1*$^{-/-}$ mice.

The hypothesis of a brain specific isoaspartyl molecular switch regulating mTOR/Akt activation (Figure 10) correlates with our quantitative analysis of the increased phosphorylation and activation of mTOR and Akt in DMSO-treated *Pcmt1*$^{-/-}$ mice as compared to DMSO-treated wild-type animals and is currently under investigation. Additionally it appears that phosphorylation of the mTOR dependent Ser-473 site of Akt as well as mTOR itself exhibited a different reaction to the drug wortmannin in *Pcmt1*$^{-/-}$ mice with dramatic decreases in phosphorylation, a change not seen in wild-type animals. Despite wortmannin reducing phosphorylation of these enzymes, *Pcmt1*$^{-/-}$ mice on wortmannin still exhibit enlarged brains, suggesting the possibility that this pathway remains somewhat activated, potentially due to the unique isomerization or deamidation prone-residues neighboring the hydrophobic motif of Akt3.

This model suggests a unique post-translational control point governing brain Akt/mTOR interaction that could theoretically be responsible for elevating the growth pathways in *Pcmt1*$^{-/-}$ mice. Additionally this model implicates PCMT1 and isoaspartyl residues as age-related switches regulating entry into apoptotic pathways as has recently been shown in BCL-xL [45] [44] and p53 [46]. Additionally, wortmannin itself has been shown to trigger apoptosis through inhibition of PI3K class kinases [55–56] in a manner somewhat opposite of Pcmt1. These data present a striking opportunity for further research into the role of these pathways and apoptosis in seizure onset within this mouse model.

Our finding that *Pcmt1*$^{-/-}$ mice are smaller than wild-type animals at the time of weaning, but gain weight at a similar rate post-weaning suggests at least two possibilities. First, *Pcmt1*$^{-/-}$ mice could have a defect in early development limiting their size but still have normal post-weaning development. Second, they could suffer neurological deficits limiting their milking instinct, leading to competition from wild-type littermates for breastfeeding time, and thus decreasing developing body mass due to nutrient shortage. This hypothesis would support the observation of normal development post-weaning, as *Pcmt1*$^{-/-}$ animals would not face littermate competition for the easily accessible chow diet. A mouse line in which *Pcmt1* could be knocked out at 21 days of age using a CRE-Lox system would help distinguish between the roles of PCMT1 in developing versus weaned animals.

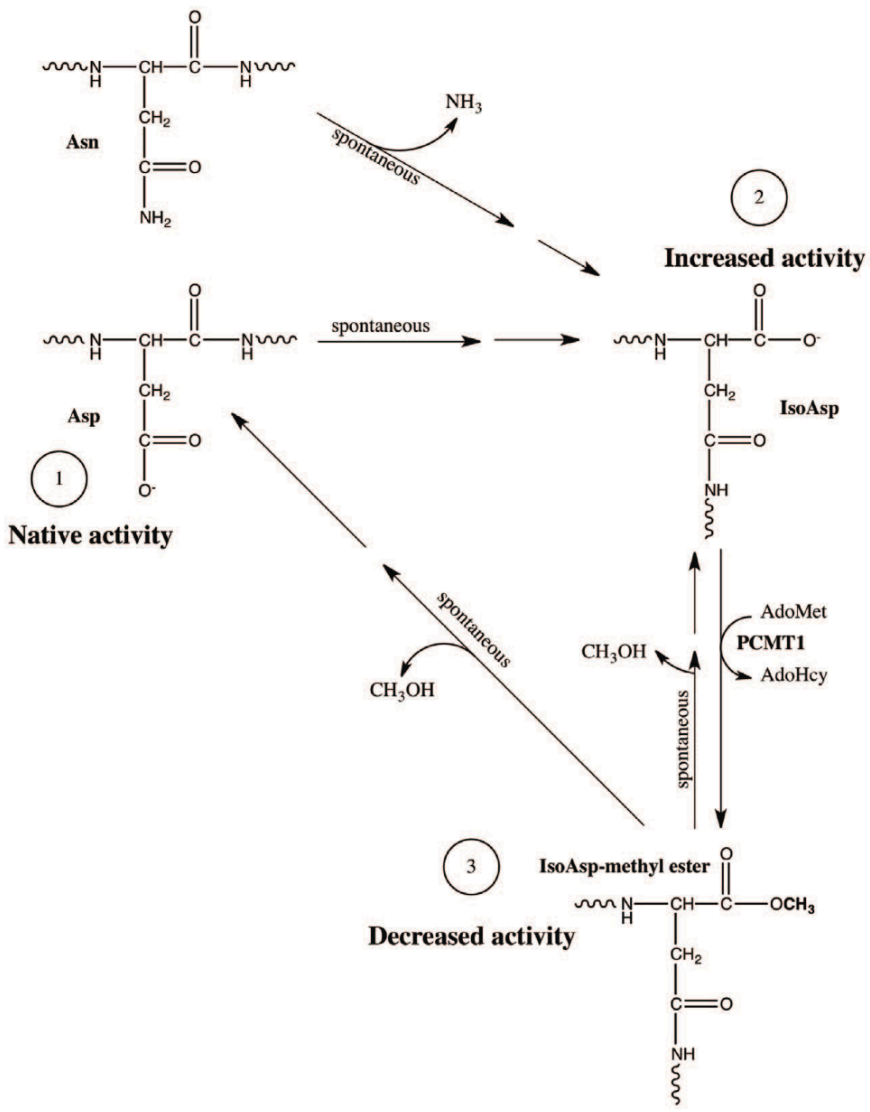

Figure 9. Simplified illustration of a hypothetical isoaspartyl switch. (1) The original Asp and Asn residues set a native activation baseline in a given protein. (2) Spontaneous deamidation or isomerization of Asn and Asp residues, respectively, through succinimide intermediates (not shown) yield isoaspartyl residues and potentially more active enzymes or better substrates for activating kinases. (3) AdoMet-dependent methylation of the isoaspartyl residue by PCMT1 yields an isoaspartyl-methyl ester, a potentially less active form. Spontaneous de-esterification via succinimide intermediates (not shown) can restore the active isoaspartyl-containing form (2), or result in reversed isomerization, returning the residue to the native aspartyl configuration (1), restoring native activity, or altered activity if the residue was initially asparagine. Such a switch may control the phosphorylation or activation of Akt3 or other proteins in the signaling pathways.
doi:10.1371/journal.pone.0046719.g009

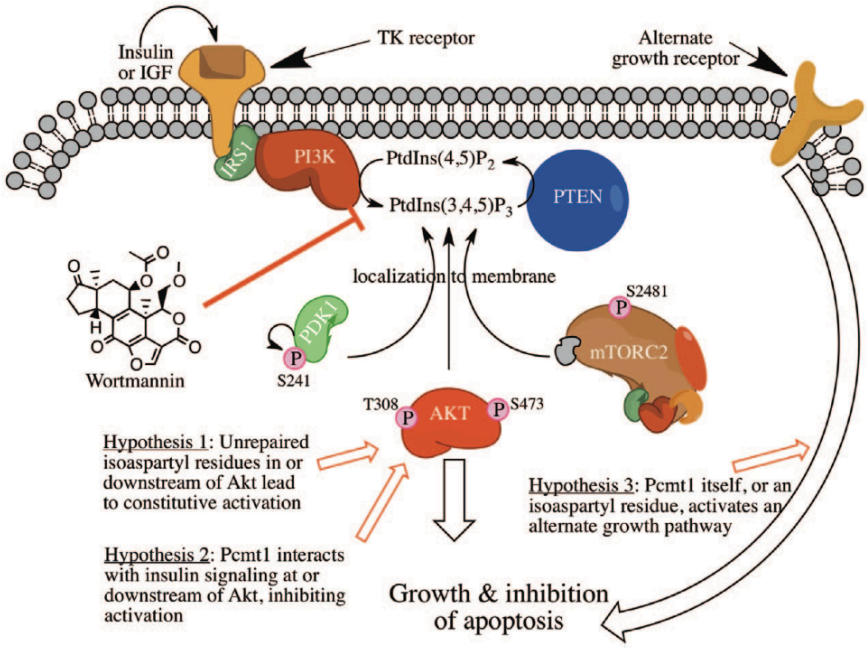

Figure 10. Possible points of interaction between *Pcmt1* and the upstream insulin-signaling pathway. Wortmannin inhibits PI3K class kinases and has been shown to inhibit insulin signaling. The elevated insulin signaling in *Pcmt1*$^{-/-}$ animals could arise from aberrant Akt activation (hypothesis 1 or 2), and/or aberrant interaction between Akt1 and mTOR (hypothesis 1 or 2) or activation of an alternate growth pathway (hypothesis 3).
doi:10.1371/journal.pone.0046719.g010

Supporting Information

Figure S1 Effect of wortmannin (WORT) on the post-weaning weight gain of wild-type (WT) and *Pcmt1*$^{-/-}$ (KO) mice. This figure shows the averaged absolute weights of the same animals whose relative weight gain is illustrated in Figure 2. In panels A-D, wild-type weight gains are shown in closed squares and *Pcmt1*$^{-/-}$ weight gains are shown in open circles. In panels E-H, weight gains of wortmannin-treated animals are shown in closed squares while those of DMSO-treated control mice are shown in open circles.
(TIFF)

Figure S2 Comparison of survival of untreated male (n = 51) and female (n = 57) Pcmt1$^{-/-}$ (KO) mice from day 21 of weaning. Untreated animals that died prior to 50 days of age were plotted on a Kaplan-Meier curve. No significant difference was observed between sexes. P = 0.334 by the Gehan-Breslow-Wilcoxon test.
(TIFF)

Acknowledgments

We would like to thank Mark Mamula for the generous gift of α-PCMT1 antibodies. We would like to thank Jonathan Wanagat, Alexander Patananan, Austin Gable and Maria Dzialo for their helpful advice on this work. Finally, we would like to acknowledge the UCLA ARC for helpful mouse husbandry advice.

Author Contributions

Conceived and designed the experiments: KBM JDL SGC. Performed the experiments: KBM JDL. Analyzed the data: KBM JDL SGC. Contributed reagents/materials/analysis tools: KBM JDL SGC. Wrote the paper: KBM JDL SGC.

References

1. Freitas AA, de Magalhaes JP (2011) A review and appraisal of the DNA damage theory of ageing. Mutation research 728: 12–22.
2. Rattan SI (2008) Increased molecular damage and heterogeneity as the basis of aging. Biological chemistry 389: 267–272.
3. Hipkiss AR (2006) Accumulation of altered proteins and ageing: causes and effects. Experimental gerontology 41: 464–473.
4. Clarke S (2003) Aging as war between chemical and biochemical processes: protein methylation and the recognition of age-damaged proteins for repair. Ageing research reviews 2: 263–285.

5. Corti A, Curnis F (2011) Isoaspartate-dependent molecular switches for integrin-ligand recognition. Journal of cell science 124: 515–522.
6. Chavous DA, Jackson FR, O'Connor CM (2001) Extension of the Drosophila lifespan by overexpression of a protein repair methyltransferase. Proceedings of the National Academy of Sciences of the United States of America 98: 14814–14818.
7. Khare S, Linster CL, Clarke SG (2011) The interplay between protein L-isoaspartyl methyltransferase activity and insulin-like signaling to extend lifespan in Caenorhabditis elegans. PloS one 6: e20850.
8. Kindrachuk J, Parent J, Davies GF, Dinsmore M, Attah-Poku S, et al. (2003) Overexpression of L-isoaspartate O-methyltransferase in Escherichia coli increases heat shock survival by a mechanism independent of methyltransferase activity. The Journal of biological chemistry 278: 50880–50886.
9. Kim E, Lowenson JD, MacLaren DC, Clarke S, Young SG (1997) Deficiency of a protein-repair enzyme results in the accumulation of altered proteins, retardation of growth, and fatal seizures in mice. Proceedings of the National Academy of Sciences of the United States of America 94: 6132–6137.
10. Yamamoto A, Takagi H, Kitamura D, Tatsuoka H, Nakano H, et al. (1998) Deficiency in protein L-isoaspartyl methyltransferase results in a fatal progressive epilepsy. The Journal of neuroscience : the official journal of the Society for Neuroscience 18: 2063–2074.
11. Kim E, Lowenson JD, Clarke S, Young SG (1999) Phenotypic analysis of seizure-prone mice lacking L-isoaspartate (D-aspartate) O-methyltransferase. The Journal of biological chemistry 274: 20671–20678.
12. Farrar C, Houser CR, Clarke S (2005) Activation of the PI3K/Akt signal transduction pathway and increased levels of insulin receptor in protein repair-deficient mice. Aging cell 4: 1–12.
13. Farrar CE, Huang CS, Clarke SG, Houser CR (2005) Increased cell proliferation and granule cell number in the dentate gyrus of protein repair-deficient mice. The Journal of comparative neurology 493: 524–537.
14. Ikegaya Y, Yamada M, Fukuda T, Kuroyanagi H, Shirasawa T, et al. (2001) Aberrant synaptic transmission in the hippocampal CA3 region and cognitive deterioration in protein-repair enzyme-deficient mice. Hippocampus 11: 287–298.
15. Carson MJ, Behringer RR, Brinster RL, McMorris FA (1993) Insulin-like growth factor I increases brain growth and central nervous system myelination in transgenic mice. Neuron 10: 729–740.
16. Lanthier J, Bouthillier A, Lapointe M, Demeule M, Beliveau R, et al. (2002) Down-regulation of protein L-isoaspartyl methyltransferase in human epileptic hippocampus contributes to generation of damaged tubulin. Journal of neurochemistry 83: 581–591.
17. Yap TA, Garrett MD, Walton MI, Raynaud F, de Bono JS, et al. (2008) Targeting the PI3K-AKT-mTOR pathway: progress, pitfalls, and promises. Current opinion in pharmacology 8: 393–412.
18. Gomez TA, Banfield KL, Clarke SG (2008) The protein L-isoaspartyl-O-methyltransferase functions in the Caenorhabditis elegans stress response. Mechanisms of ageing and development 129: 752–758.
19. Lowenson JD, Kim E, Young SG, Clarke S (2001) Limited accumulation of damaged proteins in l-isoaspartyl (D-aspartyl) O-methyltransferase-deficient mice. The Journal of biological chemistry 276: 20695–20702.
20. Gomez TA, Clarke SG (2007) Autophagy and insulin/TOR signaling in Caenorhabditis elegans pcm-1 protein repair mutants. Autophagy 3: 357–359.
21. Hazeki O, Hazeki K, Katada T, Ui M (1996) Inhibitory effect of wortmannin on phosphatidylinositol 3-kinase-mediated cellular events. Journal of lipid mediators and cell signalling 14: 259–261.
22. Ui M, Okada T, Hazeki K, Hazeki O (1995) Wortmannin as a unique probe for an intracellular signalling protein, phosphoinositide 3-kinase. Trends in biochemical sciences 20: 303–307.
23. Laplante M, Sabatini DM (2009) mTOR signaling at a glance. Journal of cell science 122: 3589–3594.
24. Lowry OH, Rosebrough NJ, Farr AL, Randall RJ (1951) Protein measurement with the Folin phenol reagent. The Journal of biological chemistry 193: 265–275.
25. Wymann MP, Bulgarelli-Leva G, Zvelebil MJ, Pirola L, Vanhaesebroeck B, et al. (1996) Wortmannin inactivates phosphoinositide 3-kinase by covalent modification of Lys-802, a residue involved in the phosphate transfer reaction. Molecular and cellular biology 16: 1722–1733.
26. Haugabook SJ, Le T, Yager D, Zenk B, Healy BM, et al. (2001) Reduction of Abeta accumulation in the Tg2576 animal model of Alzheimer's disease after oral administration of the phosphatidyl-inositol kinase inhibitor wortmannin. FASEB journal : official publication of the Federation of American Societies for Experimental Biology 15: 16–18.
27. Shivakrupa R, Bernstein A, Watring N, Linnekin D (2003) Phosphatidylinositol 3′-kinase is required for growth of mast cells expressing the kit catalytic domain mutant. Cancer research 63: 4412–4419.
28. Jindal A, Mahesh R, Singh K, Bhatt S, Gautam B, et al. (2011) Ameliorative Effect of Wortmannin and Rapamycin Treatment on Obesity Markers in High Fat Diet Feed Rats. Indian Journal of Pharmaceutical Education and Research 45: 333–338.
29. Gunther R, Abbas HK, Mirocha CJ (1989) Acute pathological effects on rats of orally administered wortmannin-containing preparations and purified wortmannin from Fusarium oxysporum. Food and chemical toxicology : an international journal published for the British Industrial Biological Research Association 27: 173–179.
30. Biddinger SB, Kahn CR (2006) From mice to men: insights into the insulin resistance syndromes. Annual review of physiology 68: 123–158.
31. Copp J, Manning G, Hunter T (2009) TORC-specific phosphorylation of mammalian target of rapamycin (mTOR): phospho-Ser2481 is a marker for intact mTOR signaling complex 2. Cancer research 69: 1821–1827.
32. Casamayor A, Morrice NA, Alessi DR (1999) Phosphorylation of Ser-241 is essential for the activity of 3-phosphoinositide-dependent protein kinase-1: identification of five sites of phosphorylation in vivo. The Biochemical journal 342 (Pt 2): 287–292.
33. Hers I, Vincent EE, Tavare JM (2011) Akt signalling in health and disease. Cellular signalling 23: 1515–1527.
34. Nave BT, Ouwens M, Withers DJ, Alessi DR, Shepherd PR (1999) Mammalian target of rapamycin is a direct target for protein kinase B: identification of a convergence point for opposing effects of insulin and amino-acid deficiency on protein translation. The Biochemical journal 344 Pt 2: 427–431.
35. Peterson RT, Beal PA, Comb MJ, Schreiber SL (2000) FKBP12-rapamycin-associated protein (FRAP) autophosphorylates at serine 2481 under translationally repressive conditions. The Journal of biological chemistry 275: 7416–7423.
36. Chiang GG, Abraham RT (2005) Phosphorylation of mammalian target of rapamycin (mTOR) at Ser-2448 is mediated by p70S6 kinase. The Journal of biological chemistry 280: 25485–25490.
37. Holz MK, Blenis J (2005) Identification of S6 kinase 1 as a novel mammalian target of rapamycin (mTOR)-phosphorylating kinase. The Journal of biological chemistry 280: 26089–26093.
38. Kosugi S, Furuchi T, Katane M, Sekine M, Shirasawa T, et al. (2008) Suppression of protein l-isoaspartyl (d-aspartyl) methyltransferase results in hyperactivation of EGF-stimulated MEK-ERK signaling in cultured mammalian cells. Biochemical and biophysical research communications 371: 22–27.
39. Cho H, Thorvaldsen JL, Chu Q, Feng F, Birnbaum MJ (2001) Akt1/PKBalpha is required for normal growth but dispensable for maintenance of glucose homeostasis in mice. The Journal of biological chemistry 276: 38349–38352.
40. Cho H, Mu J, Kim JK, Thorvaldsen JL, Chu Q, et al. (2001) Insulin resistance and a diabetes mellitus-like syndrome in mice lacking the protein kinase Akt2 (PKB beta). Science 292: 1728–1731.
41. Easton RM, Cho H, Roovers K, Shineman DW, Mizrahi M, et al. (2005) Role for Akt3/protein kinase Bgamma in attainment of normal brain size. Molecular and cellular biology 25: 1869–1878.
42. Yang ZZ, Tschopp O, Baudry A, Dummler B, Hynx D, et al. (2004) Physiological functions of protein kinase B/Akt. Biochemical Society transactions 32: 350–354.
43. Tokuda S, Mahaffey CL, Monks B, Faulkner CR, Birnbaum MJ, et al. (2011) A novel Akt3 mutation associated with enhanced kinase activity and seizure susceptibility in mice. Human molecular genetics 20: 988–999.
44. Cimmino A, Capasso R, Muller F, Sambri I, Masella L, et al. (2008) Protein isoaspartate methyltransferase prevents apoptosis induced by oxidative stress in endothelial cells: role of Bcl-Xl deamidation and methylation. PloS one 3: e3258.
45. Sambri I, Capasso R, Pucci P, Perna AF, Ingrosso D (2011) The microRNA 15a/16–1 cluster down-regulates protein repair isoaspartyl methyltransferase in hepatoma cells: implications for apoptosis regulation. The Journal of biological chemistry 286: 43690–43700.
46. Lee JC, Kang SU, Jeon Y, Park JW, You JS, et al. (2012) Protein L-isoaspartyl methyltransferase regulates p53 activity. Nature communications 3: 927.
47. Huang J, Manning BD (2009) A complex interplay between Akt, TSC2 and the two mTOR complexes. Biochemical Society transactions 37: 217–222.
48. Woodgett JR (2005) Recent advances in the protein kinase B signaling pathway. Current opinion in cell biology 17: 150–157.
49. Bozulic L, Hemmings BA (2009) PIKKing on PKB: regulation of PKB activity by phosphorylation. Current opinion in cell biology 21: 256–261.
50. Poduri A, Evrony GD, Cai X, Elhosary PC, Beroukhim R, et al. (2012) Somatic activation of AKT3 causes hemispheric developmental brain malformations. Neuron 74: 41–48.
51. Furuchi T, Homma H (2007) [Role of isomerized protein repair enzyme, PIMT, in cellular functions]. Yakugaku zasshi : Journal of the Pharmaceutical Society of Japan 127: 1927–1936.
52. Cournoyer P, Desrosiers RR (2009) Valproic acid enhances protein L-isoaspartyl methyltransferase expression by stimulating extracellular signal-regulated kinase signaling pathway. Neuropharmacology 56: 839–848.
53. Furuchi T, Sakurako K, Katane M, Sekine M, Homma H (2010) The role of protein L-isoaspartyl/D-aspartyl O-methyltransferase (PIMT) in intracellular signal transduction. Chemistry & biodiversity 7: 1337–1348.
54. Ryu J, Song J, Heo J, Jung Y, Lee SJ, et al. (2011) Cross-regulation between protein L-isoaspartyl O-methyltransferase and ERK in epithelial mesenchymal transition of MDA-MB-231 cells. Acta pharmacologica Sinica 32: 1165–1172.
55. Padmore L, Radda GK, Knox KA (1996) Wortmannin-mediated inhibition of phosphatidylinositol 3-kinase activity triggers apoptosis in normal and neoplastic B lymphocytes which are in cell cycle. International immunology 8: 585–594.
56. Rasul A, Ding C, Li X, Khan M, Yi F, et al. (2012) Dracorhodin perchlorate inhibits PI3K/Akt and NF-kappaB activation, up-regulates the expression of p53, and enhances apoptosis. Apoptosis : an international journal on programmed cell death.

Supplemental Material:

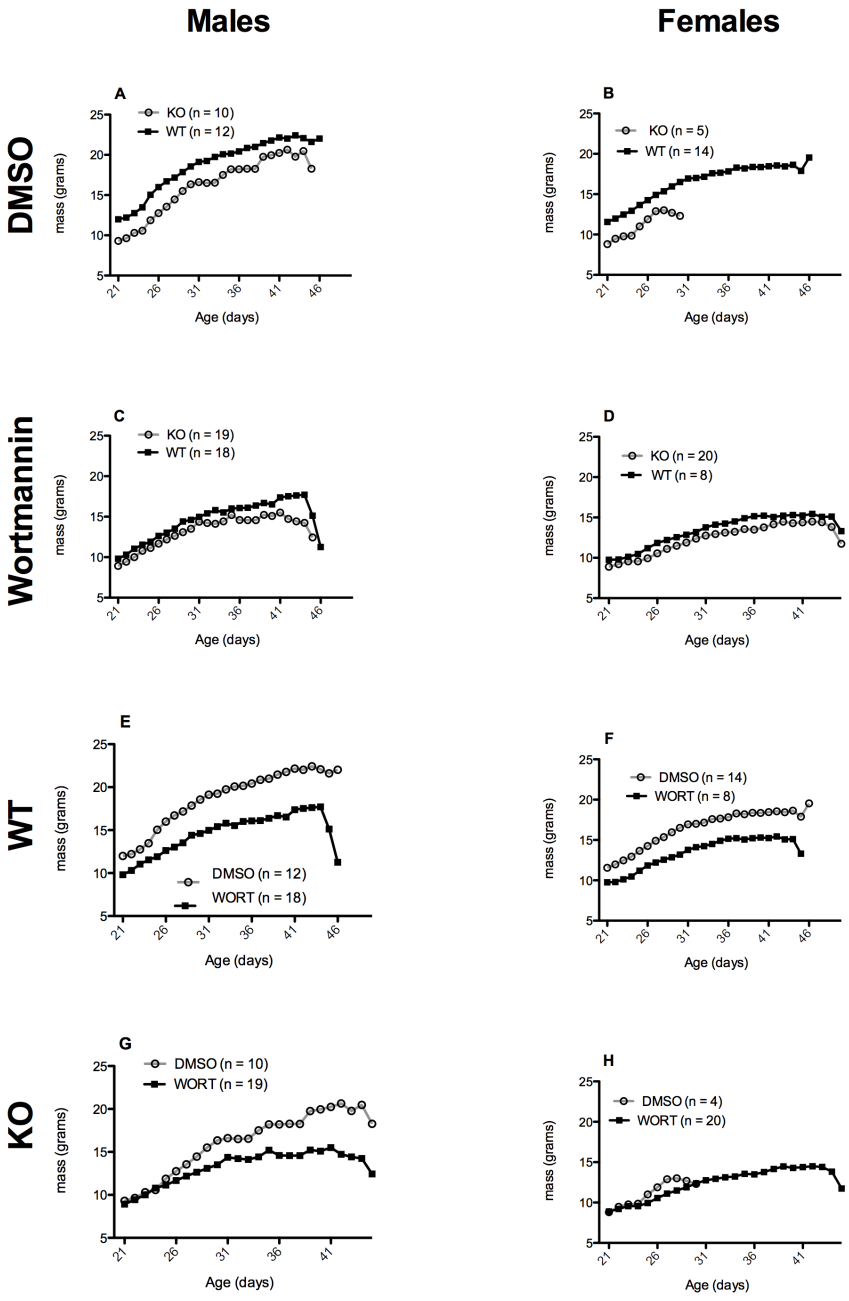

Figure S1: Effect of wortmannin (WORT) on the post-weaning weight gain of wild-type (WT) and *Pcmt1*$^{-/-}$ (KO) mice. This figure shows the averaged absolute weights of the same animals whose relative weight gain is illustrated in Figure 2. In panels

A-D, wild-type weight gains are shown in closed squares and *Pcmt1*$^{-/-}$ weight gains are shown in open circles. In panels E-H, weight gains of wortmannin-treated animals are shown in closed squares while those of DMSO-treated control mice are shown in open circles.

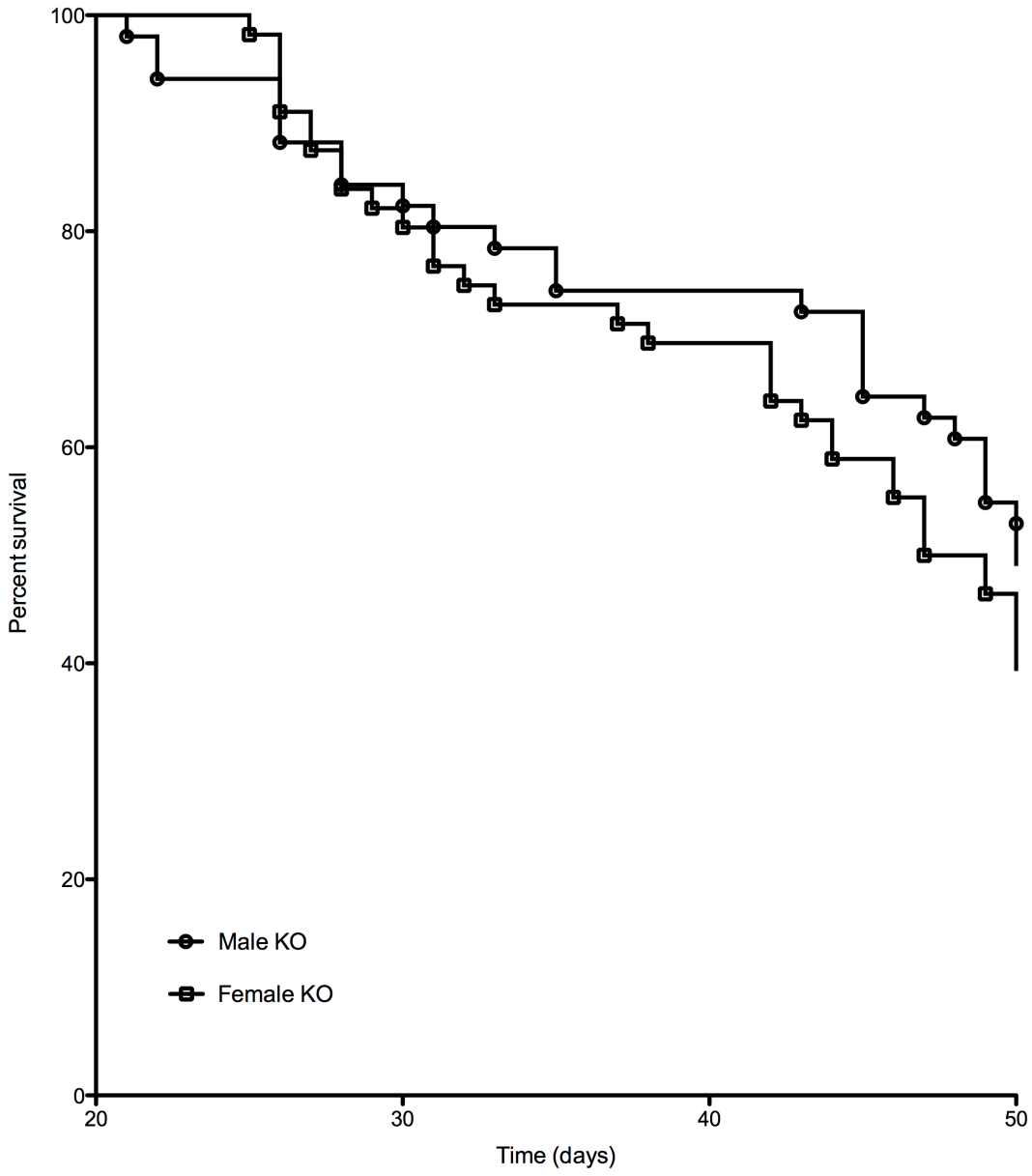

Figure S2: Comparison of survival of untreated male (n = 51) and female (n = 57) Pcmt1$^{-/-}$ (KO) mice from day 21 of weaning. Untreated animals that died prior to 50 days of age were plotted on a Kaplan-Meier curve. No significant difference was observed between sexes. P = 0.334 by the Gehan-Breslow-Wilcoxon test.

CHAPTER 3

Generation of a Novel *Lcmt1* Hypomorphic mouse model

ABSTRACT

Protein phosphatase 2A is a heterotrimeric protein composed of structural, catalytic, and targeting subunits responsible for controlling the phosphatase's function. PP2A assembly is governed by a variety of mechanisms, one of which is C-terminal methylation by the leucine carboxyl methyltransferase LCMT1. PP2A is nearly stoichiometrically methylated in the cytosol, and although some PP2A targeting subunits bind independently of methylation, methylation is required for the binding of others. To examine the role of this methylation reaction in mammalian tissues, we generated a mouse possessing a gene trap cassette in intron 1 of the *Lcmt1* gene. Rather than being a true knockout, these mice display reduced *Lcmt1* transcript and protein levels in a tissue-specific manner. LCMT1 activity and methylation of PP2A were reduced in a pattern similar to *Lcmt1* transcript expression, suggesting that LCMT1 is the only PP2A methyltransferase. These mice demonstrate a slight insulin resistance phenotype indicating a role for this methyltransferase in the governance of insulin signaling in peripheral tissue. Tissues from these animals will be vital to the identification of methylation-sensitive substrates of PP2A.

INTRODUCTION

Tightly controlled protein phosphorylation and dephosphorylation is vital to effective cellular function in mammalian cells[1]. The extent of phosphorylation at a given site is balanced by the opposing actions of protein kinases and protein phosphatases[2,3]. Over one third of the proteome is believed to be phosphorylated by the 540 murine (518 human) protein kinases at tyrosine, serine, and threonine residues [4,5,6]. These phosphorylation events overwhelmingly occur on serine and threonine residues with a ratio of approximately 1800:200:1 for pS:pT:pY modifications respectively[7]. Tyrosine phosphorylation, catalyzed by protein tyrosine kinases coded for by 90 genes in the human genome, is opposed by four families of protein tyrosine phosphatases encoded by 107 distinct genes with each phosphatase largely specific to a single substrate[8,9]. In striking contrast to the biological strategy involved with the removal of tyrosine phosphorylation, the catalysis of phosphate removal from the thousands of substrates of the 428 human protein serine/threonine kinases is catalyzed by only a handful of protein serine/threonine phosphatases[10]. The most prolific of these phosphatases, protein phosphatase 1 and protein phosphatase 2A (PP2A), catalyze the removal of over 90% of serine and threonine phosphorylation [10]. The disparity between the numbers of serine/threonine kinases and phosphatases has been reconciled by the broad substrate specificity of the catalytic subunits of phosphatases whose activity was thought to be governed mainly by proximity to phosphorylated substrates[11]. Advances in molecular biology and in vivo diagnostics have revealed, however, that phosphatase specificity is an extraordinarily tightly controlled process [12].

In the case of PP2A, the most abundant protein phosphatase[13], this regulation arises from multiple control points: posttranslational modifications, small molecule activators and inhibitors, the presence of regulatory subunits, as well as other types of protein-protein interactions[12]. A basic level of substrate control is provided by the composition of the heterotrimeric subunits composing PP2A [14]. PP2A exists in the cytosol primarily as a dimer consisting of the catalytic (C) and scaffolding (A) subunits, to which a variety of targeting or regulatory (B) subunits associate, altering the specificity of the phosphatase[15]. The complexity of PP2A composition arises from the enormity of distinct PP2A holoenzyme assemblies formed by proteins coded for by the two similar yet functionally non-redundant genes responsible for PP2A catalytic subunits[16,17], the two genes coding for non-redundant PP2A scaffolding subunits[18,19], and the four endogenous unrelated families of PP2A B subunits encoded by multiple genes with a variety of splice variants giving rise to at least 23 differential B subunits [12,14,20,21,22]. The vast array of subunits available for integration into PP2A holoenzymes are themselves regulated by spatial and temporal means as well as a strict regime of post-translational modifications regulating assembly[23,24].

Many of these modifications lie on the C-terminal “tail” of PP2A, a 6 amino acid sequence (TPDYFL) which is solvent exposed, unstructured, and yet highly conserved [12,13,25,26,27]. This tail contains 3 known post-translational modification sites: T304 phosphorylation, Y307 phosphorylation, and L309 methylation[12]. These modifications, responsible for opposing actions on the phosphatase, are often associated with deactivation (T304, Y307

phosphorylation)[28,29,30] and activation (L309 methylation) of PP2A[31,32,33]. Moreover, genetic experiments have revealed that phospho-mimetic PP2A mutants at Y307 are unable to be methylated, yet the same mutations at T304 allow methylation, suggesting likely interplay between these modifications[34,35]. Insight into PP2A methylation comes in the form of crystal structures of PP2A suggesting carboxyl-terminal charge neutralization as a result of methylation could be a causative factor in promoting phosphatase assembly and activation[26,27].

Carboxyl methylation of the C-terminus at L309 is a dynamic process catalyzed by the leucine carboxyl methyltransferase, LCMT1, and demethylation by the predominantly nuclear methylesterase PME-1 [34,36,37,38]. LCMT1 is a class 1 *S*-adenosylmethionine-dependent methyltransferase with PP2A as its only known substrate[39]. Although knockout of LCMT1 has been reported as lethal, hindering its study [40], extensive mutational analysis has revealed that L309 methylation is necessary for binding of the B α (PR55) subunit, and positively influences the binding of the B' family members[41], subunits thought to protect against oncogenic transformation[42]. On the other hand methylation appears to decrease the binding of polyoma middle T and α 4 binding [34,43,44,45]. Other B subunit families appear to bind irrespective of C-terminal methylation[35,46,47].

The complexity of the interaction between LCMT1 and PP2A has been demonstrated in several previous studies. Neither PP2A loss of function mutants, in which active site residues are mutated [34], nor wild-type PP2A that has been subject to small molecule or protein inhibitors [48,49], can be methylated by LCMT1. Additionally peptides mimicking the C-terminal tail of PP2A are not

substrates of LCMT1[38]. The crystal structure of LCMT1 suggests that other interactions of the methyltransferase with PP2A, in addition to L309, are necessary for methyltransferase activity[50]. Recently co-crystal structures of LCMT1 with PP2A shed light on this complex protein interaction, revealing not only surface interactions between the active site of the methyltransferase and the C-terminal tail of PP2A, but also an interaction between a domain of LCMT1 and the active site of PP2A[13]! These studies suggest an additional role for the methyltransferase in binding to and blocking the activity of free PP2Ac isoforms until they can be associated into appropriate holoenzyme trimers[13].

Significant evidence exists implicating a role for PP2A in onset of AD and progression of neurofibrillary tangles (NFTs) associated with the disease[51,52,53]. Peptide inhibitors of PP2A are seen to be increased in brains of AD patients[54] implicating loss of phosphatase function in the disease. Later it was discovered that PP2A was responsible both for directly catalyzing tau dephosphorylation as well as indirectly through regulation of GSK-3 β [55], one of the major tau kinases[56]. Of interest to this study, experiments in animal models revealed that addition of a methyltransferase inhibitor was capable of inducing the tau hyperphosphorylation indicative of the disease[57]. Further evidence suggesting a correlation between tau hyperphosphorylation and reduced methylation of PP2A arose from evidence suggesting high plasma homocysteine levels correlated with demethylated PP2A and AD[58], and that down-regulation of LCMT1 correlated with tau hyperphosphorylation[52]. Increased expression of LCMT1 in neuroblastoma cells has also been shown to alter actin assembly, promoting tau-positive processes and

inducing neuritogenesis[59]. In humans, however, despite evidence suggesting a role for LCMT1 and PP2A in AD, genetic variation of these enzymes in patient populations did not appear to alter late-onset AD[60].

In an attempt to further elucidate the role of *Lcmt1* and PP2A methylation in higher organisms, I characterized an *Lcmt1* hypomorphic mouse model. Here I describe in detail the biological as well as the phenotypic effects on a reduction in LCMT1. Although the loss of the *Lcmt1* gene previously was reported to be lethal [40], in this report we confirm the generation of animals homozygous for the presence of a gene trap cassette in the first intron of *Lcmt1*. Although the gene trap is homozygous, we are able to confirm both transcript as well as protein level expression, albeit at a reduced level. *Lcmt1* expression is affected in a tissue dependent manner, with the largest decreases seen in cardiac and skeletal muscle and smaller decreases seen in brain liver and kidneys. Decreases in PP2A methylation as well as concomitant increases in demethylation were observed in these hypomorphic mice.

METHODS

Animal Husbandry

Mice were kept on a 12-hour light/dark cycle and allowed *ad libitum* access to water and NIH-31 7013 chow (18% protein, 6% fat, 5% fiber, Harlan Teklad, Madison, WI). Experimental animals were housed in same-sex cages with two or three other mice. All protocols were approved by the UCLA Animal Research Committee (Protocol 1993-109-62).

Lcmt1$^{-/-}$ Mouse Generation

Lcmt1$^{+/-}$ mice were generated through insertion of a gene trap cassette in the 1st intron of *Lcmt1* by the International Gene Trap Consortium[61]. Animals were kept on a 12hr light/dark cycle and fed modified NIH diet ad libitum. Animals used in this study are the result of at least 3 back-crossings with C57BL/6 animals.

Genotyping

The site of gene trap cassette insertion was localized through consecutive PCR amplification to intron 1 of *Lcmt1*. Primers were subsequently designed flanking this site of insertion (Forward: CCTTTCTGGGTGAGCTCTTG, Reverse: AGATGAGCATCGGAATCTGG; 1899 nucleotide product) as well as primers lying within the gene trap cassette itself (Forward: ATTATTTGCCCGATGTACGC, Reverse: AGATGAGCATCGGAATCTGG; 524 nucleotide product).

Glucose Tolerance & Glucose Stimulated Insulin Secretion Test

Animals were fasted overnight for 15 hours by placement in fresh cages prior to beginning this experiment. Blood glucose measurements were recorded with an Accucheck Active blood glucose meter (Roche, Mannheim, Germany) and Accucheck Active glucose test strips (Roche, Mannheim, Germany) requiring approximately 1-2 μ L of blood per measurement. The tail vein of each animal was nicked with a fresh scalpel and blood glucose measurements as well as a blood samples were collected. Blood sample were collected into 50 μL of PBS-EDTA anti-coagulation buffer (10 mM sodium phosphate, 2 mg/mL ethylenediaminetetraacetic acid, 137.9 mM sodium chloride) and immediately placed on ice post-collection for the duration of the experiment. Following this initial measurement, animals were subsequently orally administered a bolus of glucose corresponding to 2 g glucose per kilogram of body weight. Blood samples were collected alongside blood glucose measurements at 5, 15, 30, and 60 minutes following glucose load and an additional glucose measurement was recorded 120 minutes post glucose load. Blood samples were centrifuged at 4 °C and 1,000 x g for 10 minutes to pellet cells and the plasma insulin was measured using a Rat/Mouse Insulin ELISA kit (Catalog # EZRMI-13K, EMD Millipore, Billerica, MA) according to the manufacturer's published instructions.

RNA Isolation, cDNA Generation & qPCR

Prior to and throughout this protocol all tools and bench space were thoroughly cleaned using RNase Away (Fischer, Torrance, CA). Animals were sacrificed by

carbon dioxide asphyxiation and tissues were dissected and immediately frozen in liquid nitrogen. Approximately 0.1 g of each tissue was then homogenized on ice in 1 mL of tri-reagent (Molecular Research Center, Cincinnati, OH), a commercially available guanidinium thiocyanate-phenol-chloroform mixture[62], using a Polytron homogenizer equipped with a PTA-7 generator. Samples were pulsed seven times for 30 seconds each pulse with one minute between pulses to prevent heating of the sample. Samples were subsequently centrifuged at 20,000 x *g* for 10 min to remove fat and high molecular weight DNA. A volume of chloroform equivalent to 1/5 of the volume of tri-reagent used was subsequently added and the sample was subsequently shaken, and further centrifuged at 20,000 x *g*. The aqueous phase was saved and added to an equivalent volume of isopropanol. The sample was then centrifuged again for 7 minutes at 20,000 x *g*, decanted, further washed with 70% ethanol, and centrifuged again for 5 minutes at 20,000 x *g*. After decanting the ethanol, the RNA pellet was dried and resuspended in 20 µL of RNase-free water. The sample was checked for purity spectrophotometrically by assessing the absorbance ratio at 260nm/280nm, expecting a near 2:1 ratio for pure RNA, and for degradation by separation on an agarose gel, visualizing the RNA with ethidium bromide and assessing the bands corresponding to 28S & 18S rRNA. The RNA pellet was treated with a TURBO DNA-free Kit (Applied Biosystems, Carlsbad, CA) to remove contaminating DNA as per manufacturers instructions. cDNA was generated using a RETROscript kit (Applied Biosystems) as per manufacturer's instructions. cDNA was plated in a 384 well plate using primers on *Lcmt1* exons 1 and 2 as well as primers on *Lcmt1* exons 2 and 3 as well as primers on the B2m gene coding beta-2

microglobulin as a control (forward: TGGTGCTTGTCTCACTGACC; reverse: TATGTTCGGCTTCCCATTCT). qPCR was performed on a 7900 HT instrument (Applied Biosystems) and data was analyzed using the $2^{-\Delta\Delta CT}$ method of quantitation [63].

In Vitro PP2A Methylation Assay

The content of methyl-esterified PP2A in soluble mouse brain proteins was determined by an assay similar to that used previously [64]. Briefly, endogenous leucine carboxyl methyltransferase was used as a reagent to catalyze the transfer of ^{3}H-methyl groups from *S*-adenosyl-L-[*methyl*-^{3}H]methionine to the endogenous target. After hydrolysis of the methyl esters formed, ^{3}H-methanol was quantified using a vapor diffusion assay. Tissues were extracted and homogenized using a Polytron homogenizer, 7 pulses of 30-seconds with 1 minute on ice between pulses, in three volume equivalents of sucrose buffer (three mL of buffer/g wet weight tissue) with phosphatase (HALT, Thermo-Pierce, Rockford, IL), and protease inhibitors (Complete, Roche, Mannheim, Germany), followed by centrifugation at 20,000 x *g*. This supernatant was used throughout the remainder of this method. Protein concentration was determined via the Lowry method after protein precipitation with trichloroacetic acid [65]. The *in vitro* methylation assay was performed by adding 2.5 µL of *S*-adenosyl-L-[*methyl*-^{3}H]methionine (1 mCi/1.8 mL; 78mCi/mmol; PerkinElmer) to 100 µg of protein extract in a 100mM pH 7.4 Tris buffer in a total volume of 25 µL. This was incubated at 37 °C for 1 h. This reaction was quenched by the addition of 2X SLB (100 mM Tris-HCl, pH 6.8, 200 mM β-

mercaptoethanol, 4% SDS, 0.1% bromophenol blue, 20% glycerol) and subsequent heating to 100 ° C for 5 minutes. These extracts were then loaded onto 4-12% RunBlue SDS gels (Expedeon, San Diego, CA) and separated by electrophoresis alongside molecular weight markers. The gel was then stained and the region corresponding to proteins of 31-41 kDa was cut into three slices. These slices were added to microfuge tubes containing 100 µL of 2 M NaOH to release the carboxyl methyl esters as methanol. This reaction was incubated in sealed scintillation tubes containing 5 mL of scintillation fluid (Safety-Solve, RPI, Mount Prospect, IL) overnight and counted using a liquid scintillation counter. All samples were assayed in triplicate and the lane corresponding to the molecular weight ladder was cut and counted as a background negative control.

Western Blotting

Mice were fasted overnight and euthanized in a CO_2 chamber prior to surgical tissue removal. Tissues were dissected, weighed, and added to 3 mL/g of sucrose buffer (250 mM sucrose, 10 mM Tris base, 1 mM EDTA, pH 7.4) with phosphatase (HALT, Thermo-Pierce, Rockford, IL) and protease inhibitors (Complete, Roche, Mannheim, Germany) and homogenized using a Polytron homogenizer with a PTA-7 generator. Homogenization was performed using seven pulses of 30 seconds with one minute on ice between pulses. Extracts were then centrifuged at 20,000 RCF and the supernatants were stored at -80 °C for utilization in further experiments. The protein concentration of the soluble extracts was determined after trichloroacetic acid precipitation by the Lowry method [65]. Aliquots containing 20 µg of protein

were added to 10 µl of a 2X SDS-sample loading buffer (100 mM Tris-HCl, pH 6.8, 200 mM β-mercaptoethanol, 4% SDS, 0.1% bromophenol blue, 20% glycerol) and then brought to a final volume of 20 µl with water and heated for 5 min at 100 °C. The samples were then loaded into lanes of twelve-well, 10 cm by 10 cm, 4-12% RunBlue SDS gels (Expedeon, San Diego, CA) in an Invitrogen XCell SureLock Mini-Cell apparatus along with parallel lanes of rainbow molecular weight markers (RPN-800V, GE Healthcare, Buckinghamshire, England). Electrophoresis was performed at 180 V for 1 h. Proteins were transferred from gels to PVDF membranes (Amersham Hybond-P, GE Healthcare) by electrophoretic transfer at 25 V for 3 h using the Invitrogen Blot Module and NuPAGE transfer buffer (Invitrogen, Grand Island, NY). Membranes were blocked overnight using 5% bovine serum albumin and then probed with the primary antibodies diluted in TBS-T buffer as described in Table 1**.** After the blot was washed in TBS-T buffer, it was incubated with horseradish peroxidase-labeled secondary antibodies as described in Table 1. Peroxidase activity was visualized after treating the blot with ECL Prime Chemiluminescent Agent (GE Healthcare) and detected on Hyblot CL film (Denville, Metuchen, NJ). Exposure times were optimized to allow linear responses. Film densitometry was performed using ImageJ densitometry software.

RESULTS & DISCUSSION

Creation of *Lcmt1* hypomorphic mouse model

A gene trap cassette localized to intron 1 of *Lcmt1* by 5'-RACE techniques was reported by the BayGenomics gene trapping consortium[61] in an attempt to generate *Lcmt1*$^{+/-}$ mice. Utilizing a PCR-based screen detecting the presence of the gene trap cassette, forward primers spanning every 1000 nucleotides of intron 1 were utilized in conjunction with a reverse primer on the gene trap cassette to localize the site of gene-trap insertion. Sequencing revealed the gene trap cassette was in fact localized into intron 1 of *Lcmt1*, 19455 nucleotides past exon 1, or at position 19729 of the gene (counting from the transcriptional start site and the first base of the initiating ATG codon designated as position 168). Sequencing additionally revealed the insertion of 3 exogenous nucleotides at the 5' end of the insertion site as well as the truncation of 194 nucleotides from the 5' end of the β-Geo gene trap vector. Animal genotyping was accomplished using primers flanking the insertion site that only amplify in absence of gene trap, as well as primers binding wholly within the β-Geo gene trap cassette that only amplify in presence of gene trap. This genotyping strategy suggested the creation of genetic knockout animals (Figure 1). Monitoring the birth ratio from heterozygotic parents revealed that these animals are born in a non-Mendelian ratio (Figure 2), suggesting *Lcmt1*$^{-/-}$ animal loss during pregnancy. Sacrifice and dissection of pregnant heterozygotic

mothers at 9.5 days post-coitus revealed a significant number of resorbing embryos; however, it is unclear whether these represented *Lcmt1*$^{-/-}$ pups (data not shown).

Sacrifice and tissue analysis of *Lcmt1*$^{-/-}$ animals revealed distinctly lower transcript levels of *Lcmt1* in *Lcmt1*$^{-/-}$ animals, but not complete ablation as should be expected with this gene trap cassette (Figure 3A) suggesting *Lcmt1*$^{-/-}$ animals are not true "knockouts", but instead "knockdowns". Interestingly, the relative decrease in *Lcmt1* transcript appeared to be tissue specific with kidney having the highest relative *Lcmt1* expression compared to wild-type animals at 58%, followed by brain at 48%, liver at 37%, heart at 6% and muscle at just 3% that of wild-type tissues (Figure 3B).

Furthermore, by comparing the results of qPCR experiments using primers for exons 2 and 3 with qPCR using primers for exons 1 and 2, we determined that an alternative start site was not being utilized by *Lcmt1* as relative transcript levels from each primer set were similar (data not shown). An alternative start site (non-exon 1), would result in exons 2/3 transcript levels being significantly higher than those from exons 1/2.

In order to determine whether these *Lcmt1*$^{-/-}$ animals were indeed able to express full length LCMT1 polypeptide we next Western blotted tissues against LCMT1. Western blotting revealed that LCMT1 protein was decreased in a tissue specific fashion similar to *Lcmt1* transcript levels. The largest decreases in expression were seen in heart and muscle tissue with *Lcmt1*$^{-/-}$ animals having LCMT1 protein levels of 2% and 13% those of wild type respectively (Figure 4). Relative LCMT1 protein level was slightly higher in the kidney at 16% that of wild

type, 22% in the liver, and the highest in the brain at 46% that of wild type. In wild-type animals LCMT1 protein was most abundant, followed by muscle, kidney, liver, and with the lowest expression, heart tissue.

Lcmt1$^{-/-}$ animals display decreased methylation of PP2A

A decrease in LCMT1 did not appear to affect global PP2A levels, but did appear to decrease methylation of PP2A (Figure 5). Analysis of steady state PP2A methylation levels via Western blotting indicated that methylation of PP2A in *Lcmt1*$^{-/-}$ animals decreased in a tissue specific manner in all tissues assayed (Figure 5). The largest decreases in PP2A methylation coincided with the largest decreases in *Lcmt1*, in muscle and heart tissue. *Lcmt1*$^{+/+}$ muscle tissue was found to have an average steady state methylation level of 95%, which was found to decrease to an average of 50% in *Lcmt1*$^{-/-}$ animals. In heart tissue, which was found to have steady state methylation of 95% we observed a drop to 66% in *Lcmt1*$^{-/-}$ animals. Substantial decreases in PP2A standard state methylation were also observed in the brain (74% and 55%) as well as the Liver (60% and 53%) in *Lcmt1*$^{+/+}$ and *Lcmt1*$^{-/-}$ animals respectively.

A methyltransferase assay utilizing endogenous LCMT1 revealed a similar decrease in PP2A methylation (Figure 6). LCMT1 activity was seen to decrease substantially in *Lcmt1*$^{-/-}$ animals with the largest decreases of 78% and 65% observed in liver and muscle. Comparatively brain exhibited a 52% decrease in methylation while heart tissue exhibited a 25% decrease. The average 45%

decrease observed in kidney tissue represented values with considerable deviation from each other and did not appear statistically significant.

Lcmt1$^{-/-}$ animals display increased insulin resistance

Due to the involvement of PP2A in halting kinase cascades involved in growth and cell signaling ,we next looked at how a decrease in PP2A methylation could affect insulin signaling in *Lcmt1*$^{-/-}$ animals. Animals were fasted overnight for 15 hours and subsequently orally administered a bolus of glucose corresponding to 2 g/kg of body weight. Following glucose load, blood samples were immediately assayed for blood sugar and collected for insulin ELISA analysis. *Lcmt1*$^{-/-}$ animals displayed decreased glucose tolerance (Figure 7A), while at the same time secreting more insulin per glucose load (Figure 7B), a phenotype often associated with insulin resistance and thought to be involved in the etiology of type-II diabetes mellitus[66,67,68].

Pcmt1$^{-/-}$ animals display increased PP2A methylation

An additional carboxyl methyltransferase, the protein L-isoaspartyl methyltransferase, PCMT1, is one of the most prolific methyltransferases within the cell, and loss of this prolific enzyme in a *Pcmt1*$^{-/-}$ mouse model has been shown to increase the cellular concentration of AdoMet and decreased AdoHcy [69]. Although PCMT1 has been implicated as an aging repair enzyme[70], *Pcmt1*$^{-/-}$ animals display phenotypes indicative of dysregulated signaling pathways, such as increased brain growth, decreased body size and early death after ~45 days of age due to tonic

clonic seizures[71,72,73]. Indeed dysregulation and constitutive activation of insulin signaling has been reported in the brains of these animals[73,74]. Although recent research suggests PCMT1 may play a role in the regulation of signal cascades [75,76], the signaling dysregulation observed in *Pcmt1*$^{-/-}$ animals may be obfuscated by increased LCMT1 activity due to the increased cytosolic AdoMet/AdoHcy ratio in these animals. Quantitative Western blotting of *Pcmt1*$^{-/-}$ and *Pcmt1*$^{+/+}$ animals for demethylated PP2A revealed an increase in PP2A demethylation in *Pcmt1*$^{-/-}$ mice without an observed increase in total PP2A (Figure 8), suggesting PP2A methylation is increased in this model. Altered methylation of PP2A, and a concomitant alteration in PP2A methylation dependent targeting could be responsible for the signaling defects observed in *Pcmt1*$^{-/-}$ animals, a possibility reinforced by experiments demonstrating that the major insulin signaling kinases are known cytosolic targets of PP2A[77,78,79], with Akt targeted by the major methylation dependent subunit[80].

FIGURES

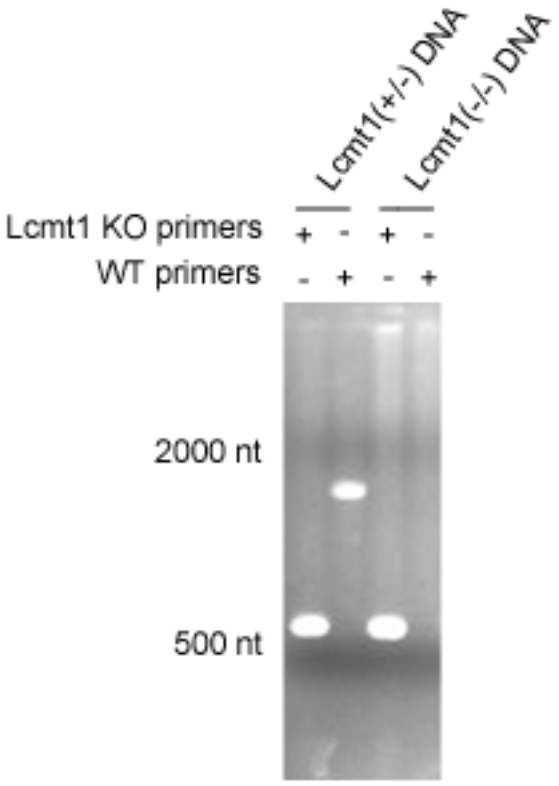

Figure 1: PCR based strategy for genotyping *Lcmt1*$^{-/-}$ animals. Primers flanking the gene trap cassette amplify a 1899 nucleotide product (WT primer) and primers inside the gene trap cassette amplifying a 524 nucleotide product were utilized in conjunction with *Lcmt1*$^{+/-}$ and *Lcmt1* $^{-/-}$ digested tail tips to confirm genotypes.

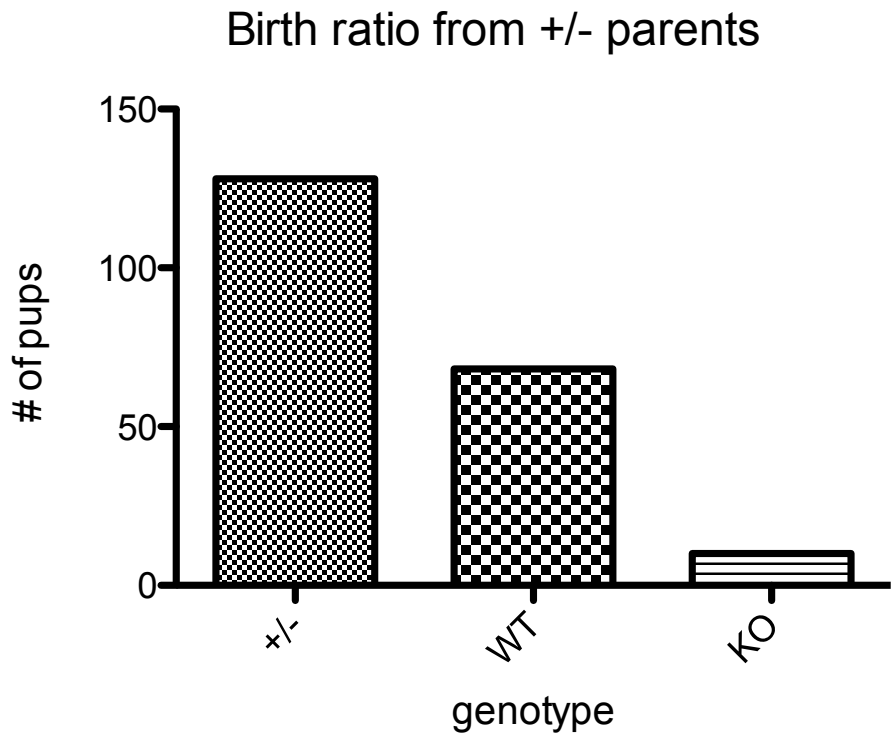

Figure 2: *Lcmt1*$^{-/-}$ animals born to heterozygotic *Lcmt1*$^{+/-}$ parents are birthed in a non-Mendelian ratio. Quantitation of all animals born to *Lcmt1*$^{+/-}$ parents. Pups were genotyped at 18 days of age. Pups were counted 1-2 days after birth and pup losses between birth and genotyping at day 18 were insignificant.

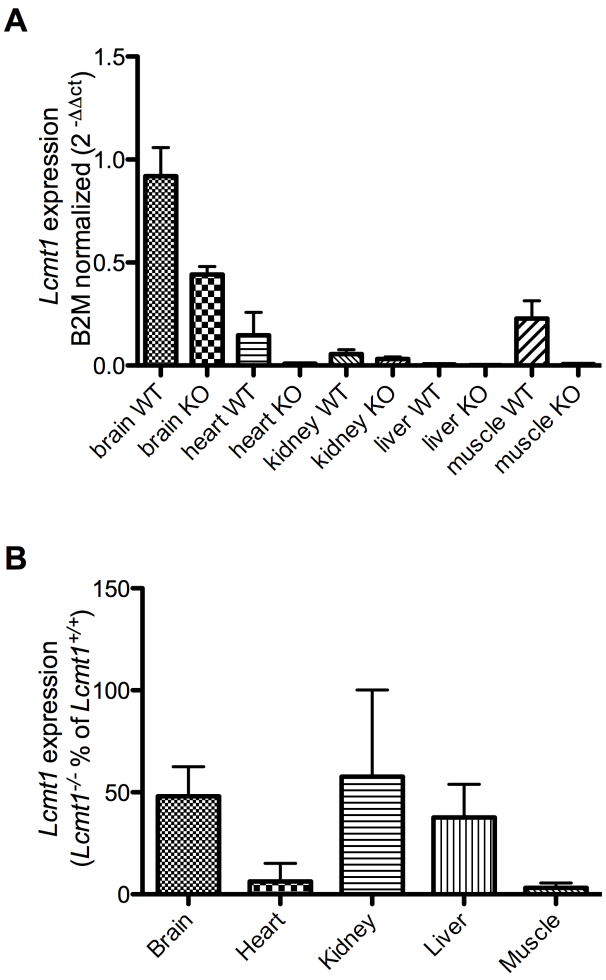

Figure 3: Transcript level quantitation of hypomorphic *Lcmt1* mice. Panel A: Representation of average *Lcmt1* transcript levels from five different tissue types in relation to beta-2 microglobulin. Error bars represent standard deviation. All *Lcmt1* hypomorphic mice displayed significantly decreased transcript as determined by Student's t-test. Panel B: Relative *Lcmt1* transcript levels in $Lcmt1^{-/-}$ mice as compared to WT counterparts. Error bars represent standard deviation.

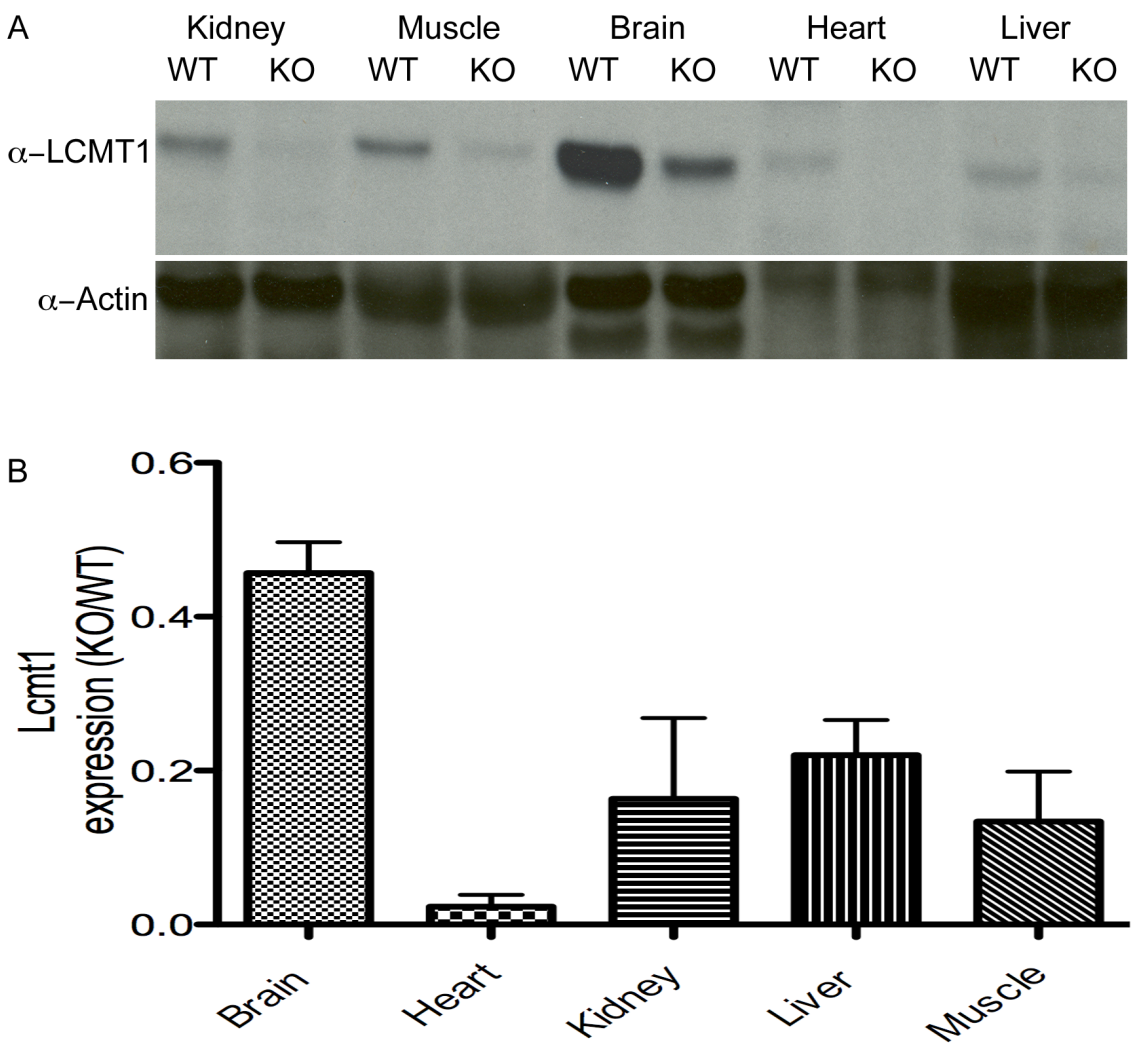

Figure 4: Quantitation of the reduction of LCMT1 expression in various tissue types in *Lcmt1*$^{-/-}$ animals compared to wild-type controls. Panel A represents Western blotting against *Lcmt1*. All five tissue types were blotted from three wild-type and three *Lcmt*$^{-/-}$ animals. β-actin was used as a loading control. All samples were run on the sale gel, however a ladder was loaded between muscle and brain samples which has been omitted from this figure. In Panel B densitometry based relative quantitation of α-LCMT1 Western blotting as compared to β-actin controls.

Error bars represent standard deviation and n = 3 for each tissue type and each genotype.

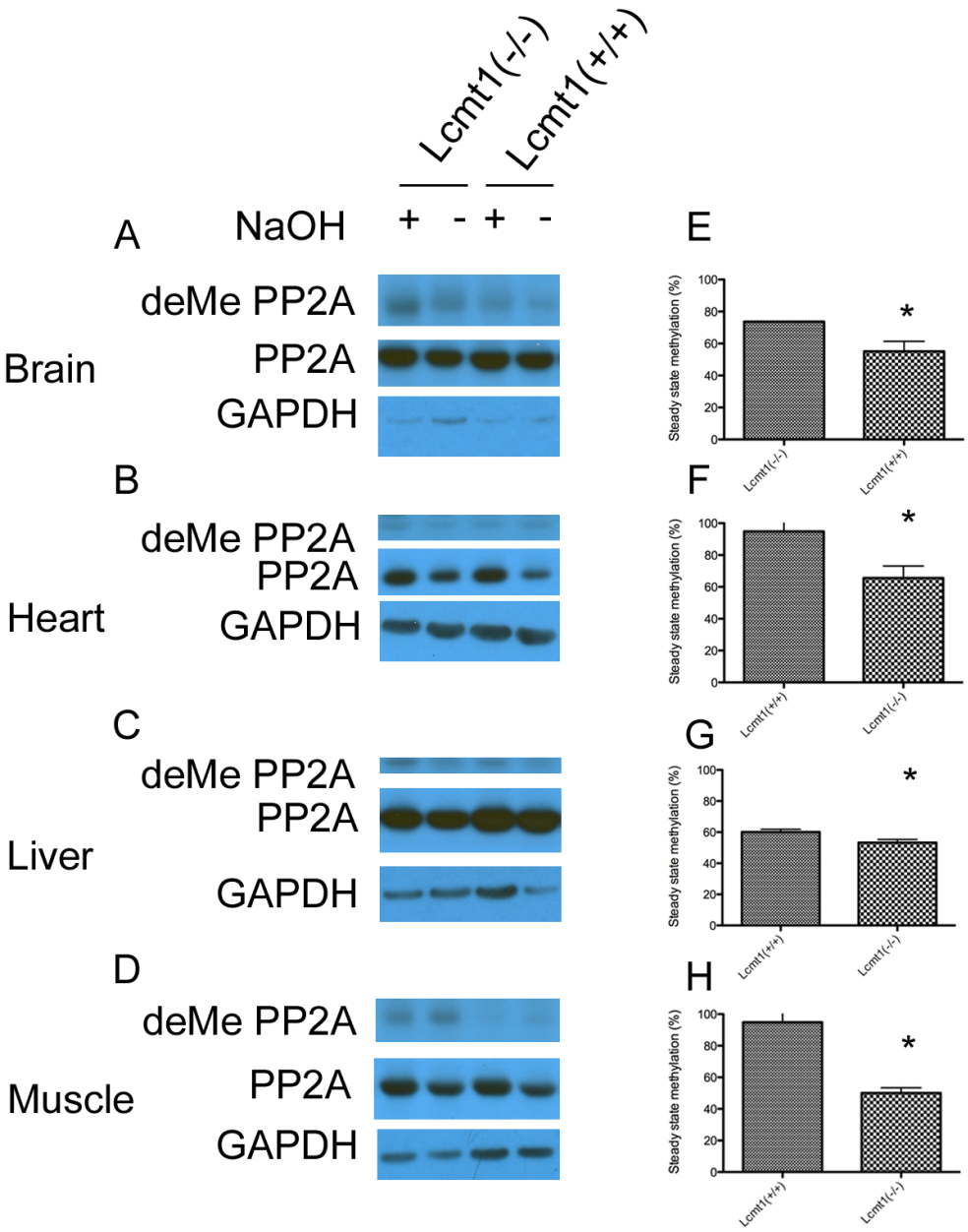

Figure 5: Quantitation of the steady state methylation of PP2A in multiple tissues of *Lcmt1*$^{-/-}$ and *Lcmt1*$^{+/+}$ mice. Panel A-D: Samples were treated either with 0.1M NaOH for 1 minute to cleave methyl esters followed by 0.1 M HCl and 0.5 M Tris to neutralize the solution (NaOH +), or a previously neutralized buffer containing the above mentioned solutions as a control (NaOH -). Samples were then

run on SDS-PAGE, blotted, and probed against demethylated PP2A C, total PP2A C and GAPDH as a loading control. The percent demethylated was calculated using the base treated sample as a completely demethylated standard from which the steady state demethylation could be subtracted to generate the steady state methylation levels outlined by Yu et al. [34]. Panels E-H represent the mean +/- SD of 4 *Lcmt1*$^{-/-}$ and 4 *Lcmt1*$^{+/+}$ samples, of which one representative sample is shown in Panel A-D. Statistical significance $p<0.05$ utilized the Student's t-test is denoted by *.

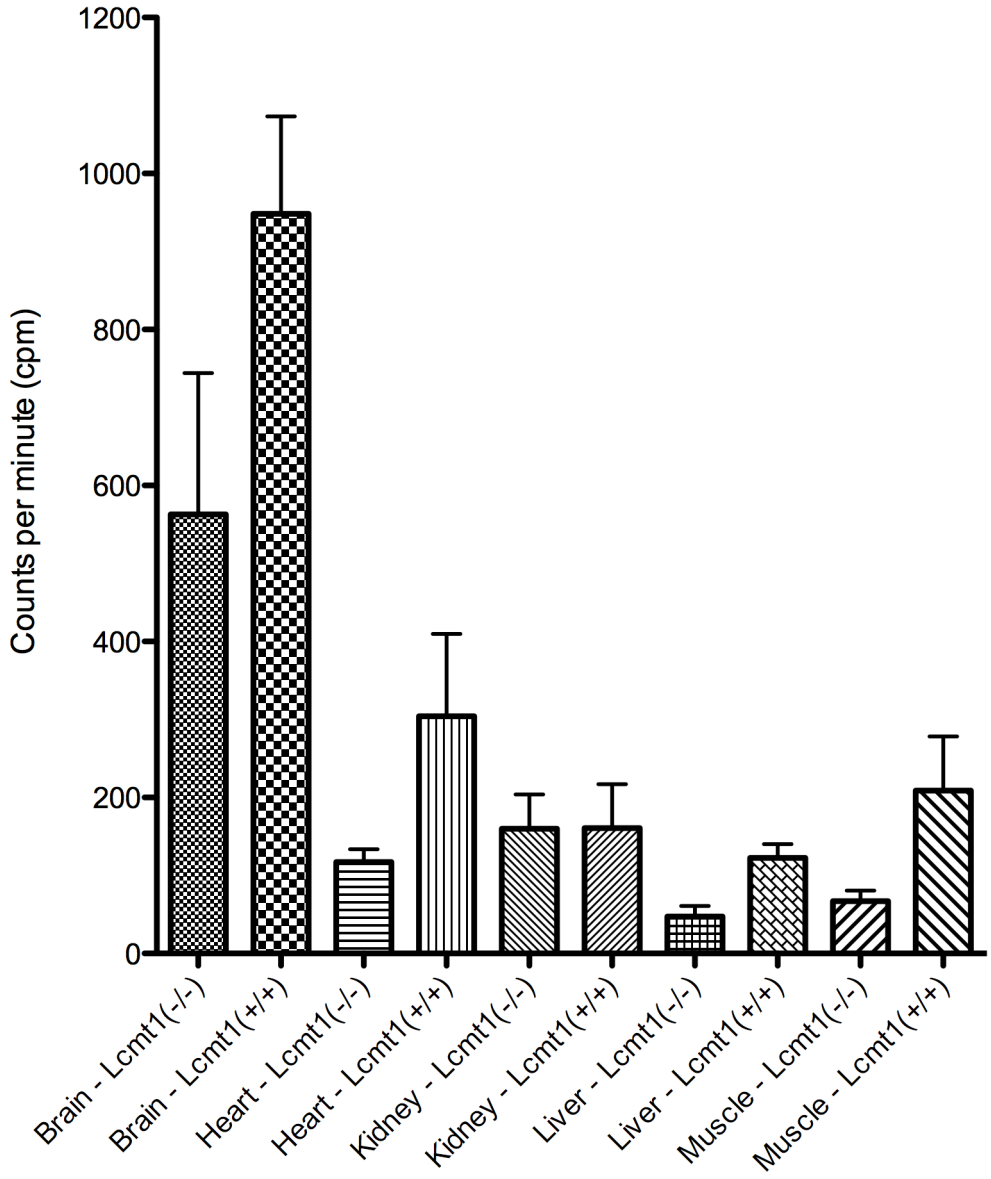

Figure 6: Quantification of *in vitro* PP2A methylation. Extracts from *Lcmt1*$^{-/-}$ and *Lcmt1*$^{+/+}$ animals were incubated with [^{3}H]AdoMet as described in Methods. Methyl esters corresponding to proteins between 31 kDa and 41 kDa were quantified and counts corresponding to PP2A methylation were plotted in the above graph. Each column represents the mean of three independent experiments utilizing tissue from

three individual mice each of which was repeated three times. Error bars represent the standard deviation.

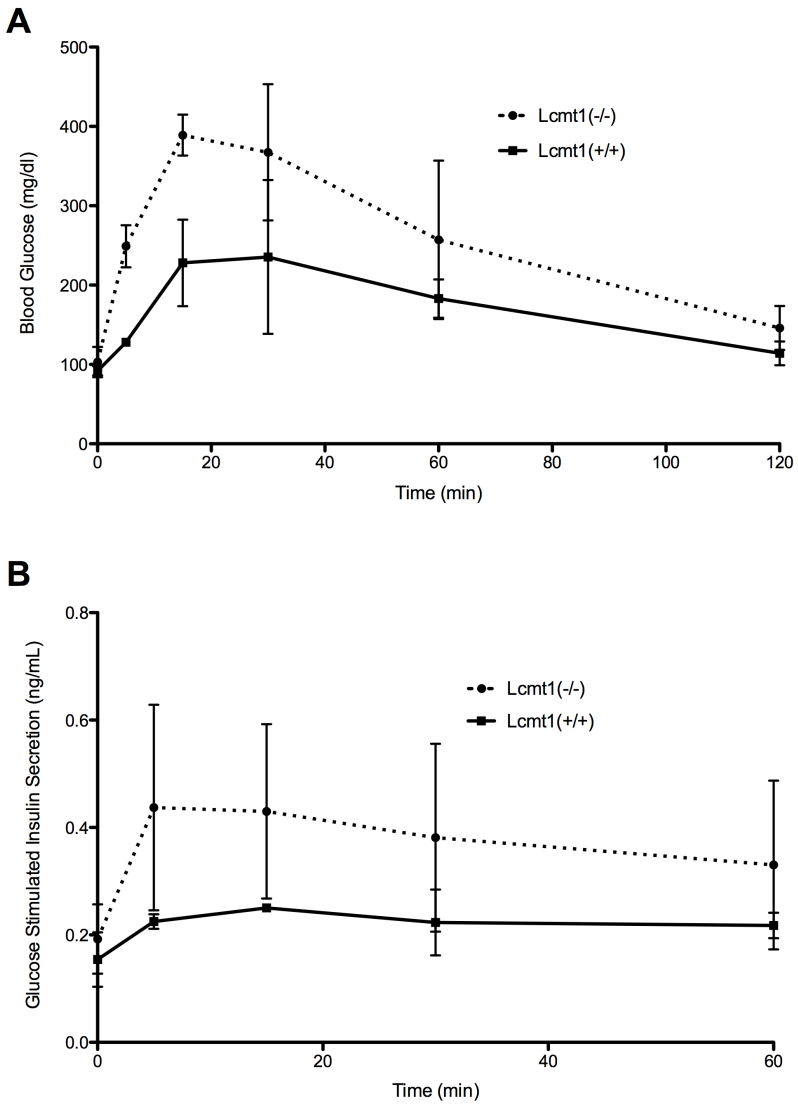

Figure 7: *Lcmt1*$^{-/-}$ animals appear to have decreased glucose tolerance and increased glucose stimulated insulin secretion. Mice were fasted overnight and administered 2 grams of glucose per kg of body mass, following this bolus of glucose blood samples were collected on the indicated time points and assayed for blood glucose, Panel A, and plasma insulin levels, Panel B.

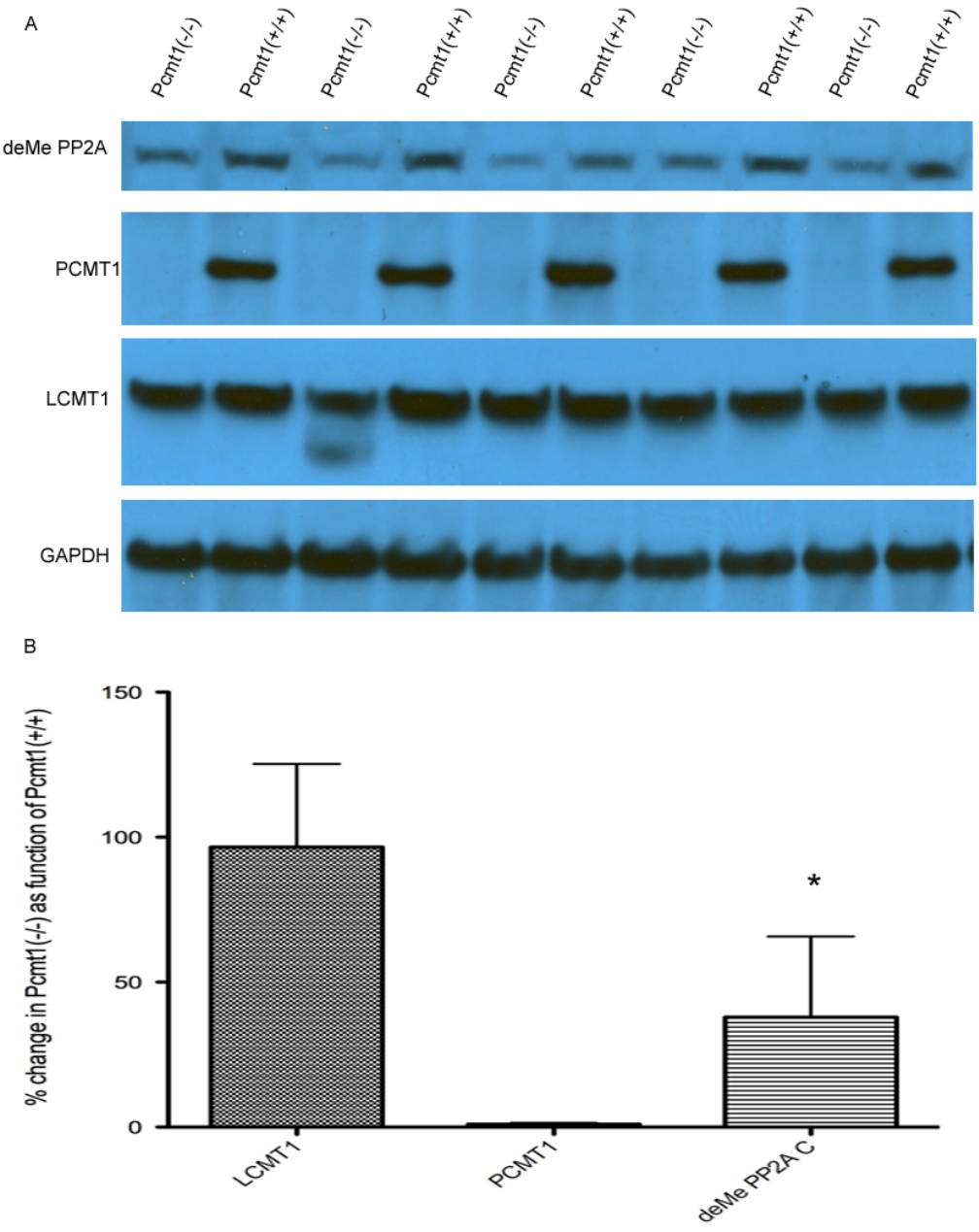

Figure 8: Demethylation of PP2A C is increased in *Pcmt1*$^{-/-}$ animals without a concomitant increase in LCMT1. Panel A depicts Western blots in brain tissue from *Pcmt1*$^{-/-}$ and *Pcmt1*$^{+/+}$ animals displaying increased demethylation of PP2A. In Panel B blots were quantitated using densitometry software and percent changes

were assessed. Error bars represent standard deviation, n = 5 for each genotype, and statistical significance as assessed by Student's t-test is represented by *.

Target	Name	Source	Dilution	Incubation time	Temperature	Polypeptide size
PP2A	α-PP2A, clone 1D6, 05-421	Millipore	1:10,000	1 h	25°C	36 kDa
deMe-PP2A	α-PP2A demethylated, clone 4B7, 05-577	Millipore	1:100	15 h	25°C	36 kDa
Me-PP2A	α-methyl-PP2A, clone 2A10, 04-1479	Millipore	1:100	15 h	25°C	36 kDa
LCMT1	α -LCMT1 (4A4) (ab77754)	Abcam	1:10,000	1 h	25°C	38 kDa
PCMT1	α-PCMT1 cultured in rabbit (non-commercial)	Gift from Dr. Mark Mamula	1:1,000	1 h	4°C	25 kDa
GAPDH	GAPDH (14C10)	Cell Signaling	1:40,000	1 h	25°C	37 kDa
Actin	α-Actin cultured in rabbit (non-commercial)	Gift from Dr. Emil Reisler	1:40,000	1 h	25°C	45 kDa
α-mouse	A-Mouse IgG, HRP secondary #7076	Cell Signaling	1:100,000	1 h	25°C	NA
α -rabbit	α-Rb Goat HRP conjugated secondary (ab721))	Abcam	1:100,000	1 h	25°C	NA

Table 1: Source of antibodies and immunoblotting protocols

REFERENCES

1. Dissmeyer N, Schnittger A (2011) The age of protein kinases. Methods in molecular biology 779: 7-52.
2. Kurosawa M (1994) Phosphorylation and dephosphorylation of protein in regulating cellular function. Journal of pharmacological and toxicological methods 31: 135-139.
3. Stock JB, Ninfa AJ, Stock AM (1989) Protein phosphorylation and regulation of adaptive responses in bacteria. Microbiological reviews 53: 450-490.
4. Caenepeel S, Charydczak G, Sudarsanam S, Hunter T, Manning G (2004) The mouse kinome: discovery and comparative genomics of all mouse protein kinases. Proceedings of the National Academy of Sciences of the United States of America 101: 11707-11712.
5. Ahn NG, Resing KA (2001) Toward the phosphoproteome. Nature biotechnology 19: 317-318.
6. Hubbard MJ, Cohen P (1993) On target with a new mechanism for the regulation of protein phosphorylation. Trends in biochemical sciences 18: 172-177.
7. Mann M, Ong SE, Gronborg M, Steen H, Jensen ON, Pandey A (2002) Analysis of protein phosphorylation using mass spectrometry: deciphering the phosphoproteome. Trends in biotechnology 20: 261-268.
8. Alonso A, Sasin J, Bottini N, Friedberg I, Osterman A, Godzik A, Hunter T, Dixon J, Mustelin T (2004) Protein tyrosine phosphatases in the human genome. Cell 117: 699-711.

9. Stoker AW (2005) Protein tyrosine phosphatases and signalling. The Journal of endocrinology 185: 19-33.

10. Shi Y (2009) Serine/threonine phosphatases: mechanism through structure. Cell 139: 468-484.

11. Hardie DG (1990) Roles of protein kinases and phosphatases in signal transduction. Symposia of the Society for Experimental Biology 44: 241-255.

12. Janssens V, Longin S, Goris J (2008) PP2A holoenzyme assembly: in cauda venenum (the sting is in the tail). Trends in biochemical sciences 33: 113-121.

13. Stanevich V, Jiang L, Satyshur KA, Li Y, Jeffrey PD, Li Z, Menden P, Semmelhack MF, Xing Y (2011) The structural basis for tight control of PP2A methylation and function by LCMT-1. Molecular cell 41: 331-342.

14. Sents W, Ivanova E, Lambrecht C, Haesen D, Janssens V (2012) The biogenesis of active protein phosphatase 2A holoenzymes: a tightly regulated process creating phosphatase specificity. The FEBS journal.

15. Mayer-Jaekel RE, Hemmings BA (1994) Protein phosphatase 2A--a 'menage a trois'. Trends in cell biology 4: 287-291.

16. Gotz J, Probst A, Ehler E, Hemmings B, Kues W (1998) Delayed embryonic lethality in mice lacking protein phosphatase 2A catalytic subunit Calpha. Proceedings of the National Academy of Sciences of the United States of America 95: 12370-12375.

17. Gu P, Qi X, Zhou Y, Wang Y, Gao X (2012) Generation of Ppp2Ca and Ppp2Cb conditional null alleles in mouse. Genesis 50: 429-436.

18. Ruediger R, Ruiz J, Walter G (2011) Human cancer-associated mutations in the Aalpha subunit of protein phosphatase 2A increase lung cancer incidence in Aalpha knock-in and knockout mice. Molecular and cellular biology 31: 3832-3844.

19. Sablina AA, Chen W, Arroyo JD, Corral L, Hector M, Bulmer SE, DeCaprio JA, Hahn WC (2007) The tumor suppressor PP2A Abeta regulates the RalA GTPase. Cell 129: 969-982.

20. Dagda RK, Zaucha JA, Wadzinski BE, Strack S (2003) A developmentally regulated, neuron-specific splice variant of the variable subunit Bbeta targets protein phosphatase 2A to mitochondria and modulates apoptosis. The Journal of biological chemistry 278: 24976-24985.

21. Zwaenepoel K, Louis JV, Goris J, Janssens V (2008) Diversity in genomic organisation, developmental regulation and distribution of the murine PR72/B" subunits of protein phosphatase 2A. BMC genomics 9: 393.

22. Jin Z, Shi J, Saraf A, Mei W, Zhu GZ, Strack S, Yang J (2009) The 48-kDa alternative translation isoform of PP2A:B56epsilon is required for Wnt signaling during midbrain-hindbrain boundary formation. The Journal of biological chemistry 284: 7190-7200.

23. Gentry MS, Hallberg RL (2002) Localization of Saccharomyces cerevisiae protein phosphatase 2A subunits throughout mitotic cell cycle. Molecular biology of the cell 13: 3477-3492.

24. Longin S, Zwaenepoel K, Martens E, Louis JV, Rondelez E, Goris J, Janssens V (2008) Spatial control of protein phosphatase 2A (de)methylation. Experimental cell research 314: 68-81.

25. Shi Y (2009) Assembly and structure of protein phosphatase 2A. Science in China Series C, Life sciences / Chinese Academy of Sciences 52: 135-146.

26. Xu Y, Xing Y, Chen Y, Chao Y, Lin Z, Fan E, Yu JW, Strack S, Jeffrey PD, Shi Y (2006) Structure of the protein phosphatase 2A holoenzyme. Cell 127: 1239-1251.

27. Cho US, Xu W (2007) Crystal structure of a protein phosphatase 2A heterotrimeric holoenzyme. Nature 445: 53-57.

28. Guo H, Damuni Z (1993) Autophosphorylation-activated protein kinase phosphorylates and inactivates protein phosphatase 2A. Proceedings of the National Academy of Sciences of the United States of America 90: 2500-2504.

29. Guo H, Reddy SA, Damuni Z (1993) Purification and characterization of an autophosphorylation-activated protein serine threonine kinase that phosphorylates and inactivates protein phosphatase 2A. The Journal of biological chemistry 268: 11193-11198.

30. Chen J, Martin BL, Brautigan DL (1992) Regulation of protein serine-threonine phosphatase type-2A by tyrosine phosphorylation. Science 257: 1261-1264.

31. Fellner T, Lackner DH, Hombauer H, Piribauer P, Mudrak I, Zaragoza K, Juno C, Ogris E (2003) A novel and essential mechanism determining specificity and activity of protein phosphatase 2A (PP2A) in vivo. Genes & development 17: 2138-2150.

32. Hombauer H, Weismann D, Mudrak I, Stanzel C, Fellner T, Lackner DH, Ogris E (2007) Generation of active protein phosphatase 2A is coupled to holoenzyme assembly. PLoS biology 5: e155.

33. Guenin S, Schwartz L, Morvan D, Steyaert JM, Poignet A, Madelmont JC, Demidem A (2008) PP2A activity is controlled by methylation and regulates oncoprotein expression in melanoma cells: a mechanism which participates in growth inhibition induced by chloroethylnitrosourea treatment. International journal of oncology 32: 49-57.

34. Yu XX, Du X, Moreno CS, Green RE, Ogris E, Feng Q, Chou L, McQuoid MJ, Pallas DC (2001) Methylation of the protein phosphatase 2A catalytic subunit is essential for association of Balpha regulatory subunit but not SG2NA, striatin, or polyomavirus middle tumor antigen. Molecular biology of the cell 12: 185-199.

35. Longin S, Zwaenepoel K, Louis JV, Dilworth S, Goris J, Janssens V (2007) Selection of protein phosphatase 2A regulatory subunits is mediated by the C terminus of the catalytic Subunit. The Journal of biological chemistry 282: 26971-26980.

36. De Baere I, Derua R, Janssens V, Van Hoof C, Waelkens E, Merlevede W, Goris J (1999) Purification of porcine brain protein phosphatase 2A leucine carboxyl methyltransferase and cloning of the human homologue. Biochemistry 38: 16539-16547.

37. Lee J, Chen Y, Tolstykh T, Stock J (1996) A specific protein carboxyl methylesterase that demethylates phosphoprotein phosphatase 2A in bovine

brain. Proceedings of the National Academy of Sciences of the United States of America 93: 6043-6047.

38. Xie H, Clarke S (1994) Protein phosphatase 2A is reversibly modified by methyl esterification at its C-terminal leucine residue in bovine brain. The Journal of biological chemistry 269: 1981-1984.

39. Schubert HL, Blumenthal RM, Cheng X (2003) Many paths to methyltransfer: a chronicle of convergence. Trends in biochemical sciences 28: 329-335.

40. Lee JA, Pallas DC (2007) Leucine carboxyl methyltransferase-1 is necessary for normal progression through mitosis in mammalian cells. The Journal of biological chemistry 282: 30974-30984.

41. Mumby M (2001) A new role for protein methylation: switching partners at the phosphatase ball. Science's STKE : signal transduction knowledge environment 2001: pe1.

42. Jackson JB, Pallas DC (2012) Circumventing cellular control of PP2A by methylation promotes transformation in an Akt-dependent manner. Neoplasia 14: 585-599.

43. Ogris E, Gibson DM, Pallas DC (1997) Protein phosphatase 2A subunit assembly: the catalytic subunit carboxy terminus is important for binding cellular B subunit but not polyomavirus middle tumor antigen. Oncogene 15: 911-917.

44. Wu J, Tolstykh T, Lee J, Boyd K, Stock JB, Broach JR (2000) Carboxyl methylation of the phosphoprotein phosphatase 2A catalytic subunit promotes its functional association with regulatory subunits in vivo. The EMBO journal 19: 5672-5681.

45. Chung H, Nairn AC, Murata K, Brautigan DL (1999) Mutation of Tyr307 and Leu309 in the protein phosphatase 2A catalytic subunit favors association with the alpha 4 subunit which promotes dephosphorylation of elongation factor-2. Biochemistry 38: 10371-10376.

46. Tolstykh T, Lee J, Vafai S, Stock JB (2000) Carboxyl methylation regulates phosphoprotein phosphatase 2A by controlling the association of regulatory B subunits. The EMBO journal 19: 5682-5691.

47. Wei H, Ashby DG, Moreno CS, Ogris E, Yeong FM, Corbett AH, Pallas DC (2001) Carboxymethylation of the PP2A catalytic subunit in Saccharomyces cerevisiae is required for efficient interaction with the B-type subunits Cdc55p and Rts1p. The Journal of biological chemistry 276: 1570-1577.

48. Floer M, Stock J (1994) Carboxyl methylation of protein phosphatase 2A from Xenopus eggs is stimulated by cAMP and inhibited by okadaic acid. Biochemical and biophysical research communications 198: 372-379.

49. Li M, Damuni Z (1994) Okadaic acid and microcystin-LR directly inhibit the methylation of protein phosphatase 2A by its specific methyltransferase. Biochemical and biophysical research communications 202: 1023-1030.

50. Tsai ML, Cronin N, Djordjevic S (2011) The structure of human leucine carboxyl methyltransferase 1 that regulates protein phosphatase PP2A. Acta crystallographica Section D, Biological crystallography 67: 14-24.

51. Sontag E, Nunbhakdi-Craig V, Sontag JM, Diaz-Arrastia R, Ogris E, Dayal S, Lentz SR, Arning E, Bottiglieri T (2007) Protein phosphatase 2A methyltransferase links homocysteine metabolism with tau and amyloid precursor protein

regulation. The Journal of neuroscience : the official journal of the Society for Neuroscience 27: 2751-2759.

52. Sontag E, Hladik C, Montgomery L, Luangpirom A, Mudrak I, Ogris E, White CL, 3rd (2004) Downregulation of protein phosphatase 2A carboxyl methylation and methyltransferase may contribute to Alzheimer disease pathogenesis. Journal of neuropathology and experimental neurology 63: 1080-1091.

53. Sontag E, Luangpirom A, Hladik C, Mudrak I, Ogris E, Speciale S, White CL, 3rd (2004) Altered expression levels of the protein phosphatase 2A ABalphaC enzyme are associated with Alzheimer disease pathology. Journal of neuropathology and experimental neurology 63: 287-301.

54. Tanimukai H, Grundke-Iqbal I, Iqbal K (2005) Up-regulation of inhibitors of protein phosphatase-2A in Alzheimer's disease. The American journal of pathology 166: 1761-1771.

55. Qian W, Shi J, Yin X, Iqbal K, Grundke-Iqbal I, Gong CX, Liu F (2010) PP2A regulates tau phosphorylation directly and also indirectly via activating GSK-3beta. Journal of Alzheimer's disease : JAD 19: 1221-1229.

56. Medina M, Avila J (2010) Glycogen synthase kinase-3 (GSK-3) inhibitors for the treatment of Alzheimer's disease. Current pharmaceutical design 16: 2790-2798.

57. Luo Y, Zhou X, Yang X, Wang J (2007) Homocysteine induces tau hyperphosphorylation in rats. Neuroreport 18: 2005-2008.

58. Vafai SB, Stock JB (2002) Protein phosphatase 2A methylation: a link between elevated plasma homocysteine and Alzheimer's Disease. FEBS letters 518: 1-4.

59. Sontag JM, Nunbhakdi-Craig V, Mitterhuber M, Ogris E, Sontag E (2010) Regulation of protein phosphatase 2A methylation by LCMT1 and PME-1 plays a critical role in differentiation of neuroblastoma cells. Journal of neurochemistry 115: 1455-1465.

60. Vazquez-Higuera JL, Mateo I, Sanchez-Juan P, Rodriguez-Rodriguez E, Pozueta A, Calero M, Dobato JL, Frank-Garcia A, Valdivieso F, Berciano J, Bullido MJ, Combarros O (2011) Genetic variation in the tau protein phosphatase-2A pathway is not associated with Alzheimer's disease risk. BMC research notes 4: 327.

61. Nord AS, Chang PJ, Conklin BR, Cox AV, Harper CA, Hicks GG, Huang CC, Johns SJ, Kawamoto M, Liu S, Meng EC, Morris JH, Rossant J, Ruiz P, Skarnes WC, Soriano P, Stanford WL, Stryke D, von Melchner H, Wurst W, Yamamura K, Young SG, Babbitt PC, Ferrin TE (2006) The International Gene Trap Consortium Website: a portal to all publicly available gene trap cell lines in mouse. Nucleic acids research 34: D642-648.

62. Chomczynski P, Sacchi N (1987) Single-step method of RNA isolation by acid guanidinium thiocyanate-phenol-chloroform extraction. Analytical biochemistry 162: 156-159.

63. Livak KJ, Schmittgen TD (2001) Analysis of relative gene expression data using real-time quantitative PCR and the 2(T)(-Delta Delta C) method. Methods 25: 402-408.

64. Lowenson JD, Kim E, Young SG, Clarke S (2001) Limited accumulation of damaged proteins in l-isoaspartyl (D-aspartyl) O-methyltransferase-deficient mice. The Journal of biological chemistry 276: 20695-20702.

65. Lowry OH, Rosebrough NJ, Farr AL, Randall RJ (1951) Protein measurement with the Folin phenol reagent. The Journal of biological chemistry 193: 265-275.

66. Mayfield J (1998) Diagnosis and classification of diabetes mellitus: new criteria. American family physician 58: 1355-1362, 1369-1370.

67. Nolan CJ (2010) Failure of islet beta-cell compensation for insulin resistance causes type 2 diabetes: what causes non-alcoholic fatty liver disease and non-alcoholic steatohepatitis? Journal of gastroenterology and hepatology 25: 1594-1597.

68. Himsworth HP (2011) Diabetes mellitus: its differentiation into insulin-sensitive and insulin-insensitive types. Diabetic medicine : a journal of the British Diabetic Association 28: 1440-1444.

69. Farrar C, Clarke S (2002) Altered levels of S-adenosylmethionine and S-adenosylhomocysteine in the brains of L-isoaspartyl (D-Aspartyl) O-methyltransferase-deficient mice. The Journal of biological chemistry 277: 27856-27863.

70. Clarke S (2003) Aging as war between chemical and biochemical processes: protein methylation and the recognition of age-damaged proteins for repair. Ageing research reviews 2: 263-285.

71. Kim E, Lowenson JD, MacLaren DC, Clarke S, Young SG (1997) Deficiency of a protein-repair enzyme results in the accumulation of altered proteins, retardation of growth, and fatal seizures in mice. Proceedings of the National Academy of Sciences of the United States of America 94: 6132-6137.

72. Kim E, Lowenson JD, Clarke S, Young SG (1999) Phenotypic analysis of seizure-prone mice lacking L-isoaspartate (D-aspartate) O-methyltransferase. The Journal of biological chemistry 274: 20671-20678.

73. Farrar C, Houser CR, Clarke S (2005) Activation of the PI3K/Akt signal transduction pathway and increased levels of insulin receptor in protein repair-deficient mice. Aging cell 4: 1-12.

74. Ikegaya Y, Yamada M, Fukuda T, Kuroyanagi H, Shirasawa T, Nishiyama N (2001) Aberrant synaptic transmission in the hippocampal CA3 region and cognitive deterioration in protein-repair enzyme-deficient mice. Hippocampus 11: 287-298.

75. Kosugi S, Furuchi T, Katane M, Sekine M, Shirasawa T, Homma H (2008) Suppression of protein l-isoaspartyl (d-aspartyl) methyltransferase results in hyperactivation of EGF-stimulated MEK-ERK signaling in cultured mammalian cells. Biochemical and biophysical research communications 371: 22-27.

76. Ryu J, Song J, Heo J, Jung Y, Lee SJ, Hong S, Cho JY (2011) Cross-regulation between protein L-isoaspartyl O-methyltransferase and ERK in epithelial mesenchymal transition of MDA-MB-231 cells. Acta pharmacologica Sinica 32: 1165-1172.

77. Ugi S, Imamura T, Maegawa H, Egawa K, Yoshizaki T, Shi K, Obata T, Ebina Y, Kashiwagi A, Olefsky JM (2004) Protein phosphatase 2A negatively regulates insulin's metabolic signaling pathway by inhibiting Akt (protein kinase B) activity in 3T3-L1 adipocytes. Molecular and cellular biology 24: 8778-8789.

78. Andrabi S, Gjoerup OV, Kean JA, Roberts TM, Schaffhausen B (2007) Protein phosphatase 2A regulates life and death decisions via Akt in a context-dependent manner. Proceedings of the National Academy of Sciences of the United States of America 104: 19011-19016.

79. Padmanabhan S, Mukhopadhyay A, Narasimhan SD, Tesz G, Czech MP, Tissenbaum HA (2009) A PP2A regulatory subunit regulates C. elegans insulin/IGF-1 signaling by modulating AKT-1 phosphorylation. Cell 136: 939-951.

80. Kuo YC, Huang KY, Yang CH, Yang YS, Lee WY, Chiang CW (2008) Regulation of phosphorylation of Thr-308 of Akt, cell proliferation, and survival by the B55alpha regulatory subunit targeting of the protein phosphatase 2A holoenzyme to Akt. The Journal of biological chemistry 283: 1882-1892.

CHAPTER 4

Interaction of Methyltransferases with Protein Phosphorylation: Quantitative Phosphoproteomics in both *Lcmt1*$^{-/-}$ and *Pcmt1*$^{-/-}$ mice

ABSTRACT

Tightly controlled protein phosphorylation is vital to effective cellular function. The tight control of this phosphorylation provided by the opposing actions of protein kinases and protein phosphatases. Two methyltransferases, the isoaspartyl methyltransferase PCMT1 and the leucine carboxyl methyltransferase LCMT1 have been implicated in the indirect control of protein phosphorylation. A mouse model deficient for the *Pcmt1* gene has been shown to display increased insulin signaling in the brain, increased brain growth, and early death after approximately 45 days of age due to tonic clonic seizures implicating a large role for PCMT1 in neuronal function. *Lcmt1* hypomorphic mice display altered methylation of PP2A, the main ser/thr phosphatase, as well as a slight insulin resistance phenotype, potentially implicating dysregulation of insulin signaling in skeletal muscle. Other studies of PCMT1 and LCMT1 in mammalian systems indicate that the influence of these methyltransferases on phosphorylation extends beyond just the insulin-signaling pathway; however, no attempt has yet been made to identify other phosphorylated proteins subject to this control. This study chronicles the development of efficient phosphoproteomic separation techniques as well as the identification of libraries of altered sites of phosphorylation in the brain and muscle of *Lcmt1* hypomorphic mice as well as the brain of *Pcmt1* deficient mice.

INTRODUCTION

Phosphorylation of proteins is one of the most common, and arguably most important post-translational modifications in eukaryotic cells[1,2]. With 2-4% of these genomes coding for kinases[3,4], and approximately 30% of the proteome phosphorylated[5,6], protein phosphorylation is presumably involved in the regulation of every aspect of cellular function. Reversible phosphorylation is generally highly regulated and often associated with activation or inactivation of an enzyme's function, or the modulation of protein-protein interactions [7,8]. Kinase-induced protein phosphorylation has been of particular interest due to its role in the activation and deactivation of the enzyme cascades involved in oncogenic transformation in mammalian cells[9]. Recently, however, there has been evidence that control of phosphorylation may be dependent on other post-translational modifications[10,11,12,13]. For example, histone lysine and arginine methylation reactions can strongly affect the ability of protein kinases to phosphorylate nearby serine and threonine residues [11,14,15]. Technological advancements within the field of mass spectrometry have exponentially expanded the discovery of histone modifications, revolutionizing the field of epigenetics, and establishing the idea of a histone "code" [15]. In this study I examine the role of two methyltransferases, distinct from protein lysine and protein arginine methyltransferases, in the control of phosphorylation events on a global proteome scale.

The protein L-isoaspartyl methyltransferase (PCMT1) is responsible for methylating and "repairing" L-isoaspartyl and D-aspartyl residues, which arise spontaneously from the respective isomerization and deamidation of aspartyl and

asparaginyl residues [16]. Loss of PCMT1 in mice has been shown to increase brain size and activate growth pathways in the brain[17,18,19]. These results have implicated a novel regulatory role for this methyltransferase in phosphorylation controlled growth pathways and spawned additional studies demonstrating an antagonistic role in activation of the insulin signaling pathway[20,21,22,23]. *Pcmt1*$^{-/-}$ mice additionally exhibit an autoimmune phenotype with T-cell hyperproliferation, increased response to mitogen stimulation, and increased phosphorylation of members of the TCR and CD28 signaling pathways[24]. An additional link between PCMT1 and phosphorylation comes through regulation of mitogen activated protein kinases[25,26]. This interaction, however, is obfuscated by experiments in cell culture reporting contradictory roles for PCMT1 both being necessary for phosphorylation of extracellular signal-regulated kinases[27], as well as the loss of PCMT1 causing hyperactivation of ERK signaling[23,28]. Although the mechanism through which the loss of this methyltransferase alters signal transduction remains unclear, isoaspartyl formation near the active site of an enzyme has been shown to confer alterations in enzymatic activity which can be restored through methylation by the isoaspartyl methyltransferase[29]. In addition to regulation of signal transduction through isoaspartyl dependent alterations in protein activity, PCMT1 has recently been implicated in the control of estrogen receptor signal transduction at a transcriptional level[30], providing an additional avenue for signal transduction control. The convergence of isoaspartyl methylation and phosphorylation pathways has additionally been bolstered by the recent

discovery of an isoaspartyl dependent method of governance of human p53, regulating both p53 transcript as well as p53 function[31].

The leucine carboxyl methyltransferase (LCMT1) is responsible for methylating the C-terminal residue (leucine-309) of the catalytic subunit of protein phosphatase 2A (PP2A) [32], its only known cellular substrate. This modification is reversed by the primarily nuclear methylesterase PME-1[33,34]. PP2A itself is a heterotrimeric protein and methylation of the C-terminal leucine by LCMT1 has been proposed to alter the subunit composition of PP2A and thus control the specificity of the enzyme[35,36,37,38,39,40]. PP2A has the potential to exhibit considerable structural complexity with both the structural (C) and scaffolding (A) subunits encoded by two distinct genes in mammals. However, the true complexity of PP2A arises from the four independent and unrelated families of B subunits (B, B', B'', B'''), coded for by multiple genes, many of which contain multiple splice variants[41,42,43]. Temporal and spatial assembly of distinct PP2A holoenzymes composed of different genes and splice variants is thought to be one of the main mechanisms for appropriately targeting PP2A to cellular substrates[43,44]. Post-translational modification of the C-terminal “tail” of PP2A has been proposed as a mechanism of subunit control[43]. Specifically, methylation is necessary for binding of Bα subunits and has been shown to strongly recruit B' family members though it may not be absolutely necessary for this binding [35,37,39].

Proteomic approaches have proved invaluable at identifying post-translational modifications, especially phosphorylation and methylation sites. Many of these studies, however, lack contextual controls and do not provide biological

function information on the control of, or influence of these modifications[6]. Phenotypic analysis of mice lacking *Pcmt1* has led to the discovery of a role for this enzyme in regulating phosphorylation and activation of growth pathways, and additional evidence suggests this enzyme may control isoaspartyl-gated molecular switches both in apoptosis and cellular adhesion pathways[45,46,47]. Although proteomic approaches have been utilized to search for isoaspartyl containing targets of this enzyme[48,49], no proteomic-based strategies have been utilized to search for novel PCMT1 dependent changes in protein phosphorylation. Additionally, despite the fact that LCMT1 has been suggested to contribute to the control of targeting of the main serine/threonine phosphatase PP2A, no proteomic approaches have yet been utilized to determine which phosphotargets of PP2A are sensitive to methylation. Interestingly, proteomic approaches have been utilized with great success to study LCMT1's counterpart, PME-1, and have elucidated a cadre of proteins believed to be targeted by PP2A only in the absence of the methylesterase [50]. However, because greater than 90% of the cytosolic portion of PP2A is reported to be methylated, a minimal increase in this methylation caused by loss of the nuclear methylesterase may provide only a part of the PP2A methylation sensitive phosphome[50].

In this study a mass spectrometric approach was used to quantify the phosphosites that differ in the absence and presence of both PCMT1 and LCMT1 using respective knockout and hypomorphic mouse models for these enzymes (CHAPTERS 2 & 3). A relatively new technology, isobaric tags for relative and absolute quantitation (iTRAQ), is utilized. The iTRAQ tag system allows covalent

labeling of peptide N-termini as well as side-chain amines with 4 isobaric tags which yield differential isotope coded reporter ions during peptide fragmentation in MS/MS [51]. Additionally through the use of multiple fractionation techniques we are able to assess which peptide separation conditions are best suited for phosphopeptide quantitation and analysis.

This phosphoproteomic experiment identified 5 sites of increased and 14 sites of decreased phosphorylation in *Lcmt1*$^{-/-}$ muscle. Analysis of *Lcmt1*$^{-/-}$ brain tissue revealed 114 increased, and 67 decreased phosphosites. *Pcmt1*$^{-/-}$ brain tissue revealed 13 sites of increased and 98 sites of decreased phosphorylation. Each of these sites provides a future avenue of research, for instance *Pcmt1*$^{-/-}$ brain tissue suggested marked dysregulation of protein kinase C (PKC), with decreases in phosphorylation of the activation, turn, and hydrophobic motif of multiple PKC isozymes. Supporting these data, decreases in the most prominent PKC substrate, the myristoylated alanine rich C-kinase substrate, were also observed, providing an additional link between PCMT1 and growth pathways in the brain[52,53].

MATERIALS & METHODS

Tissue and protein extraction

Brain and quadricep muscles were carefully dissected out from 6 *Lcmt1*$^{-/-}$ and 6 *Lcmt1*$^{+/+}$ age-matched mice, as well as 6 *Pcmt1*$^{-/-}$ and 6 *Pcmt1*$^{+/+}$ age-matched mice immediately post-sacrifice using CO_2 asphyxiation. All procedures were performed in accordance with UCLA ARC protocols. Post-dissection the tissues were weighed and placed in 5 volumes of RIPA buffer (50 mM Tris-HCl pH 8.0, 150 mM NaCl, 0.5% sodium deoxycholate, 1% Triton X-100, and 1 mM phenylmethylsulfonyl fluoride (PMSF) with phosphatase (HALT, Thermo-Pierce, Rockford, IL) and protease inhibitors (Complete, Roche, Mannheim, Germany). These whole tissue samples were immediately homogenized on ice using a Polytron homogenizer and a PTA7 generator. Samples were subjected to seven 30-seconds pulses with one minute on ice between pulses. The protein concentration of the crude extracts was determined after trichloroacetic acid precipitation by the Lowry method [54] repeated in quintuplicate. An aliquot of each protein extract (3 mg) was standardized into a total volume of 530 µL of RIPA buffer and solubilized by adding 318 mg of urea for a final urea concentration of 10 M, reduced with 8.48 µL of tris(2-carboxyethyl)phosphine (TCEP) (Sigma-Aldrich St. Louis, MO) and incubated for 1 hour at 60 °C. The samples were brought back to pH 8 with solid ammonium bicarbonate, re-reduced with 16.96 mg TCEP, and cysteine blocking was performed with a final concentration of 4 mM iodoacetamide for 1 hour at room temperature in the dark. Each protein extract was then digested with 600 µg of modified trypsin overnight (Promega, Fitchburg, WI) and quenched with 18 µL trifluoroacetic acid.

Separation/Enrichment

IMAC Enrichment of phosphorylated peptides was achieved using an ÄKTA Purifier (GE Healthcare, Piscataway, NJ, USA) equipped with an analytical guard column (62 µL packing volume) (Upchurch Scientific, Oak Harbor, WA) packed with 5 nm TiO_2 beads (GL Sciences, Tokyo, Japan). Lyophilized peptides were resuspended in 250 µL of wash solution (35% acetonitrile, 200 mM NaCl, 0.3% trifluoroacetic acid) and run over the TiO_2 column with an additional 3.9 mL of wash solution to remove non-phosphorylated peptides. This was followed by 3.5 mL of rinse solution (5% acetonitrile, 0.1% trifluoroacetic acid) and finally peptides were eluted onto a C18 macrotrap peptide column (Michron Bioresources, Auburn, CA) with 15 mL of elution solution (1 M KH_2PO_4). The C18 column was then further washed with 17.1 mL of rinse solution. Phosphopeptides were then eluted from the C18 column with 400 µL of organic elution solution (50% acetonitrile, 0.1% trifluoroacetic acid) and this eluent was lyophilized to dryness under vacuum using a SpeedVac concentrator.

iTRAQ labeling

Trypsin-digested peptides were iTRAQ labeled as outlined in the iTRAQ Reagents 4plex Applications Protocol (AB Sciex, Foster City, CA). Briefly, phosphopeptides were resuspended in 30 µL of dissolution buffer, and each iTRAQ reagent vial was brought up in 70 µL of ethanol. One iTRAQ vial was used to label the enriched phosphopeptide sample from a single mouse and labeling was allowed to proceed

for 1 hour at room temperature before the reaction was quenched with the addition of trifluoroacetic acid to 1% final concentration. For *Pcmt1*$^{-/-}$ and *Lcmt1*$^{-/-}$ and their wild-type controls, the order of iTRAQ labeling was alternated between experiments to compensate for differences between reporter ion recognition. For example knockout samples were labeled with 114 and 115 iTRAQ tags in the first experiment, 114 and 116 in the second experiment, 115 and 117 in the third experiment while wild-type animals were labeled with 116 and 117 in the first experiment, 115 and 117 in the second experiment, and 114 and 116 in the third experiment. Labeling efficiency (greater than 99%) was confirmed by MS/MS analysis on a QSTAR mass spectrometer (Applied Biosystems, Foster City, CA) and subsequently corresponding iTRAQ-tagged knockout and wild-type samples were combined.

High pH C18 fractionation

High *p*H reverse phase chromatography was performed using an ÄKTA Purifier (GE Healthcare, Piscataway, NJ, USA) equipped with a 1 x 100 mm Gemini 3 µm C18 column (Phenomenex, Torrance, CA). Lyophilized phosphopeptides were reconstituted in 1% buffer A (20 mM ammonium formate, *p*H 10) and loaded onto the column. High organic buffer B was composed of 50% acetonitrile with 20 mM ammonium formate The gradient went from 1% B to 21% B over 1.1 mL, to 62% B over 5.4 mL, and then directly to 100% B. The flow rate was 80 µL/min. Sixteen samples were collected and dried down using a SpeedVac concentrator.

LC-MS/MS

All peptides were analyzed on an LTQ Orbitrap Velos equipped with a nano- Acquity UPLC and samples were fragmented using HCD mode. Peptides were eluted using a 90 minute gradient. Data was searched using Protein Prospector and the UniProt Mus musculus database. The data was searched utilizing trypsin cleavage and accounting for up to one missed cleavage site. Additionally carbamidomethylation of cysteine residues was used as a fixed modification as well as N-terminal iTRAQ labeling. Furthermore acetylation of amino termini, oxidation of methionine residues, iTRAQ labeling of lysine residues, loss of N-terminal methionine as well as phosphorylation of serine, threonine and tyrosine were all set as variable modifications. Data was searched initially with a 20-ppm tolerance of the parent ion, (HCD) and 20-ppm tolerance for HCD MS/MS.

RESULTS & DISCUSSION

Introduction to the experimental design

In this experiment I examined alterations in phosphoproteins in the brain and quadricep muscle of *Lcmt1*$^{-/-}$ mice as well as the brain of *Pcmt1*$^{-/-}$ mice. *Lcmt1*$^{-/-}$ hypomorphic mice have reduced *Lcmt1* expression in a tissue specific manner (CHAPTER 3). The smallest change in LCMT1 occurs in brain tissue where *Lcmt1*$^{-/-}$ animals have a 54% decrease in LCMT1 protein levels as compared to *Lcmt1*$^{+/+}$ animals. The largest decreases are seen in heart and muscle, where *Lcmt1*$^{-/-}$ animals have 98% and 87% decreases in LCMT1 as compared to *Lcmt1*$^{+/+}$ mice (CHAPTER 3). In *Lcmt1*$^{-/-}$ animals, LCMT1 activity and methylation of PP2A largely correlated with LCMT1 protein levels (CHAPTER 3). Despite the fact that *Lcmt1*$^{-/-}$ animals show the smallest LCMT1 change in brain tissue, this tissue displays the highest expression of both LCMT1 and PP2A in wild-type animals, implicating the importance of these two proteins in cellular function in the brain (CHAPTER 3). Additionally, brain tissue possesses the largest number of both phosphorylation sites and phosphoproteins, many of which are implicated in human disease, making it a tantalizing target for phosphoproteomic analysis[55]. Muscle tissue was selected based on the enormous reduction in LCMT1 and PP2A methylation in *Lcmt1*$^{-/-}$ mice in this tissue. Additionally *Lcmt1*$^{-/-}$ mice displayed a slight insulin resistance phenotype (CHAPTER 3), which could potentially arise from dysregulated insulin signaling in peripheral tissue such as muscle, making it an interesting phosphoproteomic target. Brain tissue from *Pcmt1*$^{-/-}$ animals was selected for study due to the high amount of phosphorylation in brain tissue as well as the

dysregulated brain insulin signaling[22] and severe neurological defects documented in these animals[18,19].

One iTRAQ experiment involving the iTRAQ labeling of muscle samples from two *Lcmt1*$^{-/-}$ and two *Lcmt1*$^{+/+}$ animals was performed. These phosphoprotein samples were subjected to minimal post-labeling separation utilizing "Method A" in Figure 1. Three separate iTRAQ labeling experiments, each involving two individual *Lcmt1*$^{-/-}$ and two individual *Lcmt1*$^{+/+}$ brain samples, for a total of twelve mice were carried out. Each of these iTRAQ experiments was run utilizing one of three different separation methodologies prior to LC-MS/MS analysis as outlined in Figure 1. This enabled me to investigate phosphoproteomic methodology in addition to the phosphoproteomic changes relevant to the *Lcmt1* hypomorphic mouse model. In a fashion identical to the analysis of *Lcmt1* brains outlined above, brains samples from six *Pcmt1*$^{-/-}$ and six *Pcmt1*$^{+/+}$ animals were utilized in three separate iTRAQ experiments (12 total mice), with two *Pcmt1*$^{-/-}$ and two *Pcmt1*$^{+/+}$ animals in each iTRAQ labeling experiment. These iTRAQ experiments were prepared according to the workflow outlined in Figure 1 and each was subjected to one of the three different separation techniques outlined in Figure 1.

Phosphoproteomic Analysis of Lcmt1$^{-/-}$ and *Lcmt1*$^{+/+}$ *Muscle*

Despite the fact that muscle tissue contains fewer phosphoproteins than other tissue types with only approximately 7% of proteins phosphorylated [55], we were able to identify 1058 distinct peptides, 510 of which contained phosphorylated residues (Table 1). This result indicates 48.5% of peptides identified by MS/MS

were phosphopeptides, an approximate 7-fold enrichment in phosphoprotein abundance from endogenous levels utilizing titanium dioxide fractionation followed by minimal treatment prior to LC-MS/MS analysis as outlined in method A (Figure 1). Phosphopeptides were discovered from 228 distinct muscular proteins. Previous phosphoproteomic studies involving muscle identify fewer than 60 phosphorylated proteins[56], suggesting the enrichment and separation strategy we used here resulted in outstanding levels of phosphoenrichment. Examining the abundance of all phosphopeptides quantitated in this tissue (Figure 2A) shows an average $\log_2(Lcmt1^{-/-}/Lcmt1^{+/+})$ ratio of 0.075, indicating that on average, there is little to no global change in phosphorylation of average phosphoproteins in the muscle of *Lcmt1*$^{-/-}$ animals. Plotting the average *Lcmt1*$^{-/-}$ iTRAQ signals against the average WT signals confirmed this trend as the phosphopeptide signals remained nearly linear at a 1:1 ratio (Figure 2B). Although the average level of phosphorylation between *Lcmt1*$^{-/-}$ animals and their WT counterparts did not change, this fits with a hypothesis that decreasing methylation of PP2A will only alter targeting of the phosphatase to specific sites, not global changes in phosphorylation.

Analyzing the iTRAQ reporters allowed the discovery of five proteins with increased phosphorylation and fourteen proteins with decreased levels of phosphorylation in the quadriceps muscle of *Lcmt1*$^{-/-}$ animals (Table 2). Eight of these phosphorylation sites are previously unreported sites of phosphorylation. The proteins identified largely corresponded with metabolic and structural proteins, some of the highest abundance proteins in cytosolic extract. We did, however, identify a sites corresponding to several low abundance proteins, such as decreased

phosphosites on protein kinase C, retinoblastoma-associated protein as well as an increased site of phosphorylation on heat-shock protein β 1. All but one of the significantly increased or decreased phosphorylation sites were serine or threonine residues, potentially indicating methylation sensitive substrates of PP2A. Increases in phosphopeptide abundance in *Lcmt1*$^{-/-}$ animals could be a result of decreased targeting by PP2A, a result of fewer methylation sensitive subunits bound to the phosphatase. Alternatively decreases in specific phosphosites in these animals could indicate PP2A substrates targeted by methylation insensitive substrates.

Phosphoproteomic Analysis of Lcmt1$^{-/-}$ and *Lcmt1*$^{+/+}$ *Brain*

Neuronal tissue is one of the most highly phosphorylated tissues, with approximately 33% of proteins being phosphoproteins [55]. IMAC phosphoprotein enrichment followed by separation method A, B, or C yielded similar levels of phosphopeptide enrichment, with 70.9%, 73.2% and 80.9% of all peptides identified by LC-MS/MS possessing a site of phosphorylation in each respective separation method. This result indicates little effect of post IMAC processing on phosphopeptide enrichment. Although enrichment was slightly higher using orthogonal purification strategies (Method B & C) far fewer peptides were identified (Table 1). IMAC followed by LC-MS/MS (method A) identified 1501 unique phosphopeptides, whereas only 714 peptides were identified utilizing IMAC followed by high pH fractionation and 16 separate LC-MS/MS runs (method B), and only 879 phosphopeptides were identified performing IMAC followed by high pH, pooling of samples and C18 cleanup prior to LC-MS/MS (method C).

Examining the abundance of all phosphopeptides quantitated (Figures 3 A, C, & E) shows an average $\log_2(Lcmt1^{-/-}/Lcmt1^{+/+})$ ratio of 0.88, 0.34, and -0.54 for separation methods A, B, and C respectively. Average iTRAQ values indicating globally increased phosphorylation (Figures 3 A & C) as well as globally decreased phosphorylation (Figure 3 E) suggest deviation in iTRAQ labeling, and this discrepancy was accounted for by normalizing to the median value and quantifying phosphopeptide alteration based on their deviation from the average. Plotting the average $Lcmt1^{-/-}$ iTRAQ signals against the average WT signals confirmed this trend as the phosphopeptide signals remained nearly linear but slightly above or below the 1:1 ratio (Figure 3 B, D, & E).

Comparing the libraries of distinct phosphopeptides identified using each separation strategy (Figure 4) shows that while all strategies discovered many of the same phosphopeptides, IMAC followed by LC-MS/MS enabled much higher peptide identification. Examining the analysis of each purification strategy as it relates to only significantly increased or decreased phosphopeptides two or more standard deviations from the median value, (Figures 5 & 6), we compile a library of reliably increased and decreased phosphosites (Table 3).

Phosphoproteomic Analysis of $Pcmt1^{-/-}$ and $Pcmt1^{+/+}$ Brain

PCMT1 is widely expressed within the brain, and a majority of phenotypes associated with the loss of this enzyme in mice are related to alterations in neurological function[18,19]. Loss of PCMT1 is associated with brain growth and increased phosphorylation of proteins within the insulin signaling pathway[20],

however, reducing phosphorylation of the insulin signaling pathway using a kinase inhibitor does not completely restore normal brain growth in these animals[57]. This finding potentially indicates an interaction between this enzyme and other pro-growth phosphorylation cascades. Analyzing *Pcmt1*$^{-/-}$ brains in a methodology identical to that used for *Lcmt1*$^{-/-}$ brains allowed us to determine both global, as well as individual, changes in *Pcmt1*$^{-/-}$ brain protein phosphorylation.

IMAC phosphoprotein enrichment from *Pcmt1*$^{-/-}$ brains and their wild-type control counterparts followed by separation method A, B, or C yielded similar levels of phosphopeptide enrichment (Table1). This result once again indicates little effect of post IMAC separation strategy on phosphopeptide enrichment. Similar the *Lcmt1* samples set, on average *Pcmt1* brain samples analyzed using orthogonal separation technique enabled far fewer peptide identifications (Table 1). IMAC followed by LC-MS/MS (method A) identified 1412 unique phosphopeptides, whereas only 398 and 297 phosphopeptides were identified utilizing method B and C, respectively.

Examining the abundance of all phosphopeptides quantitated (Figures 7 A, C & E) shows an average $\log_2$(*Pcmt1*$^{-/-}$/*Pcmt1*$^{+/+}$) ratio of 0.88, 0.34, and -0.54 using methods A, B and C, respectively. Globally increased phosphorylation in *Pcmt1*$^{-/-}$ animals (Figure 7 A & E) as well as globally decreased phosphorylation (Figures 7 C) suggest deviation in iTRAQ labeling, and this discrepancy was accounted for by normalizing to the median value, and determining significantly altered phosphosites based on their deviation from this value, identical to the strategy used to determine significance in *Lcmt1*$^{-/-}$ brain samples. Plotting the average *Pcmt1*$^{-/-}$ iTRAQ signal

against the average *Pcmt1*$^{+/+}$ signal confirmed the phosphopeptide signals remained nearly linear but slightly above or below the 1:1 ratio (Figure 7 B, D, & E).

Comparing the libraries of distinct phosphopeptides identified using each separation strategy (Figure 8) shows that while all strategies discovered many of the same phosphopeptides, IMAC followed by LC-MS/MS with little post-IMAC processing (separation method A) enabled much higher peptide identification. Cross-referencing the significantly increased and decreased phosphopeptides from each study (Figures 9 & 10) enabled the compilation of a library of a altered phosphosites discovered in multiple studies (Table 4).

Overview of Results

This study created a library of reliable tissue specific alterations in phosphorylation in *Lcmt1*$^{-/-}$ and *Pcmt1*$^{-/-}$ mouse models. This data has already provided potentially novel methylation sensitive substrates for PP2A as well as novel sites of interaction for the isoaspartyl methyltransferase. Phosphosites identified to be increased or decreased in *Pcmt1*$^{-/-}$ mice are being cross-referenced with gene expression data obtained from gene-chip experiments (unpublished data) in an attempt to better understand these alterations. Increased phosphorylation is observed in proteins already known to be associated with PCMT1, such as microtubules and their associated proteins[49]. Interestingly this study also suggests a role for PCMT1 in calcium signaling as calcium/calmodulin-dependent 3',5'-cyclic nucleotide phosphodiesterase 1B, calcium/calmodulin-dependent protein kinase kinase 2, Calcium/calmodulin-dependent protein kinase kinase 1,

and multiple isotypes of Protein kinase C, all involved in propagating the calcium response, were observed to have decreased phosphorylation in *Pcmt1*$^{-/-}$ brain.

Comparing multiple sample preparation techniques enabled the correlation of separation strategies, phospho-enrichment efficiency, and peptide identification. These results suggest a less is more approach, with fewer post-IMAC peptide separation steps yielding considerably higher numbers of LC-MS/MS peptide identifications. A possible explanation for this result is that orthogonal separation did not yield a lower number of peptides, but that artifactual salts resulting from high pH fractionation decreased the MS/MS sensitivity, obfuscating the detection of peptides in these studies.

ACKNOWLEDGEMENTS

I want to thank Drs. Kevan Shokat, Al Burlingame, and Jon Trinidad for the valuable use of their lab space, materials and equipment throughout the course of this study. Additionally I would like to thank Nick Hertz, a graduate student in the lab of Drs. Shokat and Burlingame for his collaboration in this study. Additionally I would like to thank Dr. Stephen Young for the creation of the *Lcmt1*$^{-/-}$ mouse model and Dr. Jon Lowenson for the generous gift of *Pcmt1*$^{-/-}$ mouse tissue.

FIGURES

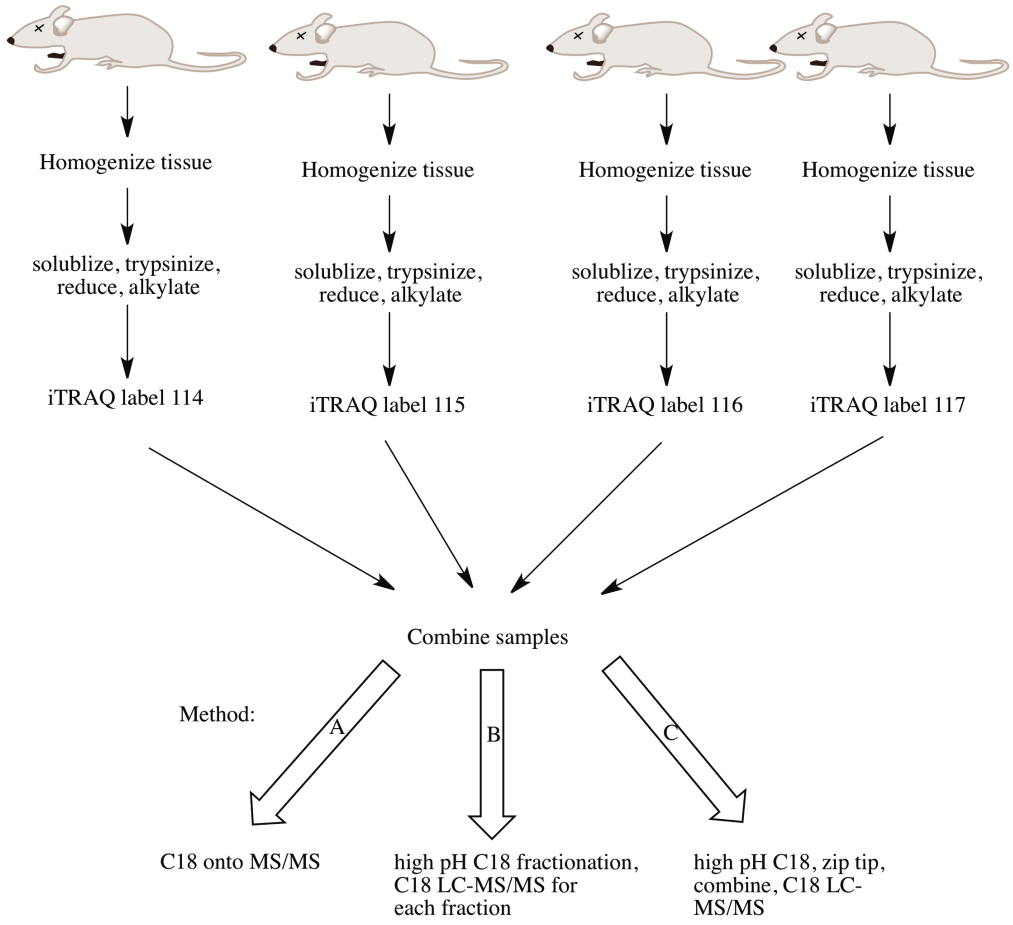

Figure 1: Overview of experimental workflow. As outlined in Materials & Methods, tissue from mice was surgically extracted, homogenized, solubilized, reduced, carbamidomethylated, trypsinized, phosphoenriched, and iTRAQ labeled. iTRAQ labeled tissues were then combined and subjected to one of 3 separation techniques: direct LC-MS/MS (Method A), high pH fractionation followed by LC-

MS/MS of each fraction (method B), or high pH C18 fractionation followed by zip tip purification and LC-MS/MS of each fraction (method C).

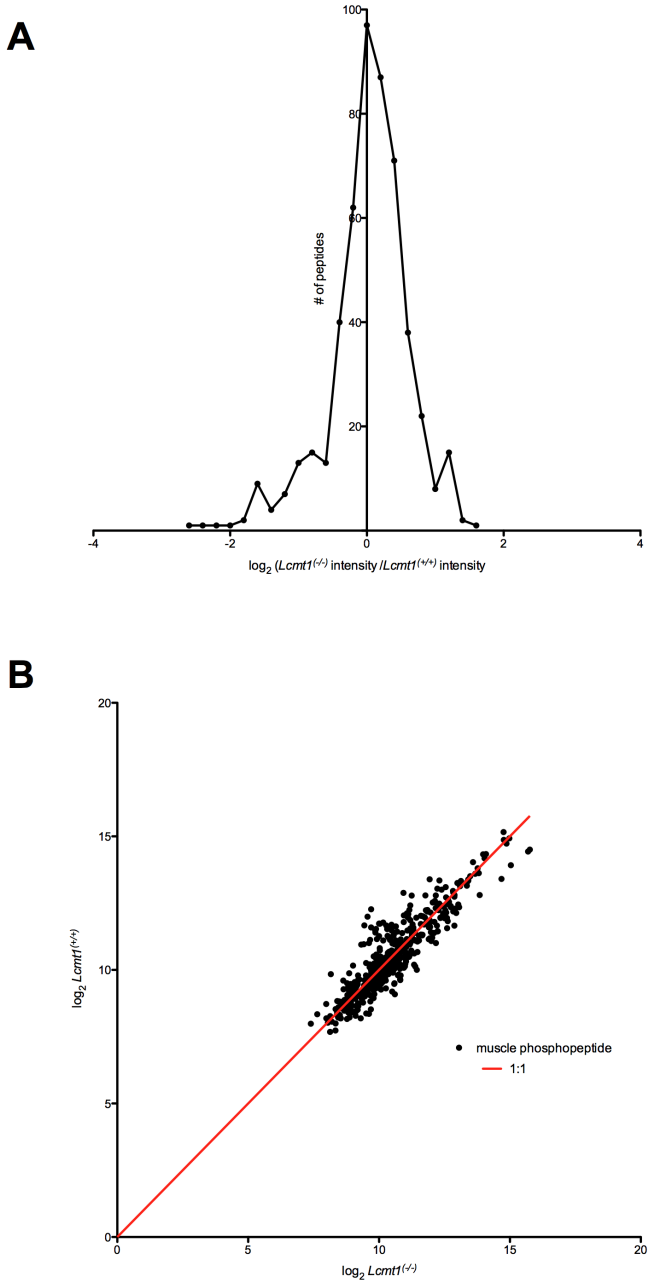

Figure 2: Comparison of *Lcmt1*$^{-/-}$ and *Lcmt1*$^{+/+}$ iTRAQ reporter ions from phosphopeptides isolated from quadricep muscle samples separated using Method A. Panel A depicts a histogram comparing the relative quantitation of phosphopeptides from *Lcmt1*$^{-/-}$ and *Lcmt1*$^{+/+}$ muscle samples identified using

method A. Log_2 normalization is utilized to decrease magnitude dependence during comparisons. The median of the value was 0.075, the average was 0.022, with a standard deviation of 0.59. Values greater than 0 indicate a greater *Lcmt1*$^{-/-}$ signal while values less than 0 indicate a greater *Lcmt1*$^{+/+}$ signal. iTRAQ reporter ions 2 standard deviations from the average were considered significantly altered in Table 2. Panel B depicts a comparative evaluation of the intensities of *Lcmt1*$^{-/-}$ and *Lcmt1*$^{+/+}$ iTRAQ reporter ions for each muscle phosphopeptide identified utilizing method A.

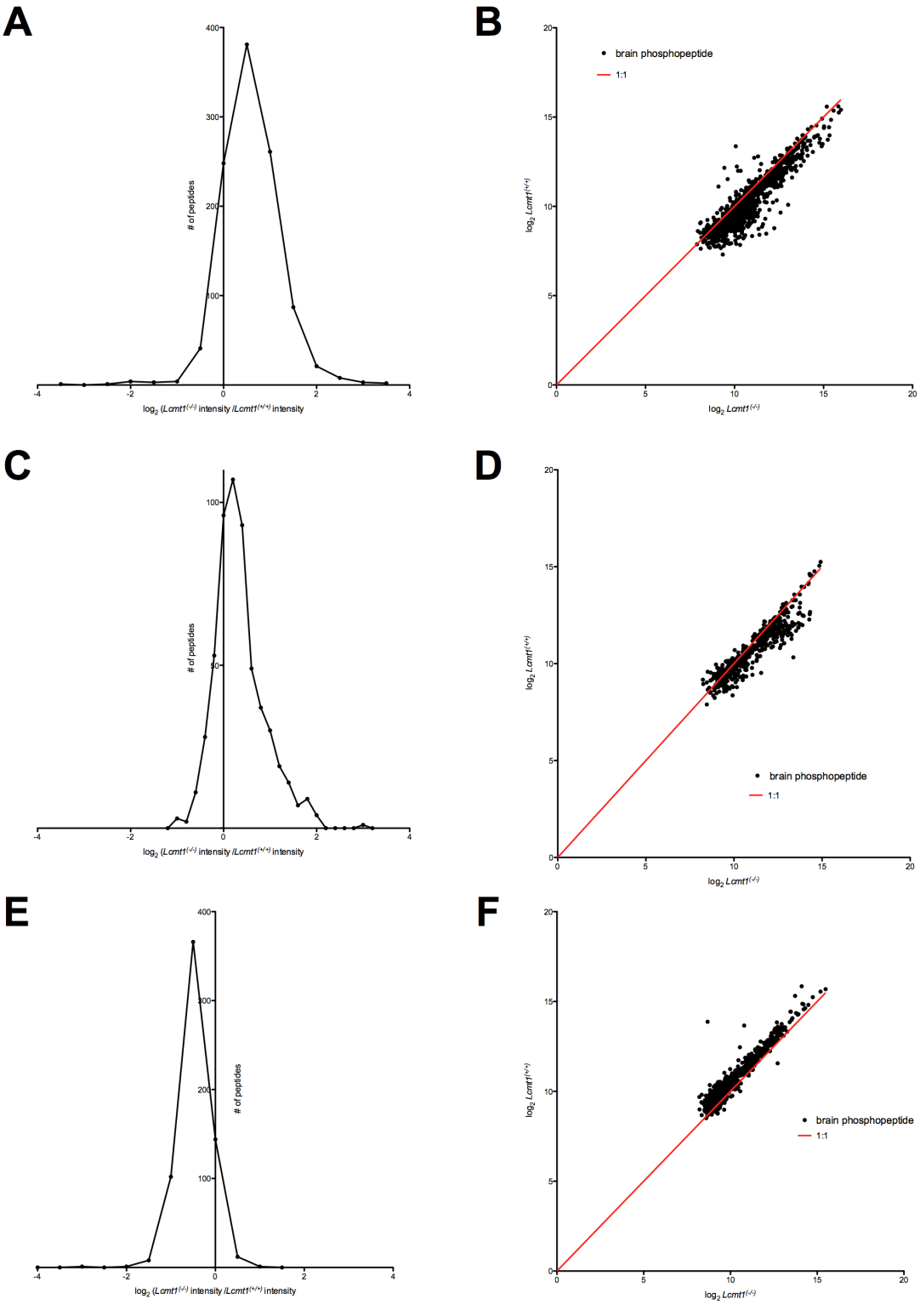
A
# of peptides
log2 (Lcmt1(-/-) intensity /Lcmt1(+/+) intensity
B
brain phosphopeptide
1:1
log2 Lcmt1(+/+)
log2 Lcmt1(-/-)
C
# of peptides
log2 (Lcmt1(-/-) intensity /Lcmt1(+/+) intensity
D
brain phosphopeptide
1:1
log2 Lcmt1(+/+)
log2 Lcmt1(-/-)
E
# of peptides
log2 (Lcmt1(-/-) intensity /Lcmt1(+/+) intensity
F
brain phosphopeptide
1:1
log2 Lcmt1(+/+)
log2 Lcmt1(-/-)

Figure 3: Comparison of *Lcmt1*$^{-/-}$ and *Lcmt1*$^{+/+}$ iTRAQ reporter ions from phosphopeptides isolated from brain samples separated using Method A, B, and C. Panel A, C, and E depict histograms comparing the relative quantitation of phosphopeptides from *Lcmt1*$^{-/-}$ and *Lcmt1*$^{+/+}$ brain samples using separation methods A, B, and C respectively. A. Log_2 normalization is utilized to decrease magnitude dependence during comparisons. Values greater than 0 indicate a greater *Lcmt1*$^{-/-}$ signal while values less than 0 indicate a greater *Lcmt1*$^{+/+}$ signal. Panels B, D, and F depict a comparative evaluation of the intensities of *Lcmt1*$^{-/-}$ and *Lcmt1*$^{+/+}$ iTRAQ reporter ions for each brain phosphopeptide identified employing method A, B, and C respectively. In panel A, the median value of peptides identified using method A was 0.76, and the average was 0.88 with a standard deviation of 0.83. In panel C, the median value of peptides identified using method B was 0.26, and the average was 0.34 with a standard deviation of 0.53. In panel E, the median value of peptides identified using method C was -0.44, and the average was -0.54 with a standard deviation of 0.35. iTRAQ reporter ions 2 standard deviations from the average were considered significantly altered in Table 3 and figures 4-6.

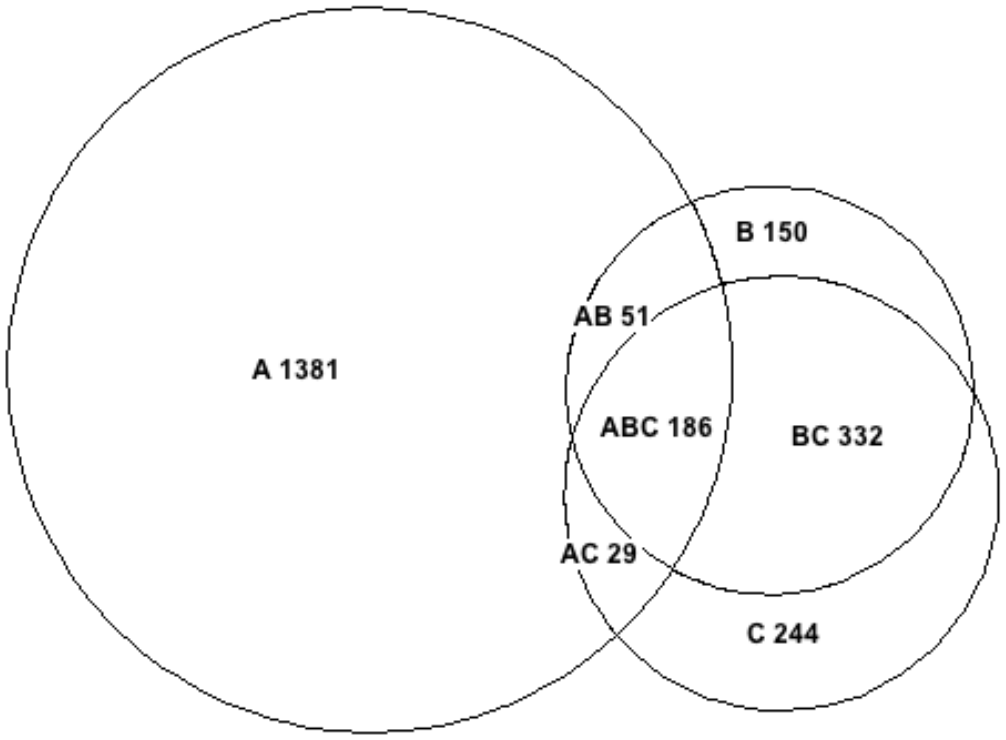

Figure 4: Unique peptides discovered in *Lcmt1*$^{-/-}$ and *Lcmt1*$^{+/+}$ animals in methods A, B, and C as well as across methods. Unique phosphopeptides from each separation technique were pooled and a Venn diagram was constructed showing overlap of peptides identified, as well as the number of unique phosphopeptides identified in each study.

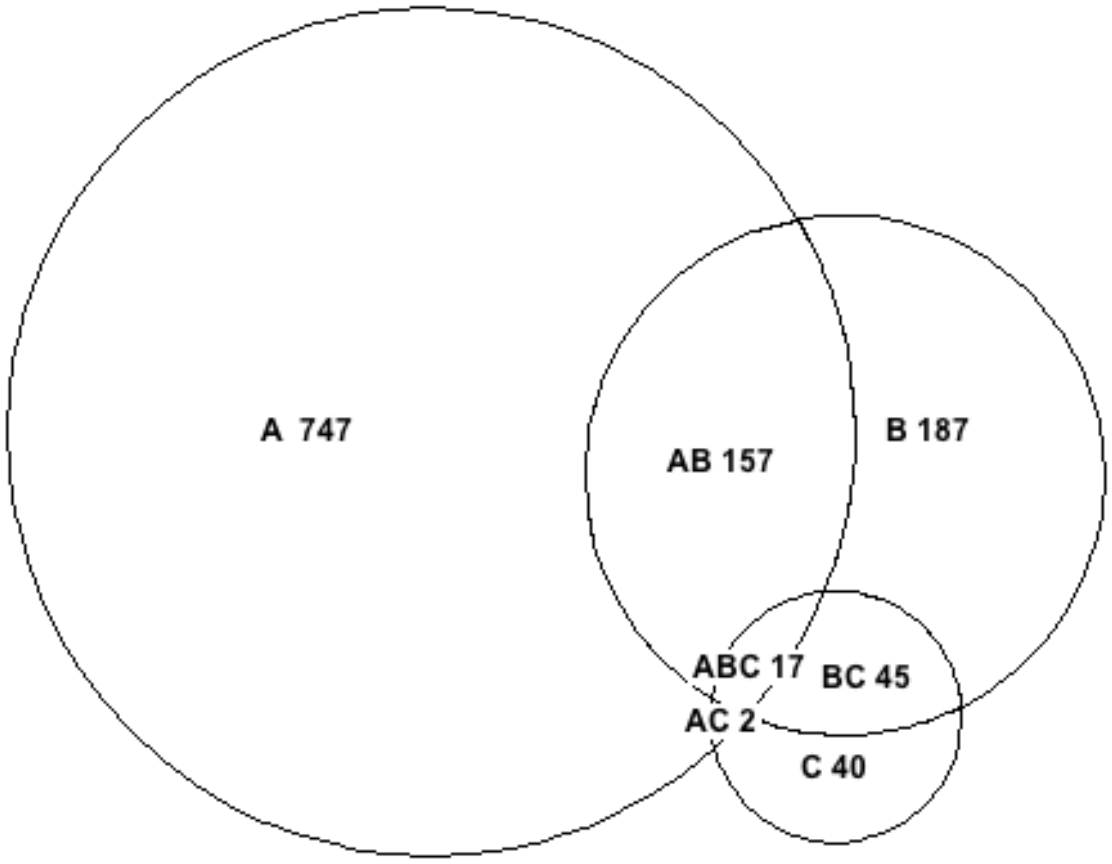

Figure 5: Venn diagram of phosphopeptides discovered in methods A, B, and C that are statistically increased in *Lcmt1*$^{-/-}$ brain samples compared to *Lcmt1*$^{+/+}$. Phosphopeptides outside of two standard deviations from the average were considered significant for construction of this Venn diagram. Phosphopeptides identified as being increased or decreased in multiple studies are considered significant.

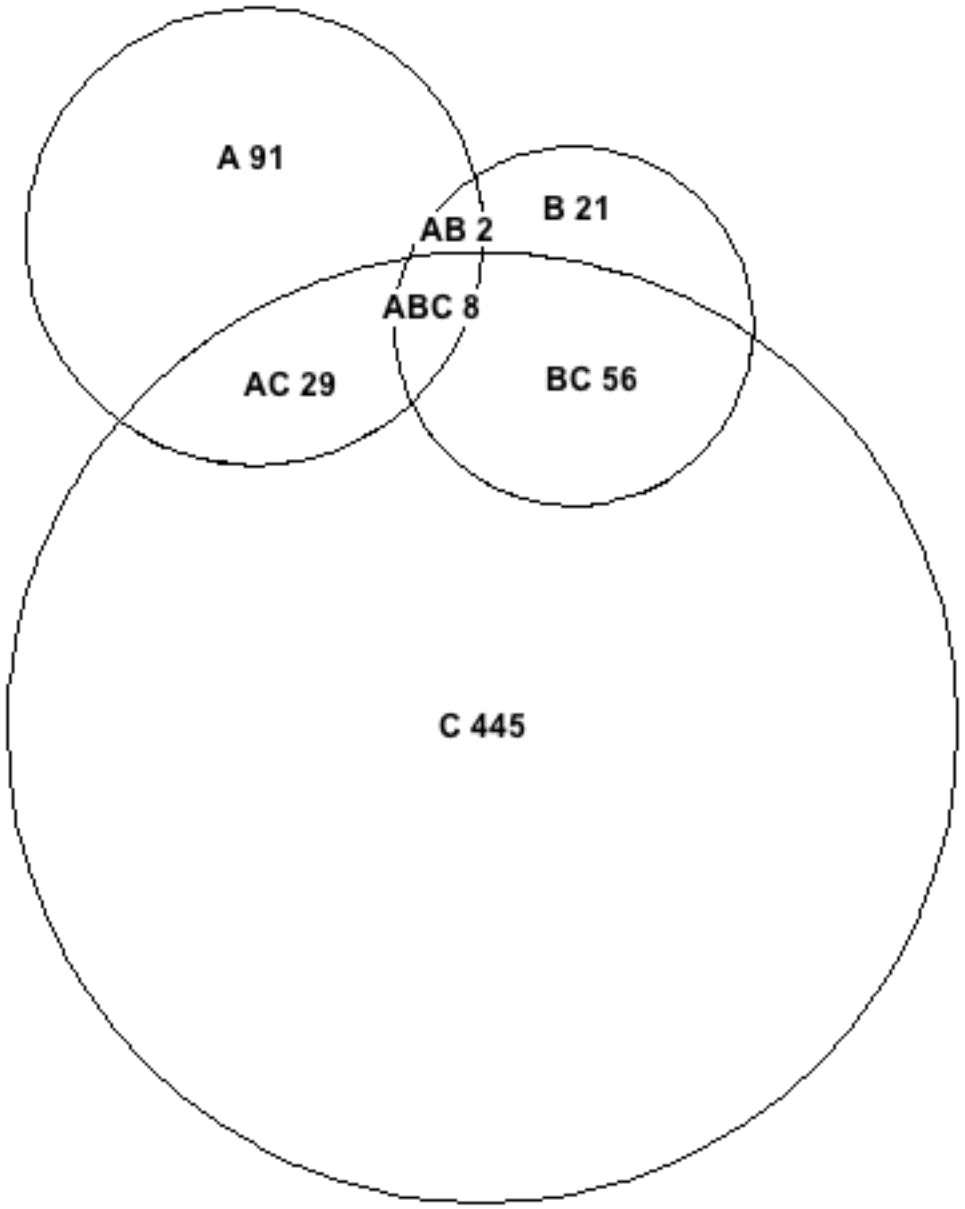

Figure 6: Venn diagram of phosphopeptides discovered in methods A, B, and C that are statistically decreased in *Lcmt1*$^{-/-}$ brain samples compared to *Lcmt1*$^{+/+}$. Phosphopeptides outside of two standard deviations from the average were considered significant for construction of this Venn diagram. Phosphopeptides

identified as being increased or decreased in multiple studies are considered significant.

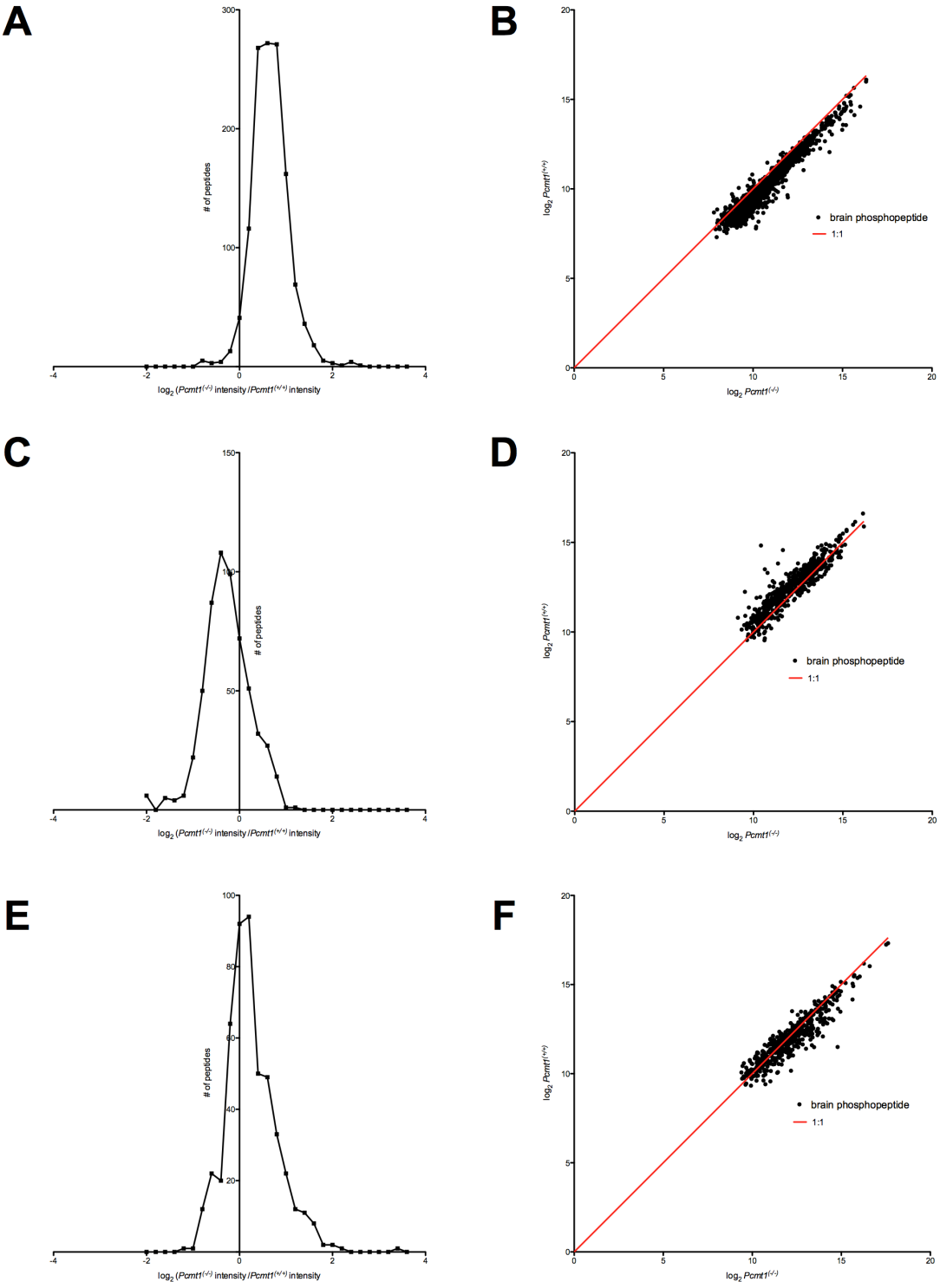
A
# of peptides
log2 (Pcmt1(-/-) intensity /Pcmt1(+/+) intensity
B
log2 Pcmt1(+/+)
log2 Pcmt1(-/-)
brain phosphopeptide
1:1
C
# of peptides
log2 (Pcmt1(-/-) intensity /Pcmt1(+/+) intensity
D
log2 Pcmt1(+/+)
log2 Pcmt1(-/-)
brain phosphopeptide
1:1
E
# of peptides
log2 (Pcmt1(-/-) intensity /Pcmt1(+/+) intensity
F
log2 Pcmt1(+/+)
log2 Pcmt1(-/-)
brain phosphopeptide
1:1

Figure 7: Comparison of *Pcmt1*$^{-/-}$ and *Pcmt1*$^{+/+}$ iTRAQ reporter ions from phosphopeptides isolated from brain samples separated using Method A, B, and C. Panel A, C, and E depict histograms comparing the relative quantitation of phosphopeptides from *Pcmt1*$^{-/-}$ and *Pcmt1*$^{+/+}$ brain samples using separation methods A, B, and C respectively. A. Log_2 normalization is utilized to decrease magnitude dependence during comparisons. Values greater than 0 indicate a greater *Pcmt1*$^{-/-}$ signal while values less than 0 indicate a greater *Pcmt1*$^{+/+}$ signal. Panels B, D, and F depict a comparative evaluation of the intensities of *Pcmt1*$^{-/-}$ and *Pcmt1*$^{+/+}$ iTRAQ reporter ions for each brain phosphopeptide identified employing method A, B, and C respectively. In panel A, the median value of peptides identified using method A was 1.21, and the average was 1.07 with a standard deviation of 0.99. In panel C, the median value of peptides identified using method B was -0.38, and the average was -0.37 with a standard deviation of 0.54. In panel E, the median value of peptides identified using method C was 0.08, and the average was 0.15 with a standard deviation of 0.55. iTRAQ reporter ions 2 standard deviations from the average were considered significantly altered in Table 4 and Figures 8-10.

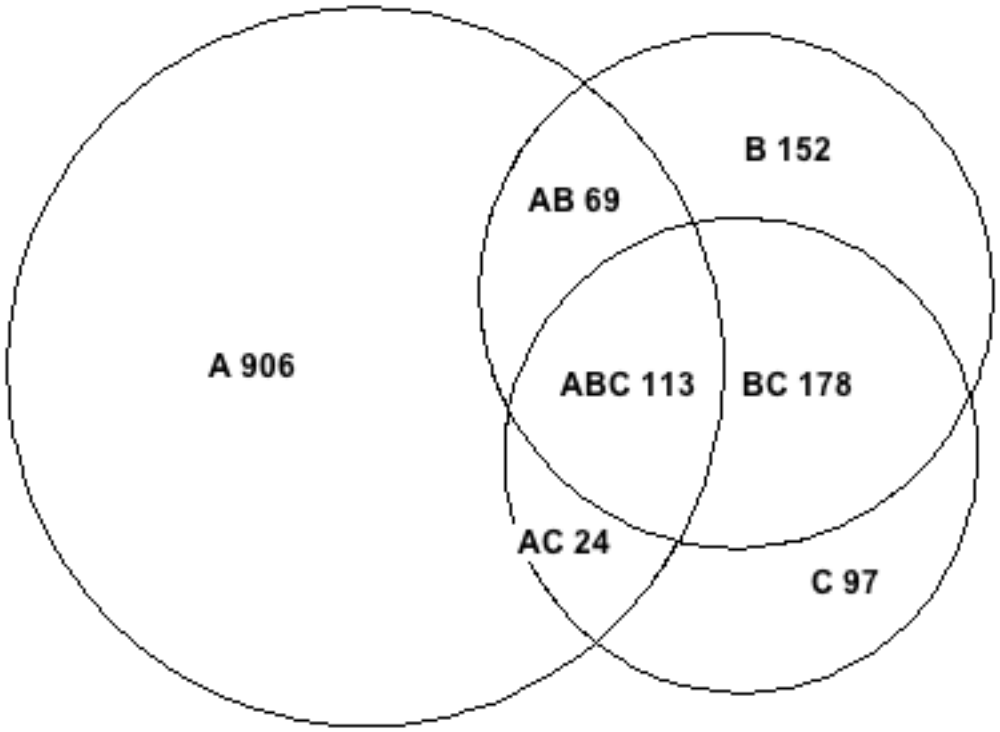

Figure 8: Venn Diagram depicting the specific peptides from *Pcmt1*$^{-/-}$ and *Pcmt1*$^{+/+}$ animals identified discovered in methods A, B, and C as well as identical peptides discovered in multiple methods. Unique phosphopeptides from each study were pooled and a Venn diagram was constructed showing overlap of peptides identified, as well as the number of unique phosphopeptides identified in each study.

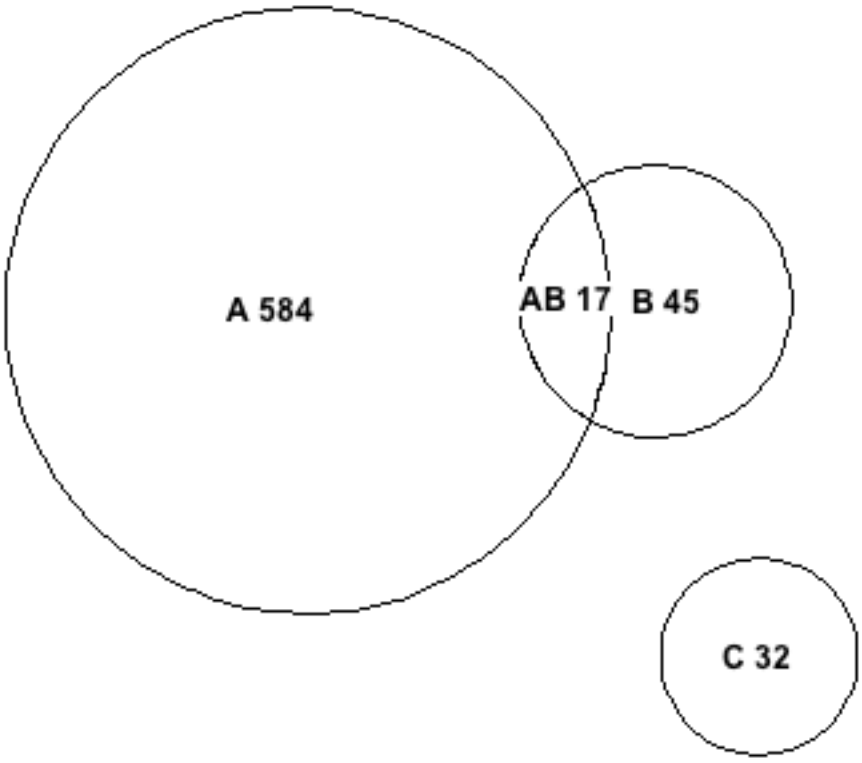

Figure 9: Venn diagram of phosphopeptides identified in methods A, B, and C statistically increased in *Pcmt1*$^{-/-}$ brain samples compared to *Pcmt1*$^{+/+}$. Phosphopeptides outside of two standard deviations from the average were considered significant for construction of this Venn diagram. Phosphopeptides identified as being increased or decreased in multiple studies are considered significant.

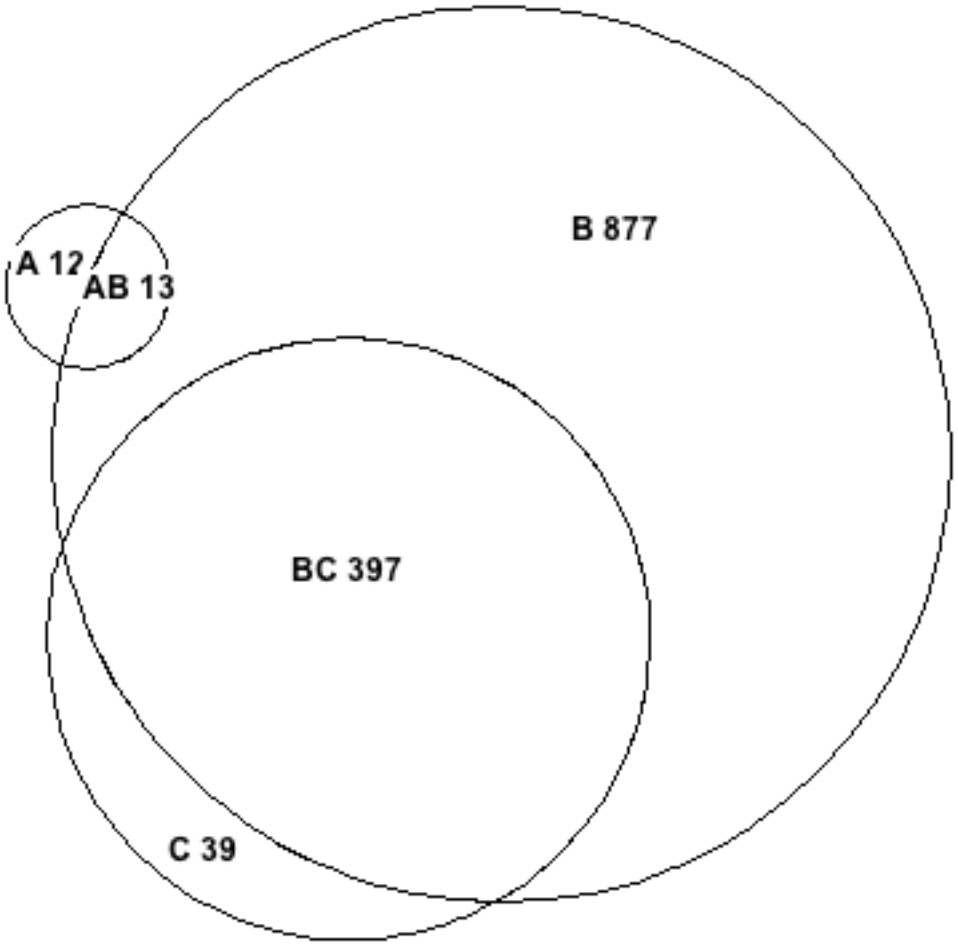

Figure 10: Venn diagram of phosphopeptides identified in methods A, B, and C statistically decreased in *Pcmt1*$^{-/-}$ brain samples compared to *Pcmt1*$^{+/+}$. Phosphopeptides outside of two standard deviations from the average were considered significant for construction of this Venn diagram. Phosphopeptides identified as being increased or decreased in multiple studies are considered significant.

Sample	Method	Peptides identified	Phospho-peptides	Non-phospho-peptides	% Phospho-peptides	Proteins represented
Lcmt1 Muscle	A	1058	510	548	48.2	228
Lcmt1 Brain	A	2117	1501	616	70.9	533
Lcmt1 Brain	B	975	714	261	73.2	262
Lcmt1 Brain	C	1087	879	208	80.9	306
Pcmt1 Brain	A	2274	1412	862	62.1	420
Pcmt1 Brain	B	585	398	187	68	158
Pcmt1 Brain	C	497	297	200	59.8	127

Table 1:

Summary of phosphopeptide identification utilizing each separation technique. Total number of peptides, number of phosphopeptides, non-phosphopeptides, the fraction of phosphopeptides, and the number of proteins represented by the peptides are compared.

Phosphopeptides discovered to be upregulated in *Lcmt1*$^{-/-}$ Muscle		
proteins	**peptides**	**phosphosite**
Dihydropyrimidinase-related protein 2	iTRAQ4plex-GLYDGPVC(Carbamidomethyl)EVSVT(Phospho)PK(iTRAQ4plex)	T509
DNA ligase 3	iTRAQ4plex-LT(Phospho)K(iTRAQ4plex)EDEQQQALQDIAS(Phospho)R	T393, S497, novel
Heat shock protein beta-1	iTRAQ4plex-SPS(Phospho)WEPFR	S15
L-lactate dehydrogenase A chain	iTRAQ4plex-S(Phospho)ADTLWGIQK(iTRAQ4plex)	S319 (novel)
Protein kinase C beta type	iTRAQ4plex-HPPVLT(Phospho)PPDQEVIR	T609

Phosphopeptides discovered to be downregulated in *Lcmt1*$^{-/-}$ Muscle		
proteins	**peptides**	**phosphosite**
Adherens junction-associated protein 1	iTRAQ4plex-M(Met-loss)WIQQLLGLSS(Phospho)M(Oxidation)SIR	S11, novel
Ankyrin repeat domain-containing protein 26	iTRAQ4plex-S(Phospho)K(iTRAQ4plex)GPS(Phospho)PLGPSARPR	S9, S13, novel
Beta-enolase	iTRAQ4plex-AAVPSGAS(Phospho)TGIYEALELRDGDK(iTRAQ4plex)	S37
Fructose-bisphosphate aldolase A	iTRAQ4plex-GILAADEST(Phospho)GSIAK(iTRAQ4plex)	S36
Fructose-bisphosphate	iTRAQ4plex-GILAADESTGS(Phospho)IAK(iTRAQ4plex)R	S39

aldolase A		
Laminin subunit alpha-3	iTRAQ4plex-AK(iTRAQ4plex)T(Phospho)LSSDSEELLNEAK(iTRAQ4plex)M(Oxidation)T(Phospho)QK(iTRAQ4plex)	T2218
Patatin-like phospholipase domain-containing protein 1	iTRAQ4plex-RLNAAY(Phospho)LDSPSK(iTRAQ4plex)R	Y262
Phosphoglycerate mutase 2	iTRAQ4plex-HY(Phospho)GGLTGLNK(iTRAQ4plex)	Y92
Protein NDRG2	iTRAQ4plex-TAS(Phospho)LTSAASIDGSR	S332
Protein odr-4 homolog	iTRAQ4plex-VTLHIC(Carbamidomethyl)S(Phospho)STK(iTRAQ4plex)K(iTRAQ4plex)	S142, novel
Retinoblastoma-associated protein	iTRAQ4plex-T(Phospho)AAIPINGSPRT(Phospho)PR	T235, T246, 1st novel
Rotatin	iTRAQ4plex-VAANALLS(Phospho)LLAVS(Phospho)RR	S1869, S1874, novel
Transient receptor potential cation channel subfamily M member 6	iTRAQ4plex-AVIAS(Phospho)ILY(Phospho)RAMAR	S648, Y651 novel
U8 snoRNA-decapping enzyme	iTRAQ4plex-SDYRS(Phospho)SHIAARPR	S97, novel

Table 2: Significantly increased and decreased phosphopeptides in *Lcmt1* Muscle.

Phosphopeptides identified as being significantly increased or decreased (2 or more standard deviations from the median) in multiple studies are considered significant.

Phosphopeptides discovered to be upregulated in *Lcmt1*$^{-/-}$ brain		
proteins	**peptides**	**phosphosite**
3-hydroxyacyl-CoA dehydratase 3	iTRAQ4plex-WLDES(Phospho)DAEM(Oxidation)ELR	S114
6-phosphofructokinase, liver type	iTRAQ4plex-TLS(Phospho)IDK(iTRAQ4plex)GF	S775
60S acidic ribosomal protein P1	iTRAQ4plex-K(iTRAQ4plex)EES(Phospho)EES(Phospho)EDDMGFGLFD	S101, S104
Actin-related protein 3B	iTRAQ4plex-HNPVFGVMS(Phospho)	S418
Alpha-enolase	iTRAQ4plex-YDLDFK(iTRAQ4plex)S(Phospho)PDDPSR	S263
Alpha-enolase	iTRAQ4plex-SGK(iTRAQ4plex)YDLDFK(iTRAQ4plex)S(Phospho) PDDPSR	S263
AP-3 complex subunit delta-1	iTRAQ4plex-VDIITEEMPENALPS(Phospho)DEDDK(iTRAQ4plex) DPNDPYR	S784
AP-3 complex subunit delta-1	iTRAQ4plex-HSSLPTES(Phospho)DEDIAPAQR	S760
AP2-associated protein kinase 1	iTRAQ4plex-S(Phospho)TQLLQAAAAEASLNK(iTRAQ4plex)	S650
Apolipoprotein E	iTRAQ4plex-NEVHTMLGQS(Phospho)TEEIR	S139
ARF GTPase-activating protein GIT1	iTRAQ4plex-SLSS(Phospho)PTDNLELSAR	S371
Ataxin-2-like protein	iTRAQ4plex-GPPQS(Phospho)PVFEGVYNNSR	S109
Bcl2 antagonist of cell	iTRAQ4plex-RMS(Phospho)DEFEGSFK(iTRAQ4plex)	S155

death		
Calcium/calmodulin-dependent 3',5'-cyclic nucleotide phosphodiesterase 1B	iTRAQ4plex-QPS(Phospho)LDVDVGDPNPDVVSFR	S465
Calcium/calmodulin-dependent 3',5'-cyclic nucleotide phosphodiesterase 1B	iTRAQ4plex-QPS(Phospho)LDVDVGDPNPDVVSFR	S465
Calcium/calmodulin-dependent protein kinase kinase 1	iTRAQ4plex-S(Phospho)FGNPFEPQAR	S458
Calcium/calmodulin-dependent protein kinase kinase 1	iTRAQ4plex-S(Phospho)FGNPFEPQAR	S458
Calcium/calmodulin-dependent protein kinase kinase 2	iTRAQ4plex-S(Phospho)FGNPFEGSR	S458
cAMP-regulated phosphoprotein 19	iTRAQ4plex-YFDS(Phospho)GDYNMAK(iTRAQ4plex)	S62
Connector enhancer of kinase suppressor of ras 2	iTRAQ4plex-LGDS(Phospho)LQDLYR	S906
Cyclin-dependent kinase-like 5	iTRAQ4plex-DLTNNNIPHLLS(Phospho)PK(iTRAQ4plex)	S407
Cyclin-Y	iTRAQ4plex-SAS(Phospho)ADNLILPR	S326
Cytoplasmic dynein 1 light intermediate chain 1	iTRAQ4plex-LIRDFQEYVEPGEDFPAS(Phospho)PQRR	S207

DCC-interacting protein 13-alpha	iTRAQ4plex-VNQSALEAVTPS(Phospho)PSFQQR	S401
Dematin	iTRAQ4plex-STS(Phospho)PPPSPEVWAESR	S92
Dematin	iTRAQ4plex-S(Phospho)TSPPPSPEVWAESR	S90
DmX-like protein 2	iTRAQ4plex-FGNVDADS(Phospho)PVEETIQDHSALK (iTRAQ4plex)	S1288
Dual specificity tyrosine-phosphorylation-regulated kinase 1A	iTRAQ4plex-IYQY(Phospho)IQSR	Y321
E3 ubiquitin-protein ligase UBR4	iTRAQ4plex-AAPPPPPPPPPLES(Phospho)SPR	S619
ELAV-like protein 2	iTRAQ4plex-TNQAILSQLYQS(Phospho)PNR	S221
Eukaryotic translation initiation factor 3 subunit C	iTRAQ4plex-QPLLLS(Phospho)EDEEDTK(iTRAQ4plex)R	S39
Eukaryotic translation initiation factor 3 subunit C	iTRAQ4plex-QPLLLS(Phospho)EDEEDTK(iTRAQ4plex)R	S39
F-actin-capping protein subunit beta	iTRAQ4plex-ELS(Phospho)QVLTQR	S263
Fructose-bisphosphate aldolase C	iTRAQ4plex-GILAADES(Phospho)VGSMAK(iTRAQ4plex)	S36
Galectin-related protein A	iTRAQ4plex-LDDGHLNNSLGS(Phospho)PVQADVYFPR	S25
Glucocorticoid receptor DNA-binding factor 1	iTRAQ4plex-TSFSVGS(Phospho)DDELGPIR	S1179
Glucose 1,6-bisphosphate	iTRAQ4plex-AVAGVMITAS(Phospho)HNR	

synthase		
Heterogeneous nuclear ribonucleoprotein H	iTRAQ4plex-HTGPNS(Phospho)PDTANDGFVR	S104
Iron-sulfur cluster assembly enzyme ISCU, mitochondrial	iTRAQ4plex-AAS(Phospho)ALLLR	novel
Kinesin light chain 2	iTRAQ4plex-ASS(Phospho)LNFLNK(iTRAQ4plex)	S579
Kinesin-like protein KIF1A	iTRAQ4plex-S(Phospho)DSLILDHQWELEK(iTRAQ4plex)	S1373
Kinesin-like protein KIF1B	iTRAQ4plex-SGLS(Phospho)LEELR	S1057
La-related protein 1	iTRAQ4plex-GLS(Phospho)ASLPDLDSESWIEVK(iTRAQ4plex)	S523
Microtubule-associated protein 1A	iTRAQ4plex-WLAES(Phospho)PVGLPPEEEDK(iTRAQ4plex)LTR	S1747
Microtubule-associated protein 1A	iTRAQ4plex-ALALVPGT(Phospho)PTR	T2182
Microtubule-associated protein 1A	iTRAQ4plex-SPFEIIS(Phospho)PPAS(Phospho)PPEMTGQR	S1768
Microtubule-associated protein 1A	iTRAQ4plex-ETS(Phospho)PTRGEPVPAWEGK (iTRAQ4plex)S(Phospho)PEQEVR	S1634
Microtubule-associated protein 1A	iTRAQ4plex-ELALS(Phospho)S(Phospho)PEDLTQDFEELK (iTRAQ4plex)R	S526
Microtubule-associated protein 1B	iTRAQ4plex-SPSLSPSPPS(Phospho)PIEK(iTRAQ4plex)	S1260

Microtubule-associated protein 1B	iTRAQ4plex-K(iTRAQ4plex)LGGDVSPT(Phospho)QIDVSQFGSFK(iTRAQ4plex)	T1499
Microtubule-associated protein 1B	iTRAQ4plex-DVMSDETNNEETES(Phospho)PSQEFVNITK(iTRAQ4plex)	S1151
Microtubule-associated protein 1B	iTRAQ4plex-ASLS(Phospho)PMDEPVPDS(Phospho)ESPVEK(iTRAQ4plex)	S1373, S1382
Microtubule-associated protein 2	iTRAQ4plex-ETS(Phospho)PETSLIQDEVALK(iTRAQ4plex)	S1161
Microtubule-associated protein 2	iTRAQ4plex-DGS(Phospho)PDAPATPEK(iTRAQ4plex)EEVAFSEYK(iTRAQ4plex)	S1352
Microtubule-associated protein 2	iTRAQ4plex-DGS(Phospho)PDAPAT(Phospho)PEK(iTRAQ4plex)EEVAFSEYK(iTRAQ4plex)	S1352
Microtubule-associated protein 2	iTRAQ4plex-VDHGAEIITQS(Phospho)PSR	S1783
mRNA cap guanine-N7 methyltransferase	iTRAQ4plex-EFGEDLVEQNSSYVQDS(Phospho)PSK(iTRAQ4plex)	S64
Neurobeachin	iTRAQ4plex-TPLENVPGNLS(Phospho)PIK(iTRAQ4plex)DPDR	S1529
Neurobeachin	iTRAQ4plex-AVPNVDAGSIIS(Phospho)DTER	S1262
Neurofilament medium polypeptide	iTRAQ4plex-GVVTNGLDVS(Phospho)PAEEK(iTRAQ4plex)	S769
Neuromodulin	iTRAQ4plex-QADVPAAVTDAAATT(Phospho)PAAEDAATK(iTRAQ4plex)	T172

NSFL1 cofactor p47	iTRAQ4plex-K(iTRAQ4plex)K(iTRAQ4plex)S(Phospho) PNELVDDLFK(iTRAQ4plex)	S114
Nuclear fragile X mental retardation-interacting protein 2	iTRAQ4plex-NDS(Phospho)WGSFDLR	S649
Pleckstrin homology domain-containing family O member 2	iTRAQ4plex-SSS(Phospho)LGDLLR	S395
Prostaglandin E synthase 3	iTRAQ4plex-DWEDDS(Phospho)DEDMSNFDR	S113
Protein FAM103A1	iTRAQ4plex-RPPES(Phospho)PPIVEEWNSR	S36
Protein FAM110B	iTRAQ4plex-ANS(Phospho)DIISLNFR	S297
Protein kinase C beta type	iTRAQ4plex-HPPVLT(Phospho)PPDQEVIR	T641
Protein kinase C gamma type	iTRAQ4plex-SPT(Phospho)SPVPVPVM(Oxidation)	T689
Protein kinase C gamma type	iTRAQ4plex-LVLASIDQADFQGFT(Phospho)YVNPDFVHPDAR	T674
Protein kinase C gamma type	iTRAQ4plex-AAPALT(Phospho)PPDRLVLASIDQADFQGFT (Phospho)YVNPDFVHPDAR	T655,T674
Protein lunapark	iTRAQ4plex-ADS(Phospho)VPNLEPSEESLVTK(iTRAQ4plex)	S411
Protein NDRG4	iTRAQ4plex-RLS(Phospho)GGAVPSASMTR	S298
Protein NDRG4	iTRAQ4plex-RLS(Phospho)GGAVPSASMTR	S298
Protein phosphatase 1 regulatory subunit 1B	iTRAQ4plex-ATLSEPGEEPQHPS(Phospho)PP	S192
Protein virilizer homolog	iTRAQ4plex-SFLSEPS(Phospho)SPGR	S1577

Protein-tyrosine kinase 2-beta	iTRAQ4plex-RNS(Phospho)LPQIPTLNLEAR	s375
Putative GTP-binding protein Parf	iTRAQ4plex-NISLS(Phospho)SEEEAEGLAGHPR	s482
R3H domain-containing protein 2	iTRAQ4plex-ASS(Phospho)FSGISILTR	s381
Regulator of microtubule dynamics protein 3	iTRAQ4plex-S(Phospho)HSLPNSLDYAQASER	s44
Reticulon-1	iTRAQ4plex-GSVS(Phospho)EDELIAAIK(iTRAQ4plex)	s352
Reticulon-1	iTRAQ4plex-GS(Phospho)VSEDELIAAIK(iTRAQ4plex)	s350
Reticulon-4	Acetyl-MEDIDQSSLVSSSADS(Phospho)PPRPPPAFK(iTRAQ4plex)	s16
Reticulon-4	Acetyl-M(Oxidation)EDIDQSSLVSSSADS(Phospho)PPRPPPAFK (iTRAQ4plex)	s16
RNA-binding protein 14	iTRAQ4plex-QPT(Phospho)PPFFGR	t206
Secretogranin-2	iTRAQ4plex-VPSPVS(Phospho)SEDDLQEEEQLEQAIK (iTRAQ4plex)	s532
Serine/arginine repetitive matrix protein 1	iTRAQ4plex-EK(iTRAQ4plex)S(Phospho)PELPEPSVR	s220
Serine/arginine repetitive matrix protein 2	iTRAQ4plex-VSS(Phospho)PVLETVQQR	s1360
Serine/arginine repetitive matrix protein 2	iTRAQ4plex-RVPS(Phospho)PTPVPK(iTRAQ4plex)	s2535

Serine/threonine-protein kinase B-raf	iTRAQ4plex-RDS(Phospho)SDDWEIPDGQITVGQR	s483
Serine/threonine-protein kinase DCLK1	iTRAQ4plex-REES(Phospho)EEGFQIPATITER	s392
Serine/threonine-protein kinase DCLK1	iTRAQ4plex-EES(Phospho)EEGFQIPATITER	s392
Serine/threonine-protein kinase PAK 1	iTRAQ4plex-DVATSPIS(Phospho)PTENNTTPPDALTR	s223
Small acidic protein	▫ iTRAQ4plex-S(Phospho)ASPDDDLGSSNWEAADLGNEER	
Sorting nexin-27	iTRAQ4plex-SES(Phospho)GYGFNVR	s49
Stathmin	iTRAQ4plex-SK(iTRAQ4plex)ESVPDFPLS(Phospho)PPK(iTRAQ4plex)	s38
Stathmin	iTRAQ4plex-RASGQAFELILS(Phospho)PR	s25
Stathmin	iTRAQ4plex-DLS(Phospho)LEEIQK(iTRAQ4plex)	s46
Stathmin	iTRAQ4plex-RAS(Phospho)GQAFELILSPR	s16
Stathmin	iTRAQ4plex-RAS(Phospho)GQAFELILS(Phospho)PR	s16
Stathmin	iTRAQ4plex-ASGQAFELILS(Phospho)PR	s26
Synaptopodin	iTRAQ4plex-VAS(Phospho)EEEEVPLVVYLK(iTRAQ4plex)	s258
Thyroid hormone receptor-associated protein 3	iTRAQ4plex-MDS(Phospho)FDEDLARPSGLLAQER	s572
TOM1-like protein 2	iTRAQ4plex-AAETVPDLPS(Phospho)PPTEAPAPASNTSTR	s479

TOM1-like protein 2	iTRAQ4plex-GIEFPM(Oxidation)ADLDALS(Phospho)PIHTPQR	s160
Transaldolase	iTRAQ4plex-TIVMGAS(Phospho)FR	s237
Transcription intermediary factor 1-beta	iTRAQ4plex-S(Phospho)GEGEVSGLLR	s473
Tubulin--tyrosine ligase-like protein 12	Acetyl-MEIQSGPQPGS(Phospho)PGR	s11
Tumor protein D54	iTRAQ4plex-HSIS(Phospho)MPVMR	s168
Ubiquitin-like modifier-activating enzyme 1	iTRAQ4plex-ATLPS(Phospho)PDK(iTRAQ4plex)LPGFK(iTRAQ4plex)	s835
Uncharacterized protein C10orf78 homolog	iTRAQ4plex-ENPPS(Phospho)PPT(Phospho)SPAAPQPR	s67/t70
Uncharacterized protein C10orf78 homolog	iTRAQ4plex-ENPPS(Phospho)PPTS(Phospho)PAAPQPR	s67/s71
Uncharacterized protein C10orf78 homolog	iTRAQ4plex-ENPPS(Phospho)PPTSPAAPQPR	s67
Vesicle-associated membrane protein 4	iTRAQ4plex-RNLLEDDS(Phospho)DEEEDFFLR	s30

Phosphopeptides discovered to be downregulated in *Lcmt1*$^{-/-}$ brain		
proteins	**peptides**	**phosphosite**
26S protease regulatory subunit 6A	Acetyl-M(Oxidation)QEM(Oxidation)NLLPTPES(Phospho)PVTR	S12

6-phosphofructokinase, liver type	iTRAQ4plex-TLS(Phospho)IDK(iTRAQ4plex)GF	s775
60S acidic ribosomal protein P1	iTRAQ4plex-K(iTRAQ4plex)EES(Phospho)EES(Phospho)EDDMGFGLFD	s101/s104
Actin-related protein 3B	iTRAQ4plex-HNPVFGVM(Oxidation)S(Phospho)	s418
Alpha-enolase	iTRAQ4plex-YDLDFK(iTRAQ4plex)S(Phospho)PDDPSR	s263
Astrocytic phosphoprotein PEA-15	iTRAQ4plex-YK(iTRAQ4plex)DIIRQPS(Phospho)EEEIIK(iTRAQ4plex)	s116
Astrocytic phosphoprotein PEA-15	iTRAQ4plex-DIIRQPS(Phospho)EEEIIK(iTRAQ4plex)	s116
Bcl2 antagonist of cell death	iTRAQ4plex-RMS(Phospho)DEFEGSFK(iTRAQ4plex)	s155
Biliverdin reductase A	iTRAQ4plex-S(Phospho)GSLEEVPNVGVNK(iTRAQ4plex)	s236
BR serine/threonine-protein kinase 1	iTRAQ4plex-NSFLGS(Phospho)PR	s563
Catechol O-methyltransferase	iTRAQ4plex-AVYQGPGS(Phospho)SPVK(iTRAQ4plex)S	s260?
Coatomer subunit epsilon	iTRAQ4plex-M(Met-loss)APPVPGAVSGGS(Phospho)GEVDELFDVK(iTRAQ4plex)	s13
Cytoplasmic dynein 1 light intermediate chain 1	iTRAQ4plex-DFQEYVEPGEDFPAS(Phospho)PQRR	s207
Dihydropyrimidinase-related protein 5	iTRAQ4plex-EMGT(Phospho)PLADT(Phospho)PTRPVTR	t509/t514

DmX-like protein 2	iTRAQ4plex-MK(iTRAQ4plex)LDHELS(Phospho)LDR	s451
Fructose-bisphosphate aldolase C	iTRAQ4plex-GILAADESVGS(Phospho)MAK(iTRAQ4plex)	s39
Galectin-related protein A	iTRAQ4plex-LDDGHLNNSLGS(Phospho)PVQADVYFPR	s25
Glucocorticoid receptor DNA-binding factor 1	iTRAQ4plex-TSFSVGS(Phospho)DDELGPIR	s1179
Glucose 1,6-bisphosphate synthase	iTRAQ4plex-AVAGVM(Oxidation)ITAS(Phospho)HNR	
GTP-binding protein 1	iTRAQ4plex-S(Phospho)RSPVDSPVPASMFAPEPS(Phospho)SPGAAR	s6/s24
Heterogeneous nuclear ribonucleoprotein H	iTRAQ4plex-HTGPNS(Phospho)PDTANDGFVR	s104
Heterogeneous nuclear ribonucleoproteins A2/B1	iTRAQ4plex-GFGDGYNGYGGGPGGGNFGGS(Phospho)PGYGGGR	s259
Importin subunit alpha-3	iTRAQ4plex-NVPQEES(Phospho)LEDSDVDADFK(iTRAQ4plex)	s56
IQ motif and SEC7 domain-containing protein 1	iTRAQ4plex-MQFS(Phospho)FEGPEK(iTRAQ4plex)	s179
MAP kinase-activating death domain protein	iTRAQ4plex-S(Phospho)LK(iTRAQ4plex) EENFVASVELWNK(iTRAQ4plex)	s1109
Microtubule-associated protein 1A	iTRAQ4plex-SPFEIIS(Phospho)PPAS(Phospho)PPEMTGQR	s1768/s1772
Microtubule-associated protein 1A	iTRAQ4plex-ELALS(Phospho)S(Phospho)PEDLTQDFEELK (iTRAQ4plex)R	s526/s527
Microtubule-associated	iTRAQ4plex-	s1634

protein 1A	ETS(Phospho)PTRGEPVPAWEGK(iTRAQ4plex)	
Microtubule-associated protein 1B	iTRAQ4plex-ES(Phospho)SPLYSPGFSDSTSAAK(iTRAQ4plex)	s1788
Microtubule-associated protein 1B	iTRAQ4plex-VLS(Phospho)PLRS(Phospho)PPLLGSESPYEDFLSADSK(iTRAQ4plex)	s1391/s1395
Microtubule-associated protein 1B	iTRAQ4plex-SPSLSPSPPS(Phospho)PIEK(iTRAQ4plex)	s1257
Microtubule-associated protein 1B	iTRAQ4plex-ES(Phospho)SPLYS(Phospho)PGFSDSTSAAK(iTRAQ4plex)	s1788/s1793
Microtubule-associated protein 2	iTRAQ4plex-VDHGAEIITQS(Phospho)PSR	s1783
Microtubule-associated protein 2	iTRAQ4plex-ARVDHGAEIITQS(Phospho)PSR	s1783
mRNA cap guanine-N7 methyltransferase	iTRAQ4plex-EFGEDLVEQNSSYVQDS(Phospho)PSK(iTRAQ4plex)	s64
Myocardin	iTRAQ4plex-SDRASLVTM(Oxidation)HILQAS(Phospho)T(Phospho)AER	novel
Neurofilament medium polypeptide	iTRAQ4plex-GVVTNGLDVS(Phospho)PAEEK(iTRAQ4plex)	s769
Phosphoacetylglucosamine mutase	iTRAQ4plex-STIGVMVTAS(Phospho)HNPEEDNGVK(iTRAQ4plex)	s64
Phosphoglycerate mutase 1	iTRAQ4plex-HGES(Phospho)AWNLENR	s14
Prostaglandin E synthase 3	iTRAQ4plex-DWEDDS(Phospho)DEDMSNFDR	s113
Prostaglandin E synthase 3	iTRAQ4plex-DWEDDS(Phospho)DEDM(Oxidation)SNFDR	s113
Prostaglandin E synthase 3	iTRAQ4plex-DVMSDETNNEETES(Phospho)	novel

	PSQEFVNITK(iTRAQ4plex)	
Protein FAM103A1	iTRAQ4plex-RPPES(Phospho)PPIVEEWNSR	s36
Protein FAM40A	iTRAQ4plex-AAS(Phospho)PPASASDLIEQQQK(iTRAQ4plex)	s335
Protein kinase C epsilon type	iTRAQ4plex-QINQEEFK(iTRAQ4plex)GFS(Phospho)YFGEDLMP	s729
Protein kinase C epsilon type	iTRAQ4plex-GFS(Phospho)YFGEDLMP	s729
Protein NDRG2	iTRAQ4plex-S(Phospho)RT(Phospho)ASLTSAASIDGSR	s328/t330
Protein phosphatase 1 regulatory subunit 1B	iTRAQ4plex-ATLSEPGEEPQHPS(Phospho)PP	s192
Serine/threonine-protein kinase B-raf	iTRAQ4plex-RDS(Phospho)SDDWEIPDGQITVGQR	s483
Serine/threonine-protein kinase PAK 1	iTRAQ4plex-DVATSPIS(Phospho)PTENNTTPPDALTR	s223
Serine/threonine-protein phosphatase 6 regulatory subunit 2	iTRAQ4plex-NVPGLAAPSS(Phospho)PTQK(iTRAQ4plex)	s670
SH3-containing GRB2-like protein 3-interacting protein 1	iTRAQ4plex-TVPAT(Phospho)PPRT(Phospho)GSPLTVATGNDQAATEAK(iTRAQ4plex)	t259/t263
SNW domain-containing protein 1	iTRAQ4plex-GPPS(Phospho)PPAPVMHS(Phospho)PSR	s224/s232
Stathmin	iTRAQ4plex-RAS(Phospho)GQAFELILSPR	s16
Stathmin	iTRAQ4plex-RAS(Phospho)GQAFELILS(Phospho)PR	s16/s25
Stathmin	iTRAQ4plex-ESVPDFPLS(Phospho)PPK(iTRAQ4plex)	s38
Stathmin	iTRAQ4plex-ASGQAFELILS(Phospho)PR	s25

Stathmin	iTRAQ4plex-AS(Phospho)GQAFELILSPR	s16
TOM1-like protein 2	iTRAQ4plex-AAETVPDLPS(Phospho)PPTEAPAPASNTSTR	s479
TOM1-like protein 2	iTRAQ4plex-GIEFPMADLDALS(Phospho)PIHTPQR	s160
Tubulin--tyrosine ligase-like protein 12	Acetyl-MEIQSGPQPGS(Phospho)PGR	s11
Uncharacterized protein C10orf78 homolog	iTRAQ4plex-ENPPS(Phospho)PPTSPAAPQPR	s67
Uncharacterized protein C10orf78 homolog	iTRAQ4plex-ENPPS(Phospho)PPT(Phospho)SPAAPQPR	s67/t70
Zinc finger Ran-binding domain-containing protein 2	iTRAQ4plex-ENVEYIEREES(Phospho)DGEYDEFGR	s120

Table 3: Altered phosphopeptides in *Lcmt1* brain samples. Phosphopeptides identified as being significantly increased or decreased (2 or more standard deviations from the median) in multiple studies are considered significant.

Phosphopeptides discovered to be upregulated in *Pcmt1*$^{-/-}$ brain		
proteins	**peptides**	**phosphosite**
26S protease regulatory subunit 6A	Acetyl-M(Oxidation)QEM(Oxidation)NLLPTPES(Phospho)PVTR	S12
5'-AMP-activated protein kinase subunit beta-2	iTRAQ4plex-DLSS(Phospho)SPPGPYGQEM(Oxidation)YVFR	S182
Ataxin-2-like protein	iTRAQ4plex-GPPQS(Phospho)PVFEGVYNNSR	S109
Dihydropyrimidinase-related protein 1	iTRAQ4plex-GM(Oxidation)YDGPVYEVPAT(Phospho)PK(iTRAQ4plex)	T509
Dihydropyrimidinase-related protein 2	iTRAQ4plex-NLHQS(Phospho)GFSLSGAQIDDNIPR	S537
ELAV-like protein 4	iTRAQ4plex-SSQALLSQLYQS(Phospho)PNR	S233
Galectin-related protein A	iTRAQ4plex-LDDGHLNNSLGS(Phospho)PVQADVYFPR	S25
Microtubule-associated protein 1B	iTRAQ4plex-DLTGQVPT(Phospho)PPVK(iTRAQ4plex)	T527
Phosphoglucomutase-1	iTRAQ4plex-AIGGIILTAS(Phospho)HNPGGPNGDFGIK(iTRAQ4plex)	S117
RNA-binding protein 14	iTRAQ4plex-QPT(Phospho)PPFFGR	T206
SH3-containing GRB2-like protein 3-interacting protein 1	iTRAQ4plex-AT(Phospho)PPPPPPPTYR	T409
Stathmin	iTRAQ4plex-ESVPDFPLS(Phospho)PPK(iTRAQ4plex)	S38

TOM1-like protein 2	iTRAQ4plex-GIEFPMADLDALS(Phospho)PIHTPQR	S160

Phosphopeptides discovered to be downregulated in *Pcmt1*$^{-/-}$ brain		
proteins	**peptides**	**phosphosite**
26S proteasome non-ATPase regulatory subunit 9	iTRAQ4plex-LASNS(Phospho)PVLPQAFAR	S128
3-hydroxyacyl-CoA dehydratase 3	iTRAQ4plex-WLDES(Phospho)DAEMELR	novel
3-hydroxyacyl-CoA dehydratase 3	iTRAQ4plex-WLDES(Phospho)DAEM(Oxidation)ELR	novel
40S ribosomal protein S3	iTRAQ4plex-DEILPTT(Phospho)PISEQK(iTRAQ4plex)	T221
5'-AMP-activated protein kinase subunit beta-2	iTRAQ4plex-DLSS(Phospho)SPPGPYGQEMYVFR	S182
Actin-related protein 3B	iTRAQ4plex-HNPVFGVMS(Phospho)	S418
Actin-related protein 3B	iTRAQ4plex-HNPVFGVM(Oxidation)S(Phospho)	S418
Alpha-enolase	iTRAQ4plex-YDLDFK(iTRAQ4plex)S(Phospho)PDDPSR	S263
Ankyrin-2	iTRAQ4plex-S(Phospho)PQGLELPLPNR	S2364
AP2-associated protein kinase 1	iTRAQ4plex-S(Phospho)TQLLQAAAAEASLNK(iTRAQ4plex)	S650
Band 4.1-like protein 1	iTRAQ4plex-SLS(Phospho)PIIGK(iTRAQ4plex)	S782
Band 4.1-like protein 3	iTRAQ4plex-GIS(Phospho)QTNLITTVTPEK(iTRAQ4plex)	S486
BolA-like protein 1	iTRAQ4plex-FEGMS(Phospho)PLQR	S81

BR serine/threonine-protein kinase 1	iTRAQ4plex-STPLPGPPGS(Phospho)PR	S508
BR serine/threonine-protein kinase 1	iTRAQ4plex-S(Phospho)PVFSFSPEPGAGDEAR	S450
BR serine/threonine-protein kinase 1	iTRAQ4plex-NSFLGS(Phospho)PR	S563
BTB/POZ domain-containing protein KCTD8	iTRAQ4plex-RNS(Phospho)ELFQSLISK(iTRAQ4plex)	S413
Calcium/calmodulin-dependent 3',5'-cyclic nucleotide phosphodiesterase 1B	iTRAQ4plex-QPS(Phospho)LDVDVGDPNPDVVSFR	S465
Calcium/calmodulin-dependent protein kinase kinase 1	iTRAQ4plex-S(Phospho)FGNPFEPQAR	S458
Calcium/calmodulin-dependent protein kinase kinase 2	iTRAQ4plex-SLS(Phospho)APGNLLTK(iTRAQ4plex)	S511
Calcium/calmodulin-dependent protein kinase kinase 2	iTRAQ4plex-S(Phospho)FGNPFEGSR	S495
Connector enhancer of kinase suppressor of ras 2	iTRAQ4plex-LGDS(Phospho)LQDLYR	S906
Creatine kinase B-type	iTRAQ4plex-VLT(Phospho)PELYAELR	T35
Cyclin-dependent kinase-like 5	iTRAQ4plex-DLTNNNIPHLLS(Phospho)PK(iTRAQ4plex)	S407

Cysteine and glycine-rich protein 1	iTRAQ4plex-GFGFGQGAGALVHS(Phospho)E	S192
Cytoplasmic phosphatidylinositol transfer protein 1	iTRAQ4plex-S(Phospho)APETLTLPDPEK(iTRAQ4plex)K (iTRAQ4plex)	S309
Dapper homolog 3	iTRAQ4plex-AFSFPVS(Phospho)PER	S10
Dematin	iTRAQ4plex-STS(Phospho)PPPSPEVWAESR	S92
Dematin	iTRAQ4plex-S(Phospho)TSPPPSPEVWAESR	S90
Dematin	iTRAQ4plex-GNS(Phospho)LPC(Carbamidomethyl) VLEQK(iTRAQ4plex)	S333
Dematin	iTRAQ4plex-DSSVPGS(Phospho)PSSIVAK(iTRAQ4plex)	S26
Dihydropyrimidinase-related protein 2	iTRAQ4plex-GLYDGPVC(Carbamidomethyl)EVSVT (Phospho)PK(iTRAQ4plex)	T509
DmX-like protein 2	iTRAQ4plex-FGNVDADS(Phospho)PVEETIQDHSALK(iTRAQ4plex)	S1288
DmX-like protein 2	iTRAQ4plex-NLAS(Phospho)PEGTLATLGLK(iTRAQ4plex)	S1856
DnaJ homolog subfamily C member 5	iTRAQ4plex-SLSTS(Phospho)GESLYHVLGLDK(iTRAQ4plex)	S12
DnaJ homolog subfamily C member 5	iTRAQ4plex-SLS(Phospho)TSGESLYHVLGLDK(iTRAQ4plex)	S10
DnaJ homolog subfamily C member 5	iTRAQ4plex-S(Phospho)LSTSGESLYHVLGLDK(iTRAQ4plex)	S8
E3 ubiquitin-protein ligase NEDD4-like	iTRAQ4plex-S(Phospho)LSSPTVTLSAPLEGAK(iTRAQ4plex)	S475
ELAV-like protein 2	iTRAQ4plex-TNQAILSQLYQS(Phospho)PNR	S221

ELAV-like protein 4	iTRAQ4plex-SSQALLSQLYQS(Phospho)PNR	S233
Endophilin-B2	iTRAQ4plex-VPVTYLELLS(Phospho)	S400
Endophilin-B2	iTRAQ4plex-GK(iTRAQ4plex)VPVTYLELLS(Phospho)	S400
Fructose-bisphosphate aldolase A	iTRAQ4plex-GILAADES(Phospho)TGSIAK(iTRAQ4plex)	S36
Fructose-bisphosphate aldolase C	iTRAQ4plex-GILAADES(Phospho)VGSM(Oxidation)AK(iTRAQ4plex)	S36
G protein-regulated inducer of neurite outgrowth 1	iTRAQ4plex-VDIVS(Phospho)PGGDNAGSLR	S182
Galectin-related protein A	iTRAQ4plex-LDDGHLNNSLGS(Phospho)PVQADVYFPR	S25
GRIP1-associated protein 1	iTRAQ4plex-TGLEELVLSEMNS(Phospho)PSR	S620
Heat shock 70 kDa protein 4L	iTRAQ4plex-S(Phospho)FDDPIVQTER	S74
IQ motif and SEC7 domain-containing protein 1	iTRAQ4plex-NSWDS(Phospho)PAFSNDVIR	S513
IQ motif and SEC7 domain-containing protein 1	iTRAQ4plex-NS(Phospho)WDSPAFSNDVIR	S510
La-related protein 1	iTRAQ4plex-S(Phospho)LPTTVPESPNYR	S743
Microtubule-associated protein 1A	iTRAQ4plex-SPFEIISPPAS(Phospho)PPEMTGQR	s1772
Microtubule-associated protein 1A	iTRAQ4plex-SPFEIIS(Phospho)PPAS(Phospho) PPEMTGQR	s1768, s1772
Microtubule-associated protein 1A	iTRAQ4plex-SPFEIIS(Phospho)PPAS(Phospho) PPEM(Oxidation)TGQR	s1768, s1772
Microtubule-associated	iTRAQ4plex-QLS(Phospho)PESLGTLQFGELSLGK	S1205

protein 1A	(iTRAQ4plex)	
Microtubule-associated protein 1A	iTRAQ4plex-ALALVPGT(Phospho)PTR	T2182
Microtubule-associated protein 1B	iTRAQ4plex-SPSLSPSPPS(Phospho)PIEK(iTRAQ4plex)	S1260
Microtubule-associated protein 2	iTRAQ4plex-SDT(Phospho)LQISDLLVSESR	T1260
Microtubule-associated protein 2	iTRAQ4plex-ETS(Phospho)PETSLIQDEVALK(iTRAQ4plex)	S1161
Microtubule-associated protein tau	iTRAQ4plex-TPSLPT(Phospho)PPTR	T509
Myosin-10	iTRAQ4plex-GGPISFSS(Phospho)SR	S1938
Myristoylated alanine-rich C-kinase substrate	iTRAQ4plex-LSGFS(Phospho)FK(iTRAQ4plex)	S163
Neurobeachin	iTRAQ4plex-TPLENVPGNLS(Phospho)PIK(iTRAQ4plex)DPDR	S1519
Nucleolin	iTRAQ4plex-NLS(Phospho)FNITEDELK(iTRAQ4plex)	S403
Polyubiquitin-B	iTRAQ4plex-TLS(Phospho)DYNIQK(iTRAQ4plex)	S133 OR S209
Protein FAM169A	iTRAQ4plex-T(Phospho)LLGSSDNVATVSNIEK (iTRAQ4plex)	T519, NOVEL
Protein kinase C beta type	iTRAQ4plex-HPPVLT(Phospho)PPDQEVIR	T609
Protein kinase C delta type	iTRAQ4plex-NLIDSM(Oxidation)DQEAFHGFS(Phospho)FVNPK(iTRAQ4plex)	S662
Protein kinase C gamma type	iTRAQ4plex-SPT(Phospho)SPVPVPVM(Oxidation)	T689

Protein kinase C gamma type	iTRAQ4plex-S(Phospho)PTSPVPVPVM(Oxidation)	S687
Protein kinase C gamma type	iTRAQ4plex-LVLASIDQADFQGFT(Phospho) YVNPDFVHPDAR	T674
Protein phosphatase 1 regulatory subunit 14A	iTRAQ4plex-QPGFPQPSPSDDPSLS(Phospho)PR	S136
Protein phosphatase 1 regulatory subunit 1B	iTRAQ4plex-ATLSEPGEEPQHPS(Phospho)PP	S192
R3H domain-containing protein 2	iTRAQ4plex-SAS(Phospho)TDLGTADVVLGR	S923
R3H domain-containing protein 2	iTRAQ4plex-ASS(Phospho)FSGISILTR	S381
Rab3 GTPase-activating protein non-catalytic subunit	iTRAQ4plex-GGFS(Phospho)PFGNTQGPSR	S448
Reticulon-1	iTRAQ4plex-GSVS(Phospho)EDELIAAIK(iTRAQ4plex)	S352
Rho guanine nucleotide exchange factor 2	iTRAQ4plex-SVSTTNIAGHFNDES(Phospho)PLGLR	S163
Ribosomal protein S6 kinase delta-1	iTRAQ4plex-SS(Phospho)PDQFLFSSLR	S779
Serine/arginine repetitive matrix protein 2	iTRAQ4plex-NSGPVSEVNTGFS(Phospho)PEVK(iTRAQ4plex)	S1305
Serine/arginine repetitive matrix protein 2	iTRAQ4plex-VSS(Phospho)PVLETVQQR	S1360
Serine/arginine-rich splicing factor 10	iTRAQ4plex-S(Phospho)FDYNYR	

Serine/threonine-protein kinase 11	iTRAQ4plex-IDS(Phospho)TEVIYQPR	S31
Serine/threonine-protein kinase PAK 1	iTRAQ4plex-DVATSPIS(Phospho)PTENNTTPPDALTR	S223
Stathmin	iTRAQ4plex-SK(iTRAQ4plex)ESVPDFPLS(Phospho) PPK(iTRAQ4plex)	S38
Stathmin	iTRAQ4plex-ESVPDFPLS(Phospho)PPK(iTRAQ4plex)	S38
Stathmin	iTRAQ4plex-ASGQAFELILS(Phospho)PR	S25
Stathmin	iTRAQ4plex-AS(Phospho)GQAFELILSPR	S16
Striatin-3	iTRAQ4plex-NLEQILNGGES(Phospho)PK(iTRAQ4plex)	S229
Stromal membrane-associated protein 2	iTRAQ4plex-DLDLLASVPS(Phospho)PSSVSR	S219
Synaptopodin	iTRAQ4plex-VAS(Phospho)EEEEVPLVVYLK (iTRAQ4plex)	S258
Syntaxin-7	iTRAQ4plex-TLNQLGT(Phospho)PQDSPELR	T41
Thyroid hormone receptor-associated protein 3	iTRAQ4plex-IDIS(Phospho)PSTFR	S679
TOM1-like protein 2	iTRAQ4plex-GIEFPMADLDALS(Phospho)PIHTPQR	S160
Transmembrane and coiled-coil domains protein 1	iTRAQ4plex-ALGVISNFQS(Phospho)SPK(iTRAQ4plex)	S409 - NOVEL
Triple functional domain protein	iTRAQ4plex-NFLNALTS(Phospho)PIEYQR	S2282
Uncharacterized protein C10orf78 homolog	iTRAQ4plex-ENPPS(Phospho)PPTSPAAPQPR	S67 OR S83 OR S99
WD repeat-containing	iTRAQ4plex-S(Phospho)SSQIPEGFGLTSGGSNYSLAR	S1151

protein 7		

Table 4: Significantly altered phosphopeptides in *Pcmt1*$^{-/-}$ brain samples.

Phosphopeptides identified as being significantly increased or decreased (2 or more standard deviations from the median) in multiple studies are considered significant.

REFERENCES

1. Dissmeyer N, Schnittger A (2011) The age of protein kinases. Methods in molecular biology 779: 7-52.
2. Schulze WX (2010) Proteomics approaches to understand protein phosphorylation in pathway modulation. Current opinion in plant biology 13: 280-287.
3. Manning G, Plowman GD, Hunter T, Sudarsanam S (2002) Evolution of protein kinase signaling from yeast to man. Trends in biochemical sciences 27: 514-520.
4. Chevalier D, Walker JC (2005) Functional genomics of protein kinases in plants. Briefings in functional genomics & proteomics 3: 362-371.
5. Hubbard MJ, Cohen P (1993) On target with a new mechanism for the regulation of protein phosphorylation. Trends in biochemical sciences 18: 172-177.
6. Ahn NG, Resing KA (2001) Toward the phosphoproteome. Nature biotechnology 19: 317-318.
7. Johnson LN, Barford D (1993) The effects of phosphorylation on the structure and function of proteins. Annual review of biophysics and biomolecular structure 22: 199-232.
8. Groban ES, Narayanan A, Jacobson MP (2006) Conformational changes in protein loops and helices induced by post-translational phosphorylation. PLoS computational biology 2: e32.

9. Chong PK, Lee H, Kong JW, Loh MC, Wong CH, Lim YP (2008) Phosphoproteomics, oncogenic signaling and cancer research. Proteomics 8: 4370-4382.

10. Turjanski AG, Vaque JP, Gutkind JS (2007) MAP kinases and the control of nuclear events. Oncogene 26: 3240-3253.

11. Rando OJ (2012) Combinatorial complexity in chromatin structure and function: revisiting the histone code. Current opinion in genetics & development 22: 148-155.

12. Linggi BE, Brandt SJ, Sun ZW, Hiebert SW (2005) Translating the histone code into leukemia. Journal of cellular biochemistry 96: 938-950.

13. Jenuwein T, Allis CD (2001) Translating the histone code. Science 293: 1074-1080.

14. Banerjee T, Chakravarti D (2011) A peek into the complex realm of histone phosphorylation. Molecular and cellular biology 31: 4858-4873.

15. Britton LM, Gonzales-Cope M, Zee BM, Garcia BA (2011) Breaking the histone code with quantitative mass spectrometry. Expert review of proteomics 8: 631-643.

16. Clarke S (2003) Aging as war between chemical and biochemical processes: protein methylation and the recognition of age-damaged proteins for repair. Ageing research reviews 2: 263-285.

17. Yamamoto A, Takagi H, Kitamura D, Tatsuoka H, Nakano H, Kawano H, Kuroyanagi H, Yahagi Y, Kobayashi S, Koizumi K, Sakai T, Saito K, Chiba T, Kawamura K, Suzuki K, Watanabe T, Mori H, Shirasawa T (1998) Deficiency in protein L-isoaspartyl methyltransferase results in a fatal progressive

epilepsy. The Journal of neuroscience : the official journal of the Society for Neuroscience 18: 2063-2074.

18. Kim E, Lowenson JD, Clarke S, Young SG (1999) Phenotypic analysis of seizure-prone mice lacking L-isoaspartate (D-aspartate) O-methyltransferase. The Journal of biological chemistry 274: 20671-20678.

19. Kim E, Lowenson JD, MacLaren DC, Clarke S, Young SG (1997) Deficiency of a protein-repair enzyme results in the accumulation of altered proteins, retardation of growth, and fatal seizures in mice. Proceedings of the National Academy of Sciences of the United States of America 94: 6132-6137.

20. Farrar C, Houser CR, Clarke S (2005) Activation of the PI3K/Akt signal transduction pathway and increased levels of insulin receptor in protein repair-deficient mice. Aging cell 4: 1-12.

21. Farrar CE, Huang CS, Clarke SG, Houser CR (2005) Increased cell proliferation and granule cell number in the dentate gyrus of protein repair-deficient mice. The Journal of comparative neurology 493: 524-537.

22. Ikegaya Y, Yamada M, Fukuda T, Kuroyanagi H, Shirasawa T, Nishiyama N (2001) Aberrant synaptic transmission in the hippocampal CA3 region and cognitive deterioration in protein-repair enzyme-deficient mice. Hippocampus 11: 287-298.

23. Kosugi S, Furuchi T, Katane M, Sekine M, Shirasawa T, Homma H (2008) Suppression of protein l-isoaspartyl (d-aspartyl) methyltransferase results in hyperactivation of EGF-stimulated MEK-ERK signaling in cultured

mammalian cells. Biochemical and biophysical research communications 371: 22-27.

24. Doyle HA, Gee RJ, Mamula MJ (2003) A failure to repair self-proteins leads to T cell hyperproliferation and autoantibody production. Journal of immunology 171: 2840-2847.

25. Furuchi T, Sakurako K, Katane M, Sekine M, Homma H (2010) The role of protein L-isoaspartyl/D-aspartyl O-methyltransferase (PIMT) in intracellular signal transduction. Chemistry & biodiversity 7: 1337-1348.

26. Cournoyer P, Desrosiers RR (2009) Valproic acid enhances protein L-isoaspartyl methyltransferase expression by stimulating extracellular signal-regulated kinase signaling pathway. Neuropharmacology 56: 839-848.

27. Ryu J, Song J, Heo J, Jung Y, Lee SJ, Hong S, Cho JY (2011) Cross-regulation between protein L-isoaspartyl O-methyltransferase and ERK in epithelial mesenchymal transition of MDA-MB-231 cells. Acta pharmacologica Sinica 32: 1165-1172.

28. Furuchi T, Homma H (2007) [Role of isomerized protein repair enzyme, PIMT, in cellular functions]. Yakugaku zasshi : Journal of the Pharmaceutical Society of Japan 127: 1927-1936.

29. Dutta T, Banerjee S, Soren D, Lahiri S, Sengupta S, Rasquinha JA, Ghosh AK (2012) Regulation of Enzymatic Activity by Deamidation and Their Subsequent Repair by Protein L-isoaspartyl Methyl Transferase. Applied biochemistry and biotechnology.

30. Park JW, Lee JC, Ha SW, Bang SY, Park EK, Yi SA, Lee MG, Kim DS, Nam KH, Yoo JH, Kwon SH, Han JW (2012) Requirement of protein l-isoaspartyl O-methyltransferase for transcriptional activation of trefoil factor 1 (TFF1) gene by estrogen receptor alpha. Biochemical and biophysical research communications 420: 223-229.

31. Lee JC, Kang SU, Jeon Y, Park JW, You JS, Ha SW, Bae N, Lubec G, Kwon SH, Lee JS, Cho EJ, Han JW (2012) Protein L-isoaspartyl methyltransferase regulates p53 activity. Nature communications 3: 927.

32. De Baere I, Derua R, Janssens V, Van Hoof C, Waelkens E, Merlevede W, Goris J (1999) Purification of porcine brain protein phosphatase 2A leucine carboxyl methyltransferase and cloning of the human homologue. Biochemistry 38: 16539-16547.

33. Lee J, Chen Y, Tolstykh T, Stock J (1996) A specific protein carboxyl methylesterase that demethylates phosphoprotein phosphatase 2A in bovine brain. Proceedings of the National Academy of Sciences of the United States of America 93: 6043-6047.

34. Ogris E, Du X, Nelson KC, Mak EK, Yu XX, Lane WS, Pallas DC (1999) A protein phosphatase methylesterase (PME-1) is one of several novel proteins stably associating with two inactive mutants of protein phosphatase 2A. The Journal of biological chemistry 274: 14382-14391.

35. Tolstykh T, Lee J, Vafai S, Stock JB (2000) Carboxyl methylation regulates phosphoprotein phosphatase 2A by controlling the association of regulatory B subunits. The EMBO journal 19: 5682-5691.

36. Wu J, Tolstykh T, Lee J, Boyd K, Stock JB, Broach JR (2000) Carboxyl methylation of the phosphoprotein phosphatase 2A catalytic subunit promotes its functional association with regulatory subunits in vivo. The EMBO journal 19: 5672-5681.

37. Wei H, Ashby DG, Moreno CS, Ogris E, Yeong FM, Corbett AH, Pallas DC (2001) Carboxymethylation of the PP2A catalytic subunit in Saccharomyces cerevisiae is required for efficient interaction with the B-type subunits Cdc55p and Rts1p. The Journal of biological chemistry 276: 1570-1577.

38. Yu XX, Du X, Moreno CS, Green RE, Ogris E, Feng Q, Chou L, McQuoid MJ, Pallas DC (2001) Methylation of the protein phosphatase 2A catalytic subunit is essential for association of Balpha regulatory subunit but not SG2NA, striatin, or polyomavirus middle tumor antigen. Molecular biology of the cell 12: 185-199.

39. Longin S, Zwaenepoel K, Louis JV, Dilworth S, Goris J, Janssens V (2007) Selection of protein phosphatase 2A regulatory subunits is mediated by the C terminus of the catalytic Subunit. The Journal of biological chemistry 282: 26971-26980.

40. Mumby M (2001) A new role for protein methylation: switching partners at the phosphatase ball. Science's STKE : signal transduction knowledge environment 2001: pe1.

41. Janssens V, Goris J (2001) Protein phosphatase 2A: a highly regulated family of serine/threonine phosphatases implicated in cell growth and signalling. The Biochemical journal 353: 417-439.

42. Sontag E (2001) Protein phosphatase 2A: the Trojan Horse of cellular signaling. Cellular signalling 13: 7-16.

43. Janssens V, Longin S, Goris J (2008) PP2A holoenzyme assembly: in cauda venenum (the sting is in the tail). Trends in biochemical sciences 33: 113-121.

44. Longin S, Zwaenepoel K, Martens E, Louis JV, Rondelez E, Goris J, Janssens V (2008) Spatial control of protein phosphatase 2A (de)methylation. Experimental cell research 314: 68-81.

45. Lanthier J, Desrosiers RR (2006) Regulation of protein L-isoaspartyl methyltransferase by cell-matrix interactions: involvement of integrin alphavbeta3, PI 3-kinase, and the proteasome. Biochemistry and cell biology = Biochimie et biologie cellulaire 84: 684-694.

46. Huebscher KJ, Lee J, Rovelli G, Ludin B, Matus A, Stauffer D, Furst P (1999) Protein isoaspartyl methyltransferase protects from Bax-induced apoptosis. Gene 240: 333-341.

47. Cimmino A, Capasso R, Muller F, Sambri I, Masella L, Raimo M, De Bonis ML, D'Angelo S, Zappia V, Galletti P, Ingrosso D (2008) Protein isoaspartate methyltransferase prevents apoptosis induced by oxidative stress in endothelial cells: role of Bcl-Xl deamidation and methylation. PloS one 3: e3258.

48. Yang H, Fung EY, Zubarev AR, Zubarev RA (2009) Toward proteome-scale identification and quantification of isoaspartyl residues in biological samples. Journal of proteome research 8: 4615-4621.

49. Vigneswara V, Lowenson JD, Powell CD, Thakur M, Bailey K, Clarke S, Ray DE, Carter WG (2006) Proteomic identification of novel substrates of a protein isoaspartyl methyltransferase repair enzyme. The Journal of biological chemistry 281: 32619-32629.

50. Ortega-Gutierrez S, Leung D, Ficarro S, Peters EC, Cravatt BF (2008) Targeted disruption of the PME-1 gene causes loss of demethylated PP2A and perinatal lethality in mice. PloS one 3: e2486.

51. Zieske LR (2006) A perspective on the use of iTRAQ reagent technology for protein complex and profiling studies. Journal of experimental botany 57: 1501-1508.

52. Sundaram M, Cook HW, Byers DM (2004) The MARCKS family of phospholipid binding proteins: regulation of phospholipase D and other cellular components. Biochemistry and cell biology = Biochimie et biologie cellulaire 82: 191-200.

53. Larsson C (2006) Protein kinase C and the regulation of the actin cytoskeleton. Cellular signalling 18: 276-284.

54. Lowry OH, Rosebrough NJ, Farr AL, Randall RJ (1951) Protein measurement with the Folin phenol reagent. The Journal of biological chemistry 193: 265-275.

55. Huttlin EL, Jedrychowski MP, Elias JE, Goswami T, Rad R, Beausoleil SA, Villen J, Haas W, Sowa ME, Gygi SP (2010) A tissue-specific atlas of mouse protein phosphorylation and expression. Cell 143: 1174-1189.

56. Gannon J, Staunton L, O'Connell K, Doran P, Ohlendieck K (2008) Phosphoproteomic analysis of aged skeletal muscle. International journal of molecular medicine 22: 33-42.

57. Mackay KB, Lowenson JD, Clarke SG (2012) Wortmannin reduces insulin signaling and death in seizure-prone pcmt1(-/-) mice. PloS one 7: e46719.

CHAPTER 5

A Short Perspective for Future Work

Search for an isoaspartyl molecular switch in the insulin signaling pathway

The etiology of the aberrant brain specific insulin signaling in *Pcmt1*$^{-/-}$ animals remains elusive. However, a brain specific isoform of the central effector of insulin signaling, Akt3, provides a promising candidate as the site of interaction between the isoaspartyl methyltransferase and the constitutively activated insulin signaling in *Pcmt1*$^{-/-}$ mice [1]. Recent work demonstrated that wortmannin-induced inhibition of PI3K-mediated insulin signaling did not markedly reduce Akt-dependent sites of phosphorylation on mTOR protein[1]. Phosphorylation of this Akt substrate occurs despite the absence of phosphorylation-induced activation of brain Akt [1], alluding to Akt as the culpable enzyme responsible for the elevated insulin signaling in these animals. These data provide evidence that the brain-specific Akt3 isoform behaves in a manner distinct from other Akt isoforms leading us to examine its protein sequence (Figure 1). Akt3 contains several likely sites of isoaspartyl formation that are absent in the other murine Akt isoforms. These residues provide the potential for a brain-specific isoaspartyl molecular switch, a mechanism for the phosphorylation independent activation of Akt in the brains of *Pcmt1*$^{-/-}$ animals. In support of this hypothesis, one of the highly conserved potentially isoaspartyl prone aspartate residues in the protein kinase domain of all Akt isoforms, D219, has been implicated in aberrant brain growth, seizure onset and Akt activation in D219V mutant mouse models[2]. The phenotype of these animals,

similar to the phenotype of *Pcmt1*$^{-/-}$ animals [3,4], could result from the loss of an isoaspartyl/repair-mediated molecular switch controlling Akt at this residue. Analysis of isoaspartyl formation in murine brain Akt could establish the link between Akt activation and the absence of protein isoaspartyl methyltransferase activity.

I hypothesize that the D219V mutation may cause aberrant signaling by ablating an isoaspartyl molecular switch at this position, or mimicking the effect of an isoaspartyl residue at this position. Isoaspartyl formation would move the carboxylic acid moiety of D219 to an alternative position, while D219V mutation would remove the carboxylic acid moiety completely, both of which could potentially activate Akt.

Continuing experiments are aimed at exploring the potential of isoaspartyl-prone residues unique to Akt3 as well, as the evolutionarily conserved D219, to form isoaspartyl residues *in vivo* and *in vitro*, as well as the frequency that these residues are repaired by the isoaspartyl methyltransferase. In order to avoid troublesome mammalian cloning of Akt3 throughout these experiments, immunoprecipitation of Akt using polyclonal pan-Akt antibodies from *Pcmt1*$^{-/-}$ and *Pcmt1*$^{+/+}$ mouse brains should provide an excellent source of Akt with which to proceed with *in vitro* isoaspartyl methylation assays. In order to examine the effect of isoaspartyl formation on Akt kinase activity, this preparation of Akt could additionally be immediately used to perform *in vitro* Akt kinase assays (Cell Signaling Technologies, Danvers, MA) to phosphorylate recombinant GSK fusion proteins containing Akt substrate recognition sites, and which are detectable by

Western blot analysis. This experiment would address whether endogenous Akt populations in *Pcmt1*$^{-/-}$ and *Pcmt1*$^{+/+}$ animals display altered activity, presumably due to increased isoaspartyl content in Akt from *Pcmt1*$^{-/-}$ animals.

Addressing whether isoaspartyl formation is not only necessary but sufficient to induce Akt activation in *Pcmt1*$^{-/-}$ animals could be addressed in two distinct manners. Crossing *Pcmt1*$^{-/-}$ mice with readily available Nmf350 animals possessing the D219V Akt mutation and subsequent monitoring of the seizure threshold and brain growth of the Nmf350/ *Pcmt1*$^{-/-}$ offspring could provide clues as to the relationship between D219 in Akt and the aberrant insulin signaling in *Pcmt1*$^{-/-}$ mice. An additive phenotypic increase in seizure activity and brain growth in Nmf350/ *Pcmt1*$^{-/-}$ offspring would demonstrate independent interactions with growth pathways, however if the phenotype of these offspring mimic those of Nmf350 it would suggest the phenotypes observed in *Pcmt1*$^{-/-}$ animals are brought on by an isomerization of D219, or some other interaction between PCMT1 and this residue.

Although the D219V mutation of Akt is known to cause seizures and aberrant Akt activation in mice, this does not implicate isomerization, and could arise from the loss of charge inherent to this mutation. Under this theory that D219V phenotypes are caused by loss of the carboxylate moiety, the creation of a mouse model possessing a mutation of D219 mimicking the carboxylic acid charge state, but incapable of isomerizing, such as D219E would resolve the effect of charge versus isomerization potential at this position. Phenotypic analysis of this animal,

as well as crosses of these animals with *Pcmt1*$^{-/-}$ mice could confirm the action of an isoaspartyl switch regulating Akt activity.

Search for PP2A methylation dependent and independent binding partners

Control of PP2A subunit assembly is vital for cellular function[5,6]. One theory proposes that the lethality associated with loss of the PP2A methyltransferase arises from dysregulated control of PP2A assembly[7,8]. Post-translational modifications are thought to be a major factor in controlling the assembly of PP2A holoenzymes[7], yet despite the crucial nature of PP2A holoenzyme assembly the role of methylation on binding of a majority of B subunits is still unclear. In *Lcmt1*$^{-/-}$ hypomorphic mice we have a potentially invaluable model for evaluating PP2A assembly under decreased PP2A methylation.

Evaluation of PP2A assembly could be achieved through multiple proteomic techniques. PP2A B subunits bound to the PP2A catalytic core could be immunoprecipitated from *Lcmt1*$^{-/-}$ and *Lcmt1*$^{+/+}$ animals using well defined commercially available antibodies specific for PP2Ac. Although commercial antibodies exist that recognize both methylated as well as demethylated species of PP2Ac these antibodies display enormous cross-reactivity; although suitable for Western blotting this cross-reactivity precludes their use in immunoprecipitation experiments. The *Lcmt1*$^{-/-}$ hypomorphic mouse model allows us to employ well-characterized antibodies against total PP2Ac, and enrich for PP2A binding partners that prefer the dominant demethylated form of PP2A found in these animals. This

would enable the creation of libraries of proteins bound to PP2A under normal methylation levels, *Lcmt1*$^{+/+}$ mice, as well as decreased methylation levels *Lcmt1*$^{-/-}$ mice.

The immunoprecipitate libraries could be separated by single or orthogonal SDS-PAGE followed by quantitative Western blotting against known PP2A B subunits, or alternatively in-gel digest followed by analysis and identification on a mass spectrometer. Qualifying and quantifying the B subunits bound to PP2A in *Lcmt1*$^{-/-}$ animals as well as *Lcmt1*$^{+/+}$ animals would allow us to correlate PP2A subunits with the alterations in the phosphoproteome of *Lcmt1*$^{-/-}$ mice in CHAPTER 4, providing a link between PP2A methylation, specific PP2A B subunit assembly, as well as the cytosolic targets of these subunits.

Cross-talk between modifications on the C-terminal tail of PP2A.

The "tail" of PP2A, evolutionarily conserved from yeast to humans, represents a solvent exposed six amino acid sequence, TPDYFL, thought to recognize acidic grooves on specific PP2A B subunits[9,10]. This small region of PP2A is responsible for three distinct protein chemistries, reversible methylation on L309, and reversible phosphorylation on Y307 and T304[11,12]. Methylation of PP2A is has been associated with assembly and activation of the phosphatase and phosphorylation of these two sites has been associated with PP2A inactivation[13,14,15,16].

Genetic experiments have revealed mutations to Y307 can prevent methylation of L309[17,18,19], suggesting the potential for cross talk between these two modifications. In order to investigate the influence of reduced methylation in *Lcmt1*$^{-/-}$ animals on Y307 phosphorylation of the PP2Ac tail, a Western blotting strategy can be employed correlating these two modifications. Y307 PP2Ac specific antibodies, however, have proven to be relatively non-specific, however, employing microcystin affinity chromatography to enrich for PP2A prior to Western analysis could potentially allow the successful Western blotting using these antibodies. This study could provide an additional role for methylation of PP2A in fine-tuning the activity of the phosphatase.

FIGURES

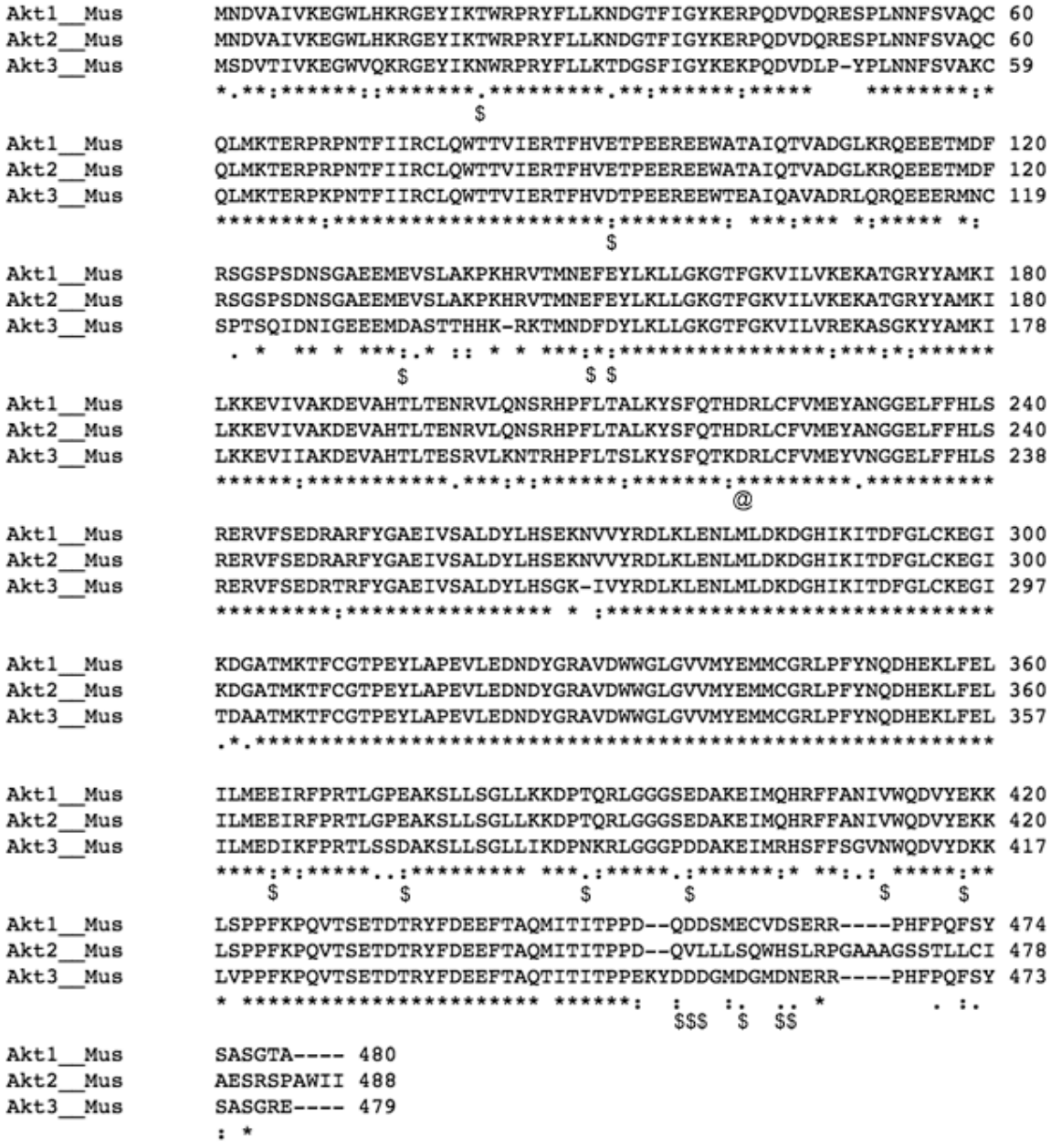

Figure 1: Sequence alignment of *Mus musculus* Akt, Akt2, and Akt3 revealing unique potentially isoaspartyl forming residues in Akt3. Sequence homology is

indicated by *, high sequence similarity is indicated by ":", low sequence similarity is indicated by ".", no sequence similarity if indicated by a blank space " ". Potentially isoaspartyl-prone residues present in Akt3 and not other Akt isoforms are indicated by $. The evolutionarily conserved D219 indicated in aberrant Akt activation is indicated by "@"

REFERENCES

1. Mackay KB, Lowenson JD, Clarke SG (2012) Wortmannin reduces insulin signaling and death in seizure-prone pcmt1(-/-) mice. PloS one 7: e46719.
2. Tokuda S, Mahaffey CL, Monks B, Faulkner CR, Birnbaum MJ, Danzer SC, Frankel WN (2011) A novel Akt3 mutation associated with enhanced kinase activity and seizure susceptibility in mice. Human molecular genetics 20: 988-999.
3. Kim E, Lowenson JD, Clarke S, Young SG (1999) Phenotypic analysis of seizure-prone mice lacking L-isoaspartate (D-aspartate) O-methyltransferase. The Journal of biological chemistry 274: 20671-20678.
4. Farrar C, Houser CR, Clarke S (2005) Activation of the PI3K/Akt signal transduction pathway and increased levels of insulin receptor in protein repair-deficient mice. Aging cell 4: 1-12.
5. Mumby M (2007) The 3D structure of protein phosphatase 2A: new insights into a ubiquitous regulator of cell signaling. ACS chemical biology 2: 99-103.
6. Wurzenberger C, Gerlich DW (2011) Phosphatases: providing safe passage through mitotic exit. Nature reviews Molecular cell biology 12: 469-482.
7. Sents W, Ivanova E, Lambrecht C, Haesen D, Janssens V (2012) The biogenesis of active protein phosphatase 2A holoenzymes: a tightly regulated process creating phosphatase specificity. The FEBS journal.

8. Lee JA, Pallas DC (2007) Leucine carboxyl methyltransferase-1 is necessary for normal progression through mitosis in mammalian cells. The Journal of biological chemistry 282: 30974-30984.

9. Cho US, Xu W (2007) Crystal structure of a protein phosphatase 2A heterotrimeric holoenzyme. Nature 445: 53-57.

10. Xu Y, Xing Y, Chen Y, Chao Y, Lin Z, Fan E, Yu JW, Strack S, Jeffrey PD, Shi Y (2006) Structure of the protein phosphatase 2A holoenzyme. Cell 127: 1239-1251.

11. Janssens V, Goris J (2001) Protein phosphatase 2A: a highly regulated family of serine/threonine phosphatases implicated in cell growth and signalling. The Biochemical journal 353: 417-439.

12. Janssens V, Longin S, Goris J (2008) PP2A holoenzyme assembly: in cauda venenum (the sting is in the tail). Trends in biochemical sciences 33: 113-121.

13. Xiong Y, Jing XP, Zhou XW, Wang XL, Yang Y, Sun XY, Qiu M, Cao FY, Lu YM, Liu R, Wang JZ (2012) Zinc induces protein phosphatase 2A inactivation and tau hyperphosphorylation through Src dependent PP2A (tyrosine 307) phosphorylation. Neurobiology of aging.

14. Liu R, Zhou XW, Tanila H, Bjorkdahl C, Wang JZ, Guan ZZ, Cao Y, Gustafsson JA, Winblad B, Pei JJ (2008) Phosphorylated PP2A (tyrosine 307) is associated with Alzheimer neurofibrillary pathology. Journal of cellular and molecular medicine 12: 241-257.

15. Chen J, Martin BL, Brautigan DL (1992) Regulation of protein serine-threonine phosphatase type-2A by tyrosine phosphorylation. Science 257: 1261-1264.

16. Guo H, Damuni Z (1993) Autophosphorylation-activated protein kinase phosphorylates and inactivates protein phosphatase 2A. Proceedings of the National Academy of Sciences of the United States of America 90: 2500-2504.

17. Yu XX, Du X, Moreno CS, Green RE, Ogris E, Feng Q, Chou L, McQuoid MJ, Pallas DC (2001) Methylation of the protein phosphatase 2A catalytic subunit is essential for association of Balpha regulatory subunit but not SG2NA, striatin, or polyomavirus middle tumor antigen. Molecular biology of the cell 12: 185-199.

18. Longin S, Zwaenepoel K, Louis JV, Dilworth S, Goris J, Janssens V (2007) Selection of protein phosphatase 2A regulatory subunits is mediated by the C terminus of the catalytic Subunit. The Journal of biological chemistry 282: 26971-26980.

19. Stanevich V, Jiang L, Satyshur KA, Li Y, Jeffrey PD, Li Z, Menden P, Semmelhack MF, Xing Y (2011) The structural basis for tight control of PP2A methylation and function by LCMT-1. Molecular cell 41: 331-342.